Dynamic Testing of Solar Domestic Hot Water Systems

Final report of the IEA Dynamic Systems Testing Group

INTERNATIONAL ENERGY AGENCY
Solar Heating & Cooling Programme

Dynamic Testing of Solar Domestic Hot Water Systems

Final report of the IEA Dynamic Systems Testing Group

Volume B

Participant contributions

Edited by

H. Visser
and
A.C. de Geus

TNO Building and Construction Research,
Delft, The Netherlands

December 1992

The DSTG final report "Dynamic Testing of Solar Domestic Hot Water Systems" consists of two Volumes which are distributed together.

The report is available under number B-92-0383/26.6.7029 from:

TNO Building and Construction Research
P.O. Box 29, NL-2600 AA Delft,
The Netherlands

The cost of the two Volumes amounts to approximately $60.-.

Information about the availability of the software tools mentioned in this report can be obtained from:

DIN Deutsches Institut für Normung
c/o Mr. E. Memmert
P.O. Box 1107, D-1000 Berlin 30,
Germany

CONTENTS OF VOLUME B OF THE DSTG FINAL REPORT

INTRODUCTION TO VOLUME B

This publication "Dynamic Testing of Solar Domestic Hot Water Systems" presents the experiences of the International Energy Agency's Dynamic Systems Testing Group (IEA DSTG) on the characterization of the thermal performance of solar domestic hot water (SDHW) systems using the dynamic test method. The complete results of the DSTG's activities are presented in two Volumes of this final report.

The coordinated work is given in the other Volume A "Development and evaluation of the dynamic test procedure" and consists of a note on the IEA and the DSTG followed by a description of dynamic SDHW system testing including dynamic testing in practice.

This Volume B "Participant contributions" contains a collection of papers of the DSTG participants and other interested researchers, describing the findings with respect to dynamic testing of SDHW systems in more detail.

Both simulated and real measuring data have been evaluated. After introduction of the solar load ratio in Paper no. 1, investigation of the adequacy of simulated test sequences is described in the Paper nos. 2 - 4. Paper no. 5 contains recommendations on measuring the quantities needed by the dynamic fitting procedure. It can serve as a starting point for reading the Paper nos. 6 - 10 describing outdoor tests of different types of SDHW systems.

Paper nos. 11 and 12 present experiences with in-situ measuring, the latter of a large solar domestic hot water and space heating system. Paper nos. 13 - 15 describe dynamic testing of solar collectors.

The nomenclature in the papers is generally the same as used in Volume A. Additional and different symbols are defined in the relevant papers.

Volume A of the DSTG final report is an IEA technical report, whereas Volume B has the status of a Working Document. However, Volume B should surely be considered to be more than just an appendix to Volume A. Hence, in Volume A, references are often made to the contributions in this Volume B for more information.

THE SOLAR LOAD RATIO, AN INDICATOR FOR THE ABILITY OF A TEST SEQUENCE TO ALLOW FOR SUBSEQUENT ACCURATE PREDICTION OF ANNUAL SYSTEM PERFORMANCE

J.-M. SUTER
Paul Scherrer Institute
Laboratory for Energy and Process Technology
CH-5232 Villigen PSI
Switzerland

1. INTRODUCTION

A crucial issue for any long-term performance prediction from a short-term test sequence is the *absence of seasonal bias*. Generally, if the test sequence used for system parameter identification is *arbitrarily* chosen, some more or less significant part of the range covered by the input variables within a year is missing in the test sequence, although these "out-of-test-range" values are included into the long-term performance calculation performed subsequently with the identified parameters. Hence, in this case there is some *extrapolation* from the test sequence input variable range to the more extended yearly input variable range, and the probability of getting a biased annual result depending on the season of the measurement period is high.

The challenge lies in the appropriate choice of the test sequence to insure that the latter correctly represents the whole year even though it is much shorter. In order to avoid a restart of the measurements later on if, in the course of data processing, the test sequence is found uncompleted, a *criterion* should be available *already at measurement time* for *checking the completeness of the data recorded*. This issue is especially important for *in-situ* testing because, in this case, the only free option in the testing conditions is the length of the measurement period. It must be recalled that the system is

operated continuously in the normal mode, i.e. supplying heat to the users during the tests as usually, and the variations of the input variables are induced only by users and weather, not by the testing staff.

2. THE SOLAR LOAD RATIO

The *in-situ* version of the dynamic system test procedure for SDHW systems has been developed using data from a solar plus supplementary system [1]. In the course of this study, it turned out that the **solar load ratio (SLR)** is a good indicator for checking the completeness of the test sequence being recorded. The solar load ratio is defined as the *dimensionless ratio of the energy received by the collector array,* $H_t A_C$, *to the heat load,* Q_L, *in the same period.* For solar plus supplementary systems, Q_L is the heat actually delivered to the load. For solar only and solar preheat systems, we have less experience; however, as explained below, a reasonable choice for Q_L seems to be the heat which would be delivered to the load if the hot water had exactly the requested demand temperature, T_D. For SDHW systems, *daily* SLR-values have to be considered.

The solar load ratio was originally introduced by Balcomb and Hedström in a totally different context [2]. The SLR method was first developed as a design tool for active space heating systems. The solar load ratio was calculated on a monthly basis as the ratio of the solar energy received by the collector array to the heating load. The latter was expressed as the product of the building heat loss coefficient times the monthly heating degree-days. Later on, the technique was modified slightly by Balcomb and McFarland [3] and applied to passive solar heated buildings. There, the SLR was defined as the ratio of the solar radiation transmitted through the glazing of the solar aperture during a one month period to the total building heating load during the same one month period.

In our case, the following considerations led to the identification of the solar load ratio as a useful indicator for daily checks of the test sequence at measurement time:

- The accurate calculation of the yearly system energy balance requires the accurate prediction of *both collector and storage efficiencies* at any step of the computer simulation performed for long-term prediction.

- The *collector efficiency* is a function of $T^*(t) = (T_C - T_{CA}) / G_t$, where T_C is the collector (fluid) temperature, T_{CA} the collector ambient temperature, and G_t the solar

irradiance in the collector plane. The *storage efficiency* is a function of $T_S(z,t)$, the time and height dependent temperature profile of the store (the store ambient temperature, T_{SA}, being nearly constant in practice). If there is an auxiliary heater keeping the temperature in the upper part of the store at the set value required by the user, the store temperature profile, $T_S(z,t)$, is affected by substantial variations mainly in the *lower, solar-only heated part.*

- As discussed above, $T^*(t)$ and $T_S(z,t)$ must cover in the test sequence the full range of values encountered in a year of real system operation, otherwise the predicted collector and storage efficiencies may be biased. However, neither $T^*(t)$ nor $T_S(z,t)$ are measured in the dynamic system test procedure which systematically avoids intrusive measurements. Thus, *indicator(s)* involving only external variables but directly related to $T^*(t)$ and $T_S(z,t)$ have to be found.

- In a *SDHW system* of the type shown in Fig. 1, the collector operating temperature, T_C, directly depends on the occurence (or non-occurence) of a hot water withdrawal. The tapped water, at temperature T_{ST}, is immediately replaced at the store bottom by cold water at the mains temperature, T_{main}, and the temperature in that store part determines the one of the liquid flowing to the collector. Of course, T_C also depends on the available solar irradiation heating up the store progressively. Hence, neither the volume of the hot water withdrawal nor the solar irradiation on the collector alone but the *quotient* of these two quantities is an *indicator of the temperature in the lower part of the store* and, consequently, of the *collector operating temperature.*

  (i) For solar plus supplementary systems, this indicator is expressed as the *dimensionless solar load ratio* $H_t A_C / [C_S (T_{ST} - T_{main})]$, where C_S is the thermal capacitance through the store. So, the SLR is the ratio of the energy received by the collector array, $H_t A_C$, to the heat delivered to the load, Q_L.

  (ii) For solar only and solar preheat systems, a slightly different expression of the SLR is needed since, in this case, Q_L varies according to *both* C_S *and* T_{ST}. Hence, Q_L does not indicate uniquely the volume of the hot water withdrawal. We propose to replace the variable temperature of the hot water delivered, T_{ST}, by the *fixed demand temperature*, T_D. Thus, $SLR = H_t A_C / [C_S (T_D - T_{main})]$, which is still a dimensionless ratio.

The solar load ratio defined in this way is *correlated* to the average collector operation temperature and to that of the solar-only heated part of the store. A high

SLR indicates high temperatures, and *vice versa.* A given temperature level may be reached with different irradiations, provided the withdrawal volume varies in such a way that the SLR remains unchanged.

For practical use of the SLR, the ranges of irradiation and heat load to be considered are to be limited by *realistic bounds* as explained below. In practice on the average, a high SLR means realistically high irradiation and low heat load.

The time scales for the analysis of SLR and T^* have still to be defined. The following considerations were made:

- The *characteristical time constant* of a *hot water storage tank* in the stand-by mode is of the order of a few days. During system operation, SDHW systems are subject to *daily* cycles, the water stored in the lower part of the storage tank staying seldom longer than one day at that location. Hence, the values of H_t and Q_L simultaneously measured on a certain day have to be combined to get the SLR-value describing some average (lower-part) store temperature *for this day.* This is the correct indicator. Hourly values would here be meaningless.

- On the contrary, the *characteristical time constant* of an *operated collector loop* is of the order of one hour. Hence, *hourly T^*-values* have been analyzed during the course

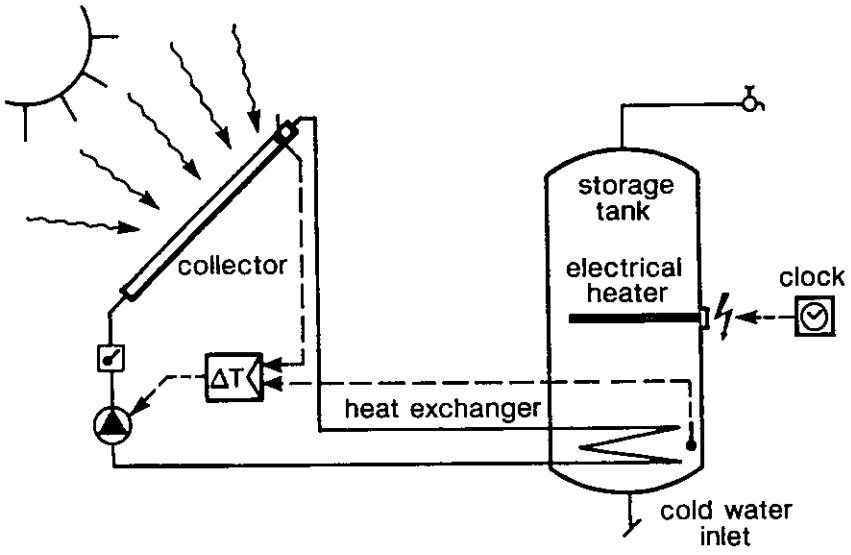

Fig. 1: Hydraulic scheme of a typical SDHW system considered here.

of the *in-situ* test procedure development, using measured data including this quantity [1].

It turned out that data covering the required range of daily SLR-values do also cover the required range of hourly T^*-values. The contrary may be false: a satisfying T^*-statistics does not necessarily implies a satisfactory SLR-statistics. Hence, *only a SLR-analysis* is required in practice and intrusive measurements as would be necessary for T^*-statistics may effectively be avoided.

3. ON-LINE HISTOGRAMS OF THE SOLAR LOAD RATIO

The SLR is used during the measurements to compute a histogram of the recorded values each day and check it for completeness. If the required criterion is fulfilled, the measurements may be stopped. The completeness check consists in a comparison with an *ideal histogram* defined as indicated below. The procedure has been developed for System #12 of Ref. [1], but is suggested to be applicable - after possible adaptations - to other systems.

Since small as well as large SLR-values are of equal importance in the statistics, at least for solar plus supplementary systems, we propose to introduce the (decimal) *logarithm* of the solar load ratio. We consider *four classes per decade* (steps of 0.25 in the logarithmic scale).

In the ideal SLR-histogram, the *lowest filled class* corresponds to a day with *low irradiation* and *high load*, hence to a typical *winter* day for which the lower store part is cold. In this situation, the store heat losses mainly arise from the upper store part kept at the set temperature. The optimal lowest SLR to be considered is given by a daily irradiation of *1.5 to 2 kWh/m²d* (5 to 7 MJ/m²d) and a withdrawal volume equal to that of the *auxiliary heated part of the store*. It is assumed here that the auxiliary heater is turned off at daylight time (operation only with off-peak electricity). Otherwise, the largest realistic daily withdrawal volume to be considered is *greater*. In this case as well as for solar-only and solar preheat systems, its value has to be estimated from other considerations as, e.g., the user's customs. A lower irradiation does not make any sense as it would correspond to a vanishing collector heat output. The optimal lowest SLR depends on the SDHW system and its users. For System #12 of Ref. [1], the value obtained is 0.84.

In the ideal SLR-histogram, the *highest filled class* corresponds to a day with *high irradiation* and *low load*. In this typical *summer* day, also the lower store part is hot during the whole day, the solar collectors heating up the mains water as soon as it is fed into the store by the hot water withdrawals. The whole storage tank is thus affected by heat losses. If it is again assumed that the auxiliary heater is turned off at daylight time, a realistic low withdrawal volume corresponds, e.g., to *one fifth of the auxiliary heated volume*. For other operating conditions of the auxiliary heater as well as for solar-only and solar preheat systems, the lowest realistic withdrawal volume to be considered has to be estimated on another way, e.g., from the user's customs. The high daily irradiation value to be selected is typically *6 kWh/m²d* (22 MJ/m²d) or 3/4 of the largest possible value at the location of interest. Usually, this is large enough to heat up the just chosen, low withdrawal volume of cold water to the demand temperature by means of the collectors. This feature may be checked using collector efficiency values from a preliminary, separate standard collector test. As the optimal lowest SLR, the optimal highest one is dependent on the system and its users. The value got for System #12 of Ref. [1] is 16.6.

In the ideal SLR-histogram, each class has an *equal number of SLR-values*, in order to get the same degree of confidence in model and parameters over the whole range of operation conditions covered during the test. However, whether this is really needed in practice, is still an open question. Obviously, a very high frequency peak in one particular histogram class should be avoided since that class would have too large a statistical weight. However, some frequency variations among the filled classes will probably have only a minor influence on the final result, the long term energy balance.

An *example* of SLR-based, statistical analysis of test sequences is given in Ref. [1].

4. FINAL REMARKS

The solar load ratio (SLR) is proposed as an indicator for the ability of a test sequence to allow for subsequent accurate prediction of the annual system performance. Its use implies on-line statistical analysis according to Section 3. Although there has been up to now only a limited validation of these ideas, we feel that they are quite *general*, and applicable to several testing situations and systems as, for example, *outdoor SDHW system testing in the laboratory*.

It is worth noting that *only the design characteristics* of the tested system and, depending on the system type, some data about the *hot water user's customs* are needed for the determination of the ideal SLR-range to be covered by the test sequence. Hence, the corresponding values may be entered into the data measuring and recording unit before starting the test, together with a minimum and, possibly, a maximum number of days per histogram class. Then, the *statistical SLR-analysis may run completely automatically*, bringing a *test cost reduction* as, in principle, no personal intervention is needed.

NOMENCLATURE (Additions to the general nomenclature)

C_S	load side thermal capacitance through the store (volume of hot water withdrawal times specific heat)
Q_L	heat delivered to the load Solar plus supplementary systems: $Q_L = C_S (T_{ST} - T_{main})$ (heat actually delivered to the load) Solar only and solar preheat systems: $Q_L = C_S (T_D - T_{main})$ (heat which would be delivered to the load if the hot water had exactly the requested demand temperature, T_D)
SLR	solar load ratio Solar plus supplementary systems: $SLR = H_t A_C / [C_S (T_{ST} - T_{main})]$ Solar only and solar preheat systems: $SLR = H_t A_C / [C_S (T_D - T_{main})]$
T_C	collector temperature (average fluid temperature in the collector)
T_D	demand temperature (hot water temperature requested by the user)
$T_S(z,t)$	time and height dependent store temperature
T_{ST}	water temperature at the top of the store
$T^*(t)$	characteristic variable for collector operation. $T^* = (T_C - T_{CA}) / G_t$
z	height of the point considered in the store

REFERENCES

[1] J.-M. Suter, M. Bolsinger, M. Gstir, Development of an *In-Situ* Short-Term Test Procedure for Solar Domestic Hot Water Systems. Contribution to the present DSTG report, Volume B

[2] J.D. Balcomb and J.C. Hedström, *A Simplified Method for Calculating Required Solar Collector Array Size for Space Heating*
Proceeding of the 1976 ISES Annual Meeting, Winnipeg, Canada, Aug. 15-20, 1976, Vol. 4

[3] J.D. Balcomb and R.D. McFarland, *A Simple Empirical Method for Estimating the Performance of a Passive Solar Heating Building of the Thermal Storage Wall Type*
Proceedings of the 2nd National Passive Solar Conference, Philadelphia, PA, USA, March 16-18, 1978

DEVELOPMENT OF SHORT TERM TEST SEQUENCES FOR OUTDOOR TESTS OF SOLAR DOMESTIC HOT WATER SYSTEMS

W. Kowalczyk, H. Visser and A.C. de Geus
TNO Building and Construction Research
P.O. Box 29, 2600 AA Delft
The Netherlands

1. INTRODUCTION

Dynamic testing of systems is used in order to either identify the system parameters or/and to predict system performance for reference conditions. In both cases a system model is used of which the complexity is always limited as compared to the real system. Because of simplifications in the model, performance prediction with the expected parameters, i.e. the most accurate parameters according to the physical meaning, is usually less accurate than the prediction with the best fitted parameters. Deviations between expected and fitted parameters are caused by the fact that more system properties are taken into account by one parameter and by correlation between the fitted parameters.

It should be noticed that it is impossible to develop a universal test sequence. When designing an optimum test period the goal is to obtain results either with given accuracy or the most accurate, for the minimum testing time. In any case, an optimum test sequence must be dedicated either to system parameter identification or to performance prediction for reference conditions. In case of parameter identification, efforts should be directed to create such heat flows in the system that searched parameters can be identified separately from the system performance. In case of performance prediction, the system during the test period should operate at conditions which are the most critical for the yearly performance for reference conditions. Hence, an optimum test period depends on the system, in case of parameter identification, and on the system and reference conditions, in case of performance prediction.

This paper describes development of outdoor test sequences for both parameter identification and yearly performance prediction. Investigations are based on simulated data. A solar plus supplementary system is studied for both types of test sequences. A solar pre-heat

system is considered for yearly performance prediction only.

2. INVESTIGATION METHOD

Outdoor test sequences in spring, summer, autumn and winter of Dutch moderate climate were investigated for both parameter identification and yearly performance prediction.
A solar domestic hot water (SDHW) system with integrated auxiliary and a pre-heat system were considered.
The following programs for dynamic SDHW system testing were used: dynamic fitting program DFP, short term performance prediction program STP and long term performance prediction program LTPP [1]. Input data for dynamic testing were obtained from model simulations. A SDHW system model, called ZBOIL4, developed by TNO was used for the simulations. The dynamic SDHW system testing programs use a system model, called P, with separate collector loop and heat store. Thermal stratification in the store is described by a plug flow model, also called register model. In ZBOIL4, the heat store is modelled using fixed-location segments for the heat balance.
In model P, the solar collector loop is characterized by at least two parameters: effective collector area A_C^* and collector loop heat loss parameter u_C^*. The heat store is described by three parameters: overall heat loss coefficient U_S, heat capacity C_S and fraction of store volume heated by the auxiliary heater f_{aux}. There are additional parameters for advanced harmonization between model and measured system, e.g. draw-off mixing parameter D_L and collector loop stratification coefficient S_C. In the investigations, parameters D_L and S_C used specifically by model P should be close to zero as no draw-off mixing and low solar stratification is expected.
Main output of the STP and LTPP program is the average net system power (system gain) which is defined as solar power delivered to the store minus store losses, i.e. power delivered to the load minus auxiliary consumption. This quantity represents an average value over the whole period for which the prediction is made.
Depending on the specific investigation, evaluation of a test sequence has been done through comparison of simulated data with those predicted by DFP, STP and LTPP, i.e.:

- parameter values identified with DFP were compared with those expected, used by ZBOIL4;
- system gain predicted with STP for short term performance was compared with that simulated by ZBOIL4;
- system gain predicted with LTPP for long term performance was compared with that simulated by ZBOIL4.

3. SOLAR DOMESTIC HOT WATER SYSTEMS INVESTIGATED

A solar plus supplementary system (see Fig. 1) was used for evaluation of test sequences both for parameter identification and yearly performance prediction. The main features of the system are: 2.4 m^2 of collector area and a store volume of 200 l of which 80 l is charged by the auxiliary heater. A pre-heat system (see Fig. 2) was used for investigation of only test sequences for yearly performance prediction. The system was derived from the previous one by reducing the hot top part. Hence, its main features are: 2.4 m^2 of collector area and a store volume of 120 l.

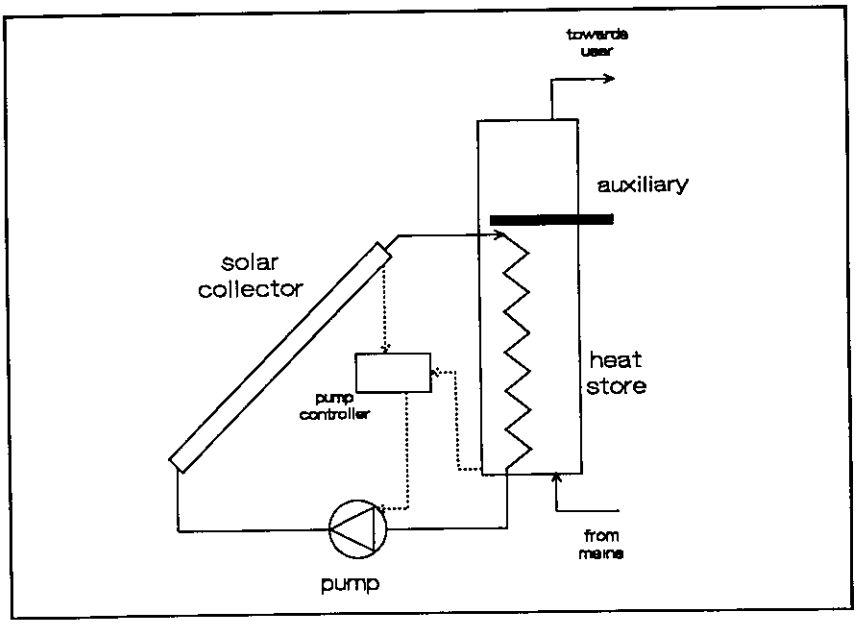

Figure 1: The simulated solar plus supplementary system.

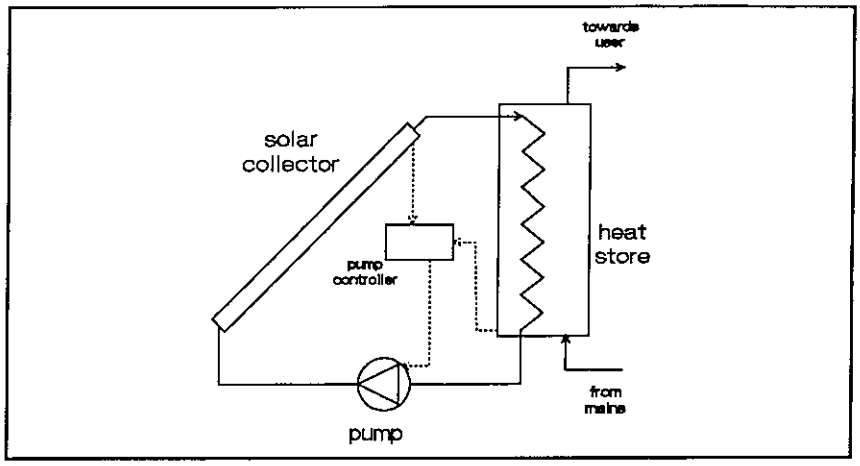

Figure 2: The simulated solar pre-heat system.

4. OUTDOOR TEST SEQUENCES FOR PARAMETER IDENTIFICATION

Outdoor test sequences for parameter identification were investigated for a SDHW system with integrated auxiliary. System performance was simulated with ZBOIL4 for four periods described in Table 1. These periods were selected from summer and winter of test reference year TRY De Bilt, the Netherlands. Test period TP1 has the best weather conditions. Winter test TP4 has the worst conditions.

Table 1: Simulated test periods.

test period	dates TRY-De Bilt	weather				
		day 1	day 2	day 3	day 4	day 5
TP1	1.07-5.07 (182-186)	good	good	good	good	good
TP2	9.07-13.07 (190-194)	good	good	bad	bad	bad
TP3	2.01-6.01 (2-6)	good	good	good	bad	bad
TP4	19.12-23.12 (353-357)	good	good	bad	bad	bad

Table 2: Simulated load profile LP1; auxiliary heater is off until 6th hour of day 3.

load profile	day	draw-off volume (l)													
		hour of the day													
		5	6	7	8	9	10	11	12	13	14	15	16	17	18
LP1	1	360	360			30	30	30	30	30	30	30	30	30	
	2														
	3	360	360	**ON**		30	30	30	30	30	30	30	30	30	
	4	360	360												

Applied water load profile LP1 is presented in Table 2. The first day of the test begins with preconditioning of the system through a large draw-off in order to adjust the states of the 'measured' and modelled system. During that day high draw-off is used and consequently relatively low temperature in the system is maintained. Under such conditions 'measured' data have information which is significant for the collector loop parameter A_C^* prediction. During the second day, there is no draw-off and collector temperature rises, so this day may be important for u_C^* prediction. At the third day, the auxiliary heater is enabled and the temperature in the store rises facilitating identification of U_S and f_{aux}. At the beginning of the fourth day, a large draw-off provides the fitting procedure with information about the end temperature profile in the store.

Identified values of parameters for load profile LP1 and all test periods are presented in Table 3. For all test periods, the worst prediction is obtained for heat loss parameters u_C^* and U_S. For test period TP1, i.e. summer days of good weather, the best fit of parameters is obtained. Test period TP1 is used in further investigations towards better prediction of parameter values.

Table 3: Expected and identified parameter values for investigated test periods and for load profile LP1. For the predictions, standard deviation has been indicated. In parentheses: relative deviation against the expected value.

test period	A_C^* [m^2]	u_C^* [W/m^2K]	U_S [W/K]	C_S [MJ/K]	f_{aux} [-]	D_L [-]	S_C [-]	Obj. [W]
expected	1.806	3.846	1.6	0.864	0.4	0	0	
TP1	1.820 ±0.034 (+0.8%)	3.353 ±0.230 (-12.8%)	2.14 ±0.25 (+33.8%)	0.851 ±0.007 (-1.5%)	0.40 ±0.01 (0.0%)	0.04 ±0.01	0.03 ±0.01	3.8
TP2	1.902 ±0.056 (+5.3%)	2.484 ±0.498 (-35.4%)	3.31 ±0.34 (+107%)	0.857 ±0.007 (-0.8%)	0.42 ±0.01 (+5.0%)	0.03 ±0.01	0.00 ±0.01	4.1
TP3	2.014 ±0.056 (+11.5%)	3.400 ±0.409 (-11.6%)	4.31 ±0.30 (+169%)	0.857 ±0.009 (-0.8%)	0.40 ±0.01 (0.0%)	0.03 ±0.01	0.01 ±0.01	2.8
TP4	1.556 ±0.055 (-13.8%)	0.096 ±0.211 (-97.5%)	4.51 ±0.47 (+182%)	0.853 ±0.022 (-1.3%)	0.43 ±0.01 (+7.5%)	0.03 ±0.01	0.00 ±0.00	4.1

Table 4: Simulated load profiles LP2 and LP3; auxiliary heater is off until 6th hour of day 3.

load profile	day	draw-off volume (l) hour of the day													
		5	6	7	8	9	10	11	12	13	14	15	16	17	18
LP2	1		360			30	30	30	30	30	30	30	30	30	
	2														
	3		360	ON		30	30	30	30	30	30	30	30	30	
	4		360												
LP3	1		360						90	90	90				
	2														
	3		360	ON					90	90	90				
	4		360												

Two other load profiles derived from load profile LP1 are described in Table 4. These load profiles were investigated for test period TP1. Identified values of parameters are presented in Table 5. The fitted parameters show no improvement as compared to the results for load

profile LP1: deviations between fitted end expected values for load profile LP2 is comparable with deviations for LP1. However, load profile LP2 is considered better because large draw-off in the morning hours may be reduced.

Table 5: Expected and identified parameter values for load profiles LP2 and LP3 and for test period TP1. For the predictions, standard deviation has been indicated. In parentheses: relative deviation against the expected value.

test period	A_C^* [m^2]	u_C^* [W/m^2K]	U_S [W/K]	C_S [MJ/K]	f_{aux} [-]	D_L [-]	S_C [-]	Obj. [W]
expected	1.806	3.846	1.6	0.864	0.4	0	0	
LP2	1.905 ±0.046 (+5.5%)	3.740 ±0.364 (-2.8%)	2.46 ±0.26 (+53.8%)	0.845 ±0.008 (-2.2%)	0.40 ±0.01 (0.0%)	0.04 ±0.01	0.01 ±0.01	3.6
LP3	1.968 ±0.046 (+9.0%)	3.642 ±0.378 (-5.3%)	2.83 ±0.23 (+76.9%)	0.847 ±0.005 (-2.0%)	0.41 ±0.01 (+2.5%)	0.04 ±0.01	0.01 ±0.01	2.7

Table 6: Simulated load profiles LP4 and LP5; auxiliary heater is on between 6.00 a.m. and 18.00 p.m.

load profile	day	draw-off volume (l) hour of the day												
		5	6	7	8	9	10	11	12	13	14	15	16	17	18
LP4	1		360	-		30	30	30	30	30	30	30	30	30	-
	2			ON											OFF
	3			ON											OFF
	4		360	ON		30	30	30	30	30	30	30	30	30	OFF
	5		360												
LP5	1		360	ON		30	30	30	30	30	30	30	30	30	OFF
	2		360	ON											OFF
	3		360	ON											OFF
	4		360	ON		30	30	30	30	30	30	30	30	30	OFF
	5		360												

In order to increase quality of prediction for parameters u_C^* and U_S, load profile LP2 has been extended by 1 day and auxiliary control has been changed. Resulting load profiles

LP4 and LP5 are described in Table 6.

Identified values of parameters are presented in Table 7. For both load profiles, deviations between fitted and expected values are within 7%. For load profile LP5, relatively large deviation for A_C^* is observed. This is caused by increased collector temperature during the first day due to system heating by the auxiliary unit.

Table 7: Expected and identified parameter values for load profiles LP4 and LP5 and for test period TP1. For the predictions, standard deviation has been indicated. In parentheses: relative deviation against the expected value.

test period	A_C^* [m^2]	u_C^* [W/m^2K]	U_S [W/K]	C_S [MJ/K]	f_{aux} [-]	D_L [-]	S_C [-]	Obj. [W]
expected	1.806	3.846	1.6	0.864	0.4	0	0	
LP4	1.782 ±0.040 (-1.3%)	3.751 ±0.427 (-2.5%)	1.71 ±0.26 (+6.9%)	0.856 ±0.009 (-0.9%)	0.40 ±0.01 (0.0%)	0.04 ±0.01	0.03 ±0.01	3.2
LP5	1.705 ±0.016 (-5.6%)	3.869 ±0.106 (+0.6%)	1.66 ±0.11 (+3.8%)	0.861 ±0.003 (-0.3%)	0.41 ±0.01 (+2.5%)	0.04 ±0.01	0.11 ±0.01	2.0

These investigations show that it is possible to design a test sequence for which system parameters are identified with small deviations against expected values. For good weather conditions and load profile LP4, deviations between fitted and expected parameters of the solar plus supplementary system is within 7%. Additionally, the standard error calculated by the DFP program is well estimated.

5. OUTDOOR TEST SEQUENCES FOR YEARLY PERFORMANCE PREDICTION

Outdoor test sequences for a solar plus supplementary system and for a solar pre-heat system were investigated. System performance was simulated with ZBOIL4 for the 1, 2, 4, 6 and 8 weeks periods described in Table 8. All test periods were preceded with 4 days of system operation in order to adjust the state of the 'measured' and modelled system at

the beginning of the test.

Attempt has been made to use the Solar Load Ratio (SLR) concept for the analysis of test sequences for system performance prediction. The SLR is defined as the non-dimensional ratio of the daily irradiation on the whole collector area $H_t A_C$ to the heat demand Q_D over a day [2]:

$$SLR = H_t A_C / Q_D \; . \qquad (1)$$

In principle, during the test period, SLR values should cover the whole SLR range determined by reference meteorological and load conditions. Varying hot water demand was applied in order to achieve more quickly the required range of SLR values: draw-off was 160 l for odd days and 80 l for even days. Reference conditions, used for yearly performance predictions, involve hot water demand of 110 l per day at 65°C, heated from 15°C, and meteorological data from test reference year TRY De Bilt, the Netherlands.

Table 8: The test periods (TRY - De Bilt)

season	start date (day number)	end date (day number)				
spring	5.04 (95)	11.04 (101)	18.04 (108)	2.05 (122)	16.05 (136)	30.05 (150)
summer	5.07 (186)	11.07 (192)	18.07 (199)	1.08 (213)	15.08 (227)	29.08 (241)
autumn	5.10 (278)	11.10 (284)	18.10 (291)	1.11 (305)	15.11 (319)	29.11 (333)
winter	5.01 (5)	11.01 (11)	18.01 (18)	1.02 (32)	15.02 (46)	1.03 (60)
duration		1 week	2 weeks	4 weeks	6 weeks	8 weeks

5.1 Test sequences for solar plus supplementary systems

Table 9 presents system gain 'measured' and predicted by the fitting program. For all sequences, 'measured' system gain is within the error bands of the predicted gain.

Table 9: System gain (W) determined by ZBOIL4 and predicted by STP for test sequences of 1, 2, 4, 6 and 8 weeks in spring, summer, autumn and winter. For the predictions, standard deviation has been indicated.

		1 week	2 weeks	4 weeks	6 weeks	8 weeks
spring	ZBOIL	138	209	169	174	190
	STP	138±3.4	210±1.8	169±1.9	174±1.3	190±1.3
summer	ZBOIL	259	202	184	184	206
	STP	259±1.0	203±1.6	184±1.6	184±1.3	206±1.4
autumn	ZBOIL	93.8	105	95.1	74.9	68.0
	STP	93.9±1.9	106±2.5	95.3±1.7	76.0±1.5	67.8±1.8
winter	ZBOIL	16.9	13.7	18.9	17.4	35.1
	STP	16.6±3.1	13.5±2.4	19.4±1.6	17.3±2.5	35.4±2.8

Table 10 shows 'measured' and predicted yearly system gain based on fitted parameters. The smallest deviation between predicted and expected yearly system gain is observed for test periods of 2 weeks and longer in spring and summer. For those periods, relative difference between predicted yearly system gain and the 'measured' value is within 3%. Twice the standard deviation given is the statistical error with a confidence interval of 95 %. So, also the error is estimated well.

Table 10: Yearly system gain (W) determined by ZBOIL4 and predicted by LTPP for test sequences of 1, 2, 4, 6 and 8 weeks in spring, summer, autumn and winter. For the predictions, standard deviation has been indicated.

		1 week	2 weeks	4 weeks	6 weeks	8 weeks
ZBOIL		119				
spring	LTPP	124±3.8	122±1.6	122±1.8	121±1.5	121±1.3
summer	LTPP	119±1.9	119±1.7	119±1.6	119±1.8	119±1.4
autumn	LTPP	129±5.1	124±4.0	125±1.9	126±2.8	125±2.1
winter	LTPP	130±6.1	134±4.0	128±2.7	127±3.6	125±4.0

Table 11 presents identified values of parameters from test sequences of 8 weeks. The agreement of the fitted parameters with the expected values is generally worse than found for test sequence LP4 (see Table 7). Nevertheless, for the sequences from which the prediction of the system performance is accurate (spring and summer), the agreement between fitted and expected values is quite acceptable. For some parameters, the error estimation is too optimistic, if the expected parameters are considered as true values. Remarkable is the increased value fitted for f_{aux}. Apparently, model P compensates neglecting of thermal conduction from the hot upper part of the store downwards through an increased fraction of the store volume heated by the auxiliary unit.

Table 11: Expected and identified parameter values from test sequences of 8 weeks in different seasons. For the predictions, standard deviation has been indicated. In parentheses: relative deviation against the expected value.

test period	AC* [m²]	uC* [W/m²K]	US [W/K]	CS [MJ/K]	faux [-]	DL [-]	SC [-]	Obj. [W]
expected	1.806	3.846	1.6	0.864	0.4	0	0	
spring (8 weeks)	1.653 ±0.018 (-8.5%)	3.400 ±0.109 (-11.6%)	1.63 ±0.06 (+1.9%)	0.812 ±0.006 (-6.0%)	0.47 ±0.01 (+17.5%)	0.06 ±0.01	0.009 ±0.003	1.8
summer (8 weeks)	1.748 ±0.023 (-3.2%)	4.198 ±0.122 (+9.2%)	1.57 ±0.06 (-1.9%)	0.811 ±0.007 (-6.1%)	0.47 ±0.01 (+17.5%)	0.07 ±0.01	0.001 ±0.003	1.6
autumn (8 weeks)	1.701 ±0.028 (-5.8%)	2.665 ±0.129 (-30.7%)	1.88 ±0.12 (+17.5%)	0.836 ±0.010 (-3.2%)	0.46 ±0.01 (+15.0%)	0.06 ±0.01	0.003 ±0.007	2.3
winter (8 weeks)	1.883 ±0.040 (+4.3%)	4.189 ±0.345 (+8.9%)	1.69 ±0.18 (+5.6%)	0.840 ±0.013 (-2.8%)	0.46 ±0.01 (+15.0%)	0.06 ±0.01	0.000 ±0.022	2.5

In Table 12 a comparison is presented between 'measured' yearly system gain and the gain predicted for tap water loads from 80 l to 200 l per day at 65°C, heated from 15°C. The deviations are less than 4%. Hence, parameter sets which give good yearly performance prediction for reference conditions can be used for accurate predictions for higher or lower hot water demands.

Table 12: Yearly system gain (W) determined by ZBOIL4 and predicted by LTPP for different tap water loads. For the predictions, standard deviation has been indicated. In parentheses: relative deviation against the expected value.

daily tap water load		80 l/d	110 l/d	140 l/d	170 l/d	200 l/d
ZBOIL		96	119	137	149	158
LTPP	parameters from 2 weeks period in spring	100±1.9 (+4%)	122±1.6 (+3%)	137±1.0 (0%)	146±0.8 (-2%)	153±0.2 (-3%)
LTPP	parameters from 8 weeks period in summer	97±1.7 (+1%)	119±1.4 (0%)	135±1.2 (-2%)	146±0.9 (-2%)	154±0.5 (-3%)

In Table 13, a comparison is presented between 'measured' system gain and the gain predicted based on fitted parameters from other sequences, for 4 weeks periods in different seasons.

Table 13: System gain (W) determined by ZBOIL4 and predicted by STP based on fitted parameters from other sequences, for periods of 4 weeks in different seasons. For the predictions, standard deviation has been indicated. In parentheses: relative deviation against the expected value.

period	spring	summer	autumn	winter
ZBOIL with expected parameters	169	184	95.1	18.9
STP with parameters from 2 weeks period in spring	169±1.3 (0%)	189±1.1 (+3%)	93.4±1.1 (-2%)	18.5±1.3 (-2%)
STP with parameters from 8 weeks period in summer	167±1.6 (-1%)	186±1.7 (+1%)	91.9±1.0 (-2%)	16.3±1.0 (-14%)

Remarkable large relative deviation for the 4 weeks period in winter based on parameters from the 8 weeks period in summer indicates that even for an accurate yearly performance prediction, the possibility remains that the parameters do not describe short term operation of the system adequately. As the system gain is relatively small for this period, the error does not influence the yearly performance very much. Nevertheless, care must be taken not to use parameters fitted from a test sequence with only good weather for winter prediction.

Prediction is shifted from interpolation to extrapolation then. Especially for systems with high store heat losses, large prediction errors for winter periods can be expected in that case, which probably will influence the accuracy of the yearly performance prediction. This means that for solar plus supplementary systems, the test sequence should not only contain days with high irradiation, but also bad weather days.

5.2 Test sequences for solar pre-heat systems

For solar pre-heat systems, investigations similar to those for the system with integrated auxiliary were performed. Table 14 presents system gain 'measured' and predicted by the fitting program. These STP results again involve self-predictions. The deviations between predicted and expected values are relatively small.

Table 14: System gain (W) determined by ZBOIL4 and predicted by STP for test sequences of 1, 2, 4, 6 and 8 weeks in spring, summer, autumn and winter. For the predictions, standard deviation has been indicated.

		1 week	2 weeks	4 weeks	6 weeks	8 weeks
spring	ZBOIL	151	209	175	179	191
	STP	151±0.7	209±1.0	175±0.2	178±0.6	191±0.9
summer	ZBOIL	251	204	188	187	207
	STP	250±4.6	204±0.6	190±2.4	189±3.0	207±1.0
autumn	ZBOIL	107	119	109	89.5	83.0
	STP	108±0.5	120±0.5	110±0.3	90.1±0.2	83.8±0.2
winter	ZBOIL	27.5	24.6	35.0	32.2	50.9
	STP	27.8±0.2	24.6±0.2	35.0±0.1	32.3±0.1	51.4±0.1

Table 15 shows 'measured' and predicted yearly system gain based on fitted parameters. Smallest deviations between predicted and expected yearly system gain are observed for test periods of 2 weeks and longer in spring and summer. For these periods, relative difference is within 4%. A systematic error between predicted and 'measured' values can be observed, which may be caused by neglect of thermal conduction in the store by

model P. For the pre-heat system, there is no f_{aux} to compensate for this. The estimated standard deviation is too small to account for the systematic error.

Table 15: Yearly system gain (W) determined by ZBOIL4 and predicted by LTPP for test sequences of 1, 2, 4, 6 and 8 weeks in spring, summer, autumn and winter. For the predictions, standard deviation has been indicated.

		1 week	2 weeks	4 weeks	6 weeks	8 weeks
ZBOIL		128				
Spring	LTPP	134±0.3	132±0.1	133±0.1	132±0.1	132±0.3
Summer	LTPP	131±1.1	130±0.4	133±0.5	133±1.3	131±0.5
Autumn	LTPP	130±1.6	135±0.9	133±0.7	134±0.7	133±0.8
Winter	LTPP	136±0.3	138±0.1	139±0.4	137±0.5	136±0.9

Table 16: Expected and identified parameter values from test sequences of 8 weeks in different seasons. For the predictions, standard deviation has been indicated. In parentheses: relative deviation against the expected value.

test period	A_C^* [m^2]	u_C^* [W/m^2K]	U_S [W/K]	C_S [MJ/K]	D_L [-]	S_C [-]	Obj. [W]
expected	1.806	3.846	1.6	0.522	0	0	
spring (8 weeks)	1.725 ±0.027 (-4.5%)	3.596 ±0.106 (-6.5%)	1.94 ±0.10 (+21.3%)	0.488 ±0.007 (-6.5%)	0.17 ±0.02	0.06 ±0.01	5.3
summer (8 weeks)	1.884 ±0.034 (+4.3%)	4.490 ±0.153 (+16.7%)	1.90 ±0.10 (+18.8%)	0.479 ±0.007 (-8.2%)	0.19 ±0.02	0.05 ±0.01	5.0
autumn (8 weeks)	1.973 ±0.024 (+9.2%)	5.045 ±0.088 (+31.2%)	2.12 ±0.14 (+32.5%)	0.513 ±0.006 (-1.7%)	0.10 ±0.01	0.06 ±0.01	1.9
winter (8 weeks)	1.976 ±0.095 (+9.4%)	4.069 ±0.321 (+5.8%)	0.81 ±0.21 (-49.4%)	0.500 ±0.022 (-4.2%)	1.44 ±0.48	0.00 ±0.03	3.7

Table 16 shows identified values of parameters from test sequences of 8 weeks. The accurate identification of parameters u_c^* and U_s appears to be difficult. As the store is not heated by auxiliary power, it is hard to determine these parameters independently from each other. Additionally, the error estimation is generally too optimistic.

Table 17 presents a comparison between 'measured' yearly system gain and the gain predicted for tap water loads from 80 l to 200 l per day at 65°C, heated from 15°C. The deviation between predicted and expected values is less than 3%. Hence again, parameter sets which give good yearly performance prediction for reference conditions can be used for accurate prediction for different hot water demands.

Table 17: Yearly system gain (W) determined by ZBOIL4 and predicted by LTPP for different tap water loads. For the predictions, standard deviation has been indicated. In parentheses: relative deviation against the expected value.

daily tap water load		80 l/d	110 l/d	140 l/d	170 l/d	200 l/d
ZBOIL		107	128	144	155	162
LTPP	parameters from 2 weeks period in spring	110±0.6 (+3%)	132±0.1 (+3%)	147±0.5 (+2%)	158±1.3 (+2%)	165±2.0 (+2%)
LTPP	parameters from 8 weeks period in summer	109±0.7 (+2%)	131±0.5 (+2%)	147±0.2 (+2%)	158±0.2 (+2%)	166±0.6 (+2%)

In Table 18 a comparison is presented between 'measured' system gain and the gain predicted based on fitted parameters from other sequences, for 4 weeks periods in different seasons. Deviations are less than 2%, even for the winter period.

Table 18: System gain (W) determined by ZBOIL4 and predicted by STP based on fitted parameters from other sequences, for periods of 4 weeks in different seasons. For the predictions, standard deviation has been indicated. In parentheses: relative deviation against the expected value.

period	spring	summer	autumn	winter
ZBOIL with expected parameters	175	188	109	35.0
STP with parameters from 2 weeks period in spring	174±0.5 (-1%)	192±0.8 (+2%)	108±0.5 (-1%)	34.9±0.4 (-1%)
STP with parameters from 8 weeks period in summer	172±1.1 (-2%)	189±0.9 (+1%)	108±0.1 (-1%)	34.4±0.1 (-2%)

6. SOLAR LOAD RATIO AS MEASURE OF TEST SEQUENCE QUALITY

Investigations of outdoor test sequences for yearly performance prediction have shown that for both solar plus supplementary and pre-heat systems, optimum test sequences were the same: periods of 2 weeks and longer in spring and summer.

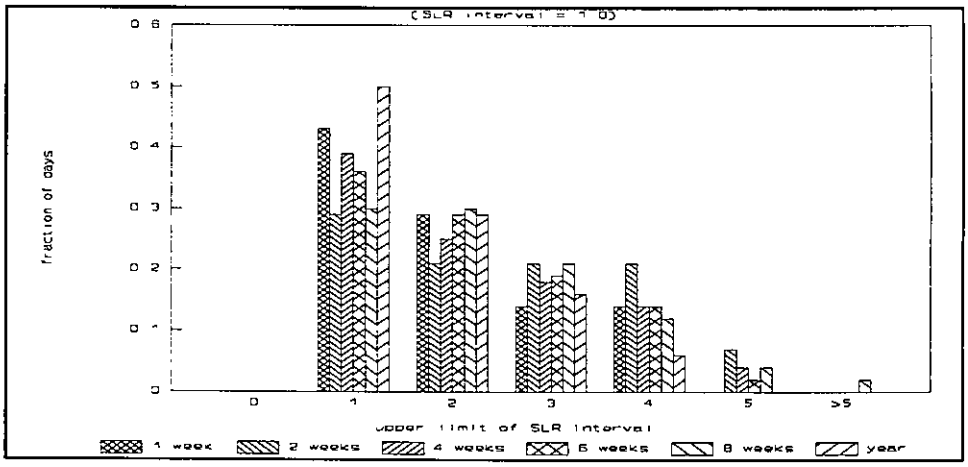

Figure 3: Frequency distribution of daily SLR for test sequences in spring and for the yearly reference conditions.

Figures 3 to 6 present frequency distribution of daily SLR over intervals of 1.0 for all investigated test periods. Additionally, distribution for the yearly reference conditions (load

of 110 l/day) is given. The optimum test sequences of 2 weeks and longer in spring and summer have higher frequency of occurrences for large SLR values as compared with the yearly distribution. These sequences also have days with low SLR values. Hence, the whole SLR range for reference conditions is well covered by the test period. That is not the case for the autumn and winter sequences. Thus, distribution of SLR enables to select optimum test periods for both types of solar systems.

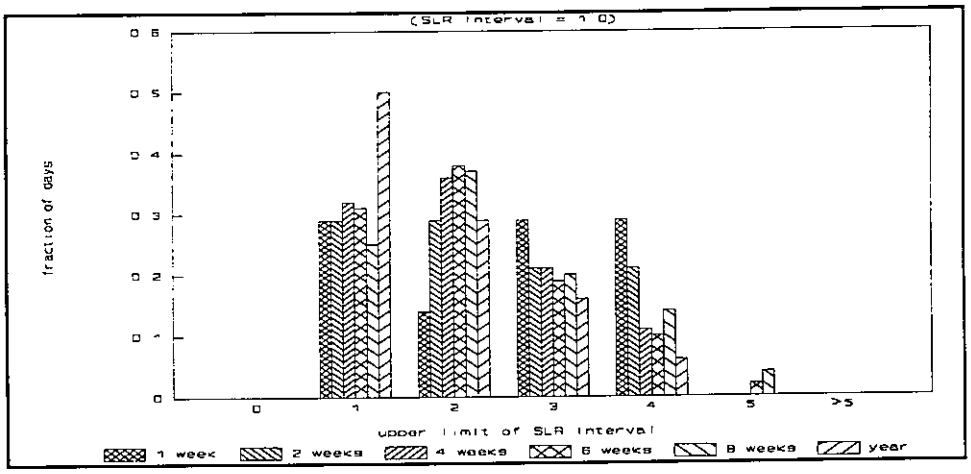

Figure 4: Frequency distribution of daily SLR for test sequences in summer and for the yearly reference conditions.

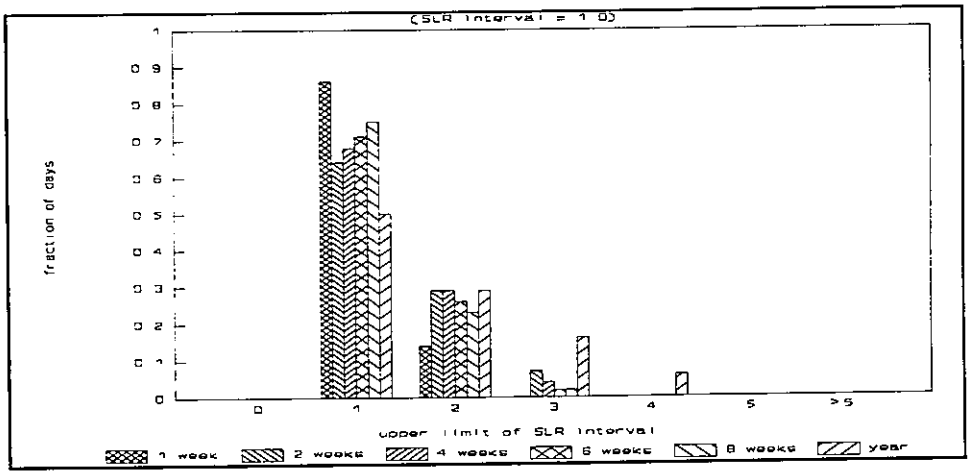

Figure 5: Frequency distribution of daily SLR for test sequences in autumn and for the yearly reference conditions.

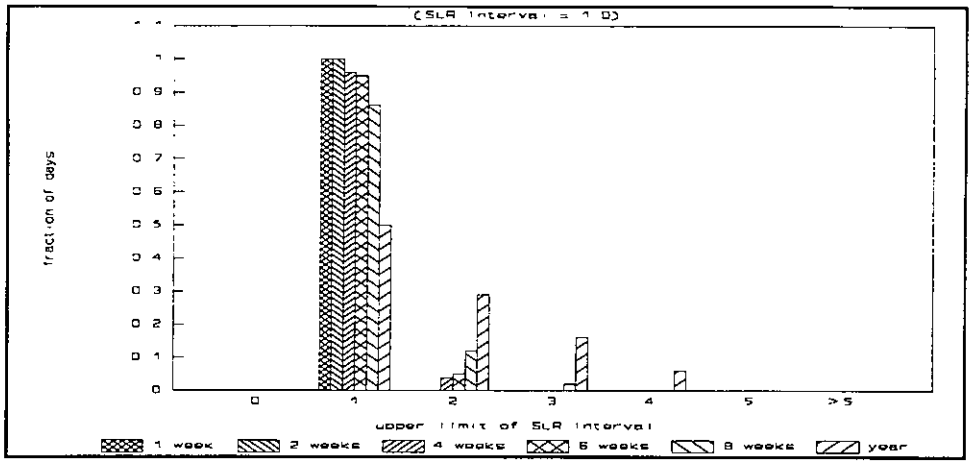

Figure 6: Frequency distribution of daily SLR for test sequences in winter and for the yearly reference conditions.

7. CONCLUSIONS

Outdoor test sequences from different seasons of Dutch climate were investigated for both parameter identification and yearly performance prediction. The investigations were based on simulated data. A solar plus supplementary system was studied for both types of test sequences. A solar pre-heat system was considered for yearly performance prediction only. The investigations have shown that it is possible to design a test sequence for which system parameters are identified with good accuracy. Such test sequence involves good weather conditions and a specific load profile. For a good test sequence, deviation between identified and expected parameters of the SDHW system with integrated auxiliary is less than 7%. Additionally, the statistical error is estimated well.

Investigations of test sequences for yearly performance prediction have shown that SLR may be used as a practical measure to evaluate quality of the test sequence. For optimum test sequences, SLR should cover the whole SLR range for reference conditions.
For an optimum test sequence, deviation between predicted and expected yearly system gain is less than 4%. Probably, part of this error is systematic caused by neglect of thermal conduction in the store by model P. If this systematic error is not considered the statistical error is estimated well. Extrapolation of yearly system gain for other tap water loads than

the reference one has a good accuracy.

Although tendencies for good test sequence design have been indicated, it seems reasonable to continue investigations on criteria for an optimum test sequence. The investigations should concentrate on analysis of conditions for which most of the system gain is obtained, both during a test period and the reference period. For solar plus supplementary systems, conditions for which most of the auxiliary power is delivered is of equal importance. Conclusions from such analysis should give more precise requirements regarding optimum test period.

REFERENCES

[1] Spirkl, W.
Dynamic SDHW system testing - program manual, version 1.18.
Ludwig Maximilians University, Munich, Germany, October, 1991.
Also included in appendix A of Volume A.

[2] Visser, H. and A.C. de Geus (ed.)
Dynamic testing of solar domestic hot water systems.
Volume A of the present DSTG final report.

DEVELOPMENT OF A SHORT TERM TEST SEQUENCE FOR INDOOR TESTS

S.J. Bennedsen and S.J. Harrison
Solar Calorimetry Laboratory
Department of Mechanical Engineering
Queen's University
Kingston, Ontario, Canada

1. INTRODUCTION

In the performance analysis of solar domestic hot water (SDHW) systems, tests are run on a given system to determine a set of parameters which describe its performance. There are generally two test methods: long term outdoor testing or monitoring, and short term static testing. Long term monitoring involves running the system under typical operating conditions for a period of up to a year. The performance of the system is then determined by time-averaging performance characteristics over the test period. Tests of this type generally are site and climate specific to the monitoring period and consequently it is difficult to make accurate performance predictions for other conditions.

Static tests are usually run indoors under a repeatable, controlled set of operating conditions (irradiation, ambient temperatures, and draw-off profile) with the system held at a quasi-equilibrium condition [1]. Individual tests can be completed in three or four days, but to get a general indication of performance several tests may be required at different operating conditions; hence, this testing can be very costly.

Recently a "dynamic" model was introduced by W. Spirkl of the University of Munich [2]. With this transient model, it was intended that test periods of only a few days could be used to estimate a set of system parameters which could be used to describe the system's long term performance.

2. EVALUATION OF THE DYNAMIC METHOD

To evaluate the potential of this dynamic test method, two activities were undertaken: 1) a simulation study was conducted to determine the capability of the method to predict long term performance from short term outdoor test sequences, and 2) an attempt was made to develop an optimum test sequence that could be conducted in an indoor test facility using the measurement techniques described in reference 1.

Part 1: To evaluate the method and to determine if systematic errors would result if testing periods were chosen from different times of the year, annual performance data for a typical solar system was produced by computer simulation [3] using weather data for a variety of North American locations representing a range of climatic regions. From this data set, specific short term test sequences representing winter and summer test periods (December and January, and June and July respectively) were chosen as data input to the parameter identification computer routine [2]. These test periods were then used separately and together to identify system performance parameters and predict performance.

Part 2: A series of very short test sequences of approximately five days length were evaluated to investigate the potential to develop an optimum test sequence that could be conducted in an indoor test facility. Each of the short term test sequences were evaluated by comparing the performance as predicted from coefficients determined from the short term test sequence against annual data developed in Part 1.

Finally the practicality and accuracy of one of the short term test sequences was evaluated experimentally and determined system parameters were compared with expected values.

2.1. The solar domestic hot water system evaluated

The SDHW system simulated is illustrated in Figure 1, and is based on a commercially available "micro-flow" preheat system. The system was a closed loop design which used a 40/60% mixture of propylene glycol and water in the solar collector/heat exchanger loop. Cold water from the bottom of the storage tank circulates through the heat exchanger to the top of the tank. Hot water is drawn off at the top of the tank according to a set draw schedule, and is replaced at the bottom of the tank with cold mains water. The system can be divided into two subsystems: the collector loop (including the heat exchanger), and the storage tank [2,4].

The collector loop is characterized by the parameters A_C^* , the effective collector area, including energy losses due to the optical properties of the system; u_C^* , the collector heat loss coefficient, a measure of energy losses to the surroundings; and S_C, the collector loop stratification parameter, which indicates the degree of temperature stratification in the storage tank due to the low collector flow rate. These parameters are all functions of the physical characteristics of the collector, heat exchanger and of the properties of the fluids.

The system was modelled with a flat-plate collector with total area of 5.23 m^2, and the collector parameters were determined from data obtained by separate test. The commercial system used a tank-in-tank heat exchanger, which could not be modeled in TRNSYS, so alternatively a constant-effectiveness heat exchanger with an effectiveness of 1 was used.

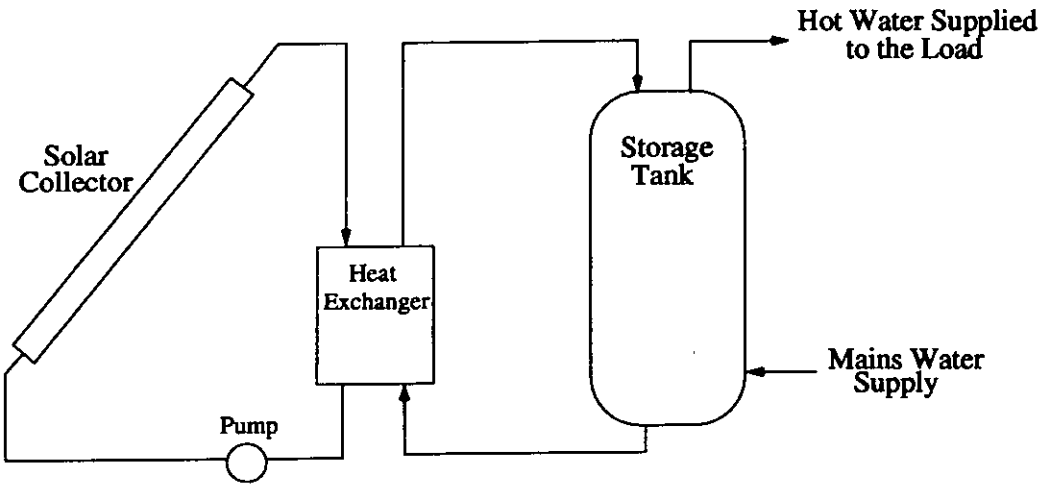

Figure 1. Schematic diagram of the "closed loop" solar domestic hot water system simulated in this study

These give:

$$A_C^* = A_C F_R(\alpha\tau) = 2.56 \text{ m}^2, \text{ and } u_C^* = F_R U_L / F_R(\alpha\tau) = 6.59 \text{ W/m}^2 \quad (1)$$

S_C was unknown and was not estimated.

The storage tank is described by the parameters U_S, the store loss coefficient, a measure of energy losses to the ambient; C_S, the store capacitance, which measures the heat capacity of the tank; and D_L, the draw-off mixing coefficient, which describes the amount of mixing in the tank during hot water draws. These parameters are dependent on the materials of the tank and the properties of the water it contains.

The store loss coefficient was set at a constant value of $U_S = 1.5$ W/K, a typical value for a water storage tank. The tank volume was 0.208 m^3. C_S, the store capacitance, was approximated by mC_p, the mass of water in the tank multiplied by the specific heat of water. The density is assumed to be 1000 kg/m^3, and C_p is assumed to be 4.19 kJ/kg K. The resulting value for C_S is then 0.863 MJ/K. D_L was unknown, but because of the nature of the tank used for the simulation, it was estimated to be much less than 1.

3. SIMULATION RESULTS

3.1. Part 1: Long Term Prediction based on Outdoor Testing

One of the claims of the Dynamic Model is that short term outdoor tests can be used for successful parameter estimation and long term performance prediction. To investigate this claim, tests were run in TRNSYS using Typical Meteorological Year (TMY) weather data for Madison, Wisconsin to simulate outdoor testing, and then the ability of the model to predict long term performance based on "outdoor" testing was examined. Summer (June and July) and winter (December and January) were considered. The parameter estimation program was run with the TRNSYS data for each season and then with data from both seasons together. These three sets of parameters were then used to model system operation for summer and winter.

The results, figure 2, show that winter performance was predicted well by the parameters fitted to winter data, and summer performance was predicted well by the parameters fitted to summer data. However, when winter parameters were used to predict summer performance, or summer parameters to predict winter performance, results were much less successful. Prediction for either season from parameters estimated using both summer and winter data was more successful.

These results support the conclusions presented in Part A of the DSTG Final Report regarding the selection of a test period and the relationship to the Solar Load Ratio, SLR which is defined as the ratio of daily irradiance striking the collector surface to the daily hot water load. Figure 3 shows calculated values of SLR for Madison. It is apparent from these results that the range of SLR's covered differs significantly from the summer period to the winter period. Consequently, parameters determined from data for a particular season may not predict the performance of the system during a different season.

These results illustrate the significance of choosing appropriate test sequences and ensuring that a suitable range of solar irradiance and load conditions are covered. The consequence of this result is that test periods covering differing seasons may be required if annual simulations are required. Alternatively, an effort must be taken to ensure that a representative range of conditions are contained in the test sequence.

3.2. Part 2: Development of a Short Term Test Sequence

As described, Part 2 of this study consisted of the evaluation of a series of very short test sequences of approximately five days length. The intention was to develop an optimum test sequence that could be conducted in an indoor test facility using the general methods described in reference 1.

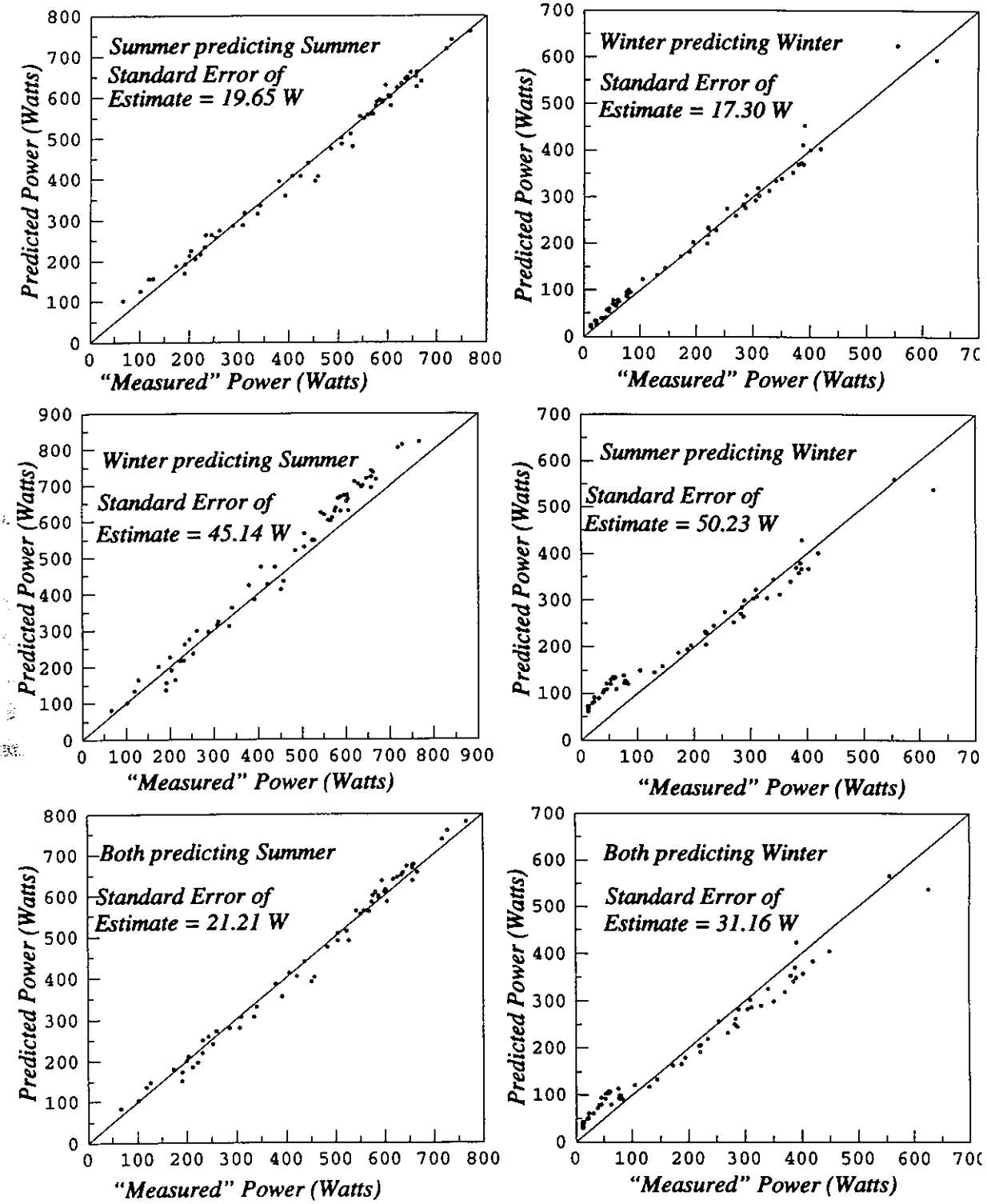

Figure 2. Predicted versus "measured" average daily power output for Madison. Values shown are for parameters predicted from simulated outdoor test periods.

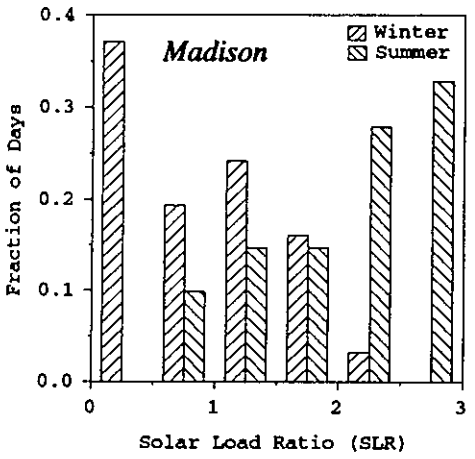

Figure 3. Values of Solar Load Ratio, SLR, calculated based on TMY weather data and a 300 L/day hot water draw at 55°C.

Initially, the test sequences were judged based on their ability to predict the system parameters. The actual parameters were known or calculated from inputs to the TRNSYS simulation. Initially ten test sequences were run. Based on what was perceived as their shortcomings in both the long and short term evaluations, another fifteen were considered. To get a good estimate, the program was started several times with different initial guesses of the parameters. The test sequence which most closely estimated the parameters was Short 9, with constant irradiance and a hot water charge at the beginning of the sequence. The smallest objective function was realized with Short 16. Some of the estimated parameters are listed in Table 1.

Another important basis for the evaluation of the test sequences is how well they predict long term performance.

Table 1: Some of the estimated parameters from the short test sequences

Test #	AC* (m2)	UC* W/m2K	US W/K	CS (MJ/K)	KL (-)	SC (-)	C (W)
3	2.2721	2.8312	1.5306	0.9139	0.0052	0.0964	15.761
8	2.3911	6.295	1.4355	0.8432	0.0155	0.2504	13.835
9	2.5621	6.6543	1.3420	0.8431	0.0189	0.2604	15.391
16	2.4230	5.5497	1.1660	0.8803	0.0027	0.1928	4.5398
21	2.2081	2.2826	1.1006	0.9085	0.0000	0.1093	18.482
22	2.1976	2.0612	1.0172	0.9312	0.0000	0.0981	23.963
†	2.56	6.6	1.5	0.863	-	-	-

† TRNSYS parameters

3.3. Long Term Prediction based on Short Test Sequences

The parameters from each of the short term tests were used in the dynamic model with weather data for the summer and winter periods for Madison, WI, as in the outdoor tests. In this case, the best results were not obtained with the best parameter fit, or with the smallest objective function. The best long term prediction for Madison was Short 22, figure 4, with constant irradiance, and with the days ordered to avoid the high temperature charge at the beginning of the test sequence.

To further evaluate this test sequence, TRNSYS was used to simulate the system's performance in other locations with different climates. The two cities used were Albuquerque, NM and Seattle, WA. Albuquerque has high temperatures and irradiation all year, and Seattle, which is similar to Madison in the summer, has very low irradiation and moderate temperatures in the winter. The same two-month periods of TMY weather data were used in these locations as were used for Madison. In Albuquerque it can be seen that at the very high output powers the system performance was over-predicted in the summer, but in the winter performance was accurately modelled.

The results for Seattle are better than those for Albuquerque in the summer, but not as good the results for the other times and locations, Figure 5. Some insight into these results can be obtained by referring to figure 6 where Solar Load Ratios are plotted for the three cities studied. It

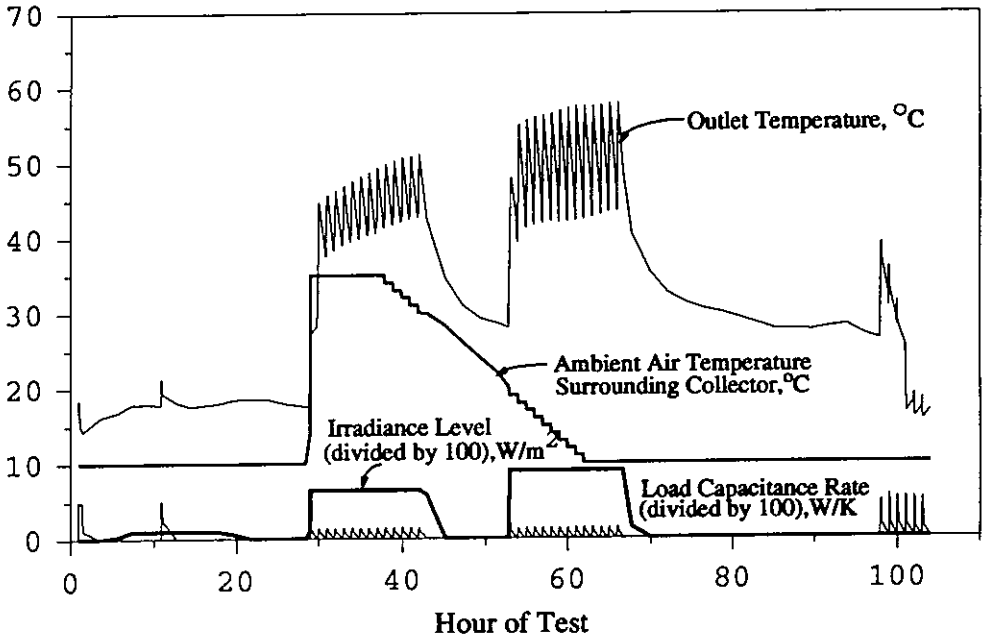

Figure 4. Plot of test sequence and results for the short 22 test.

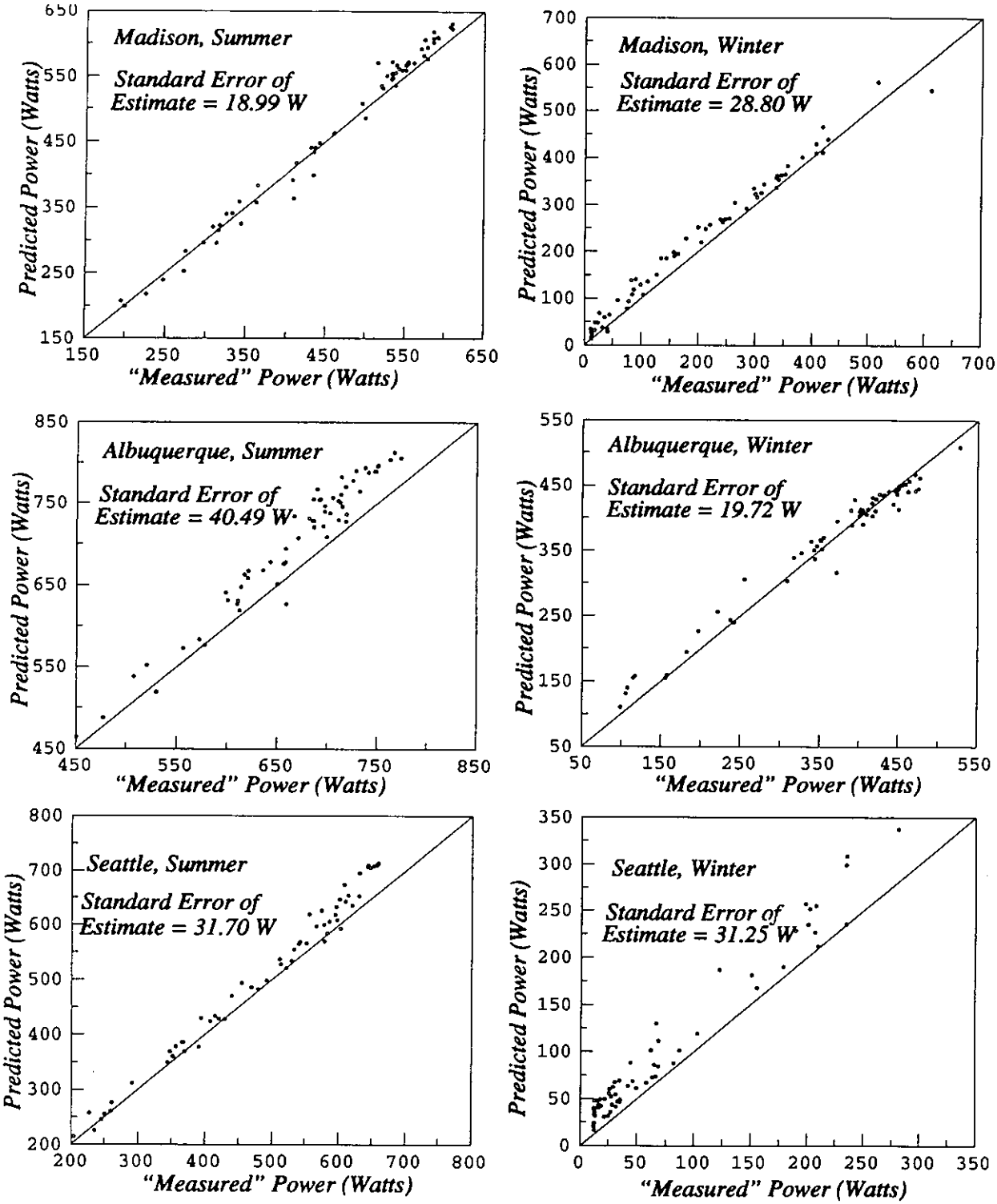

Figure 5. "Measured" versus predicted output power for three cities. Predicted form parameters fit to test sequence Short 22.

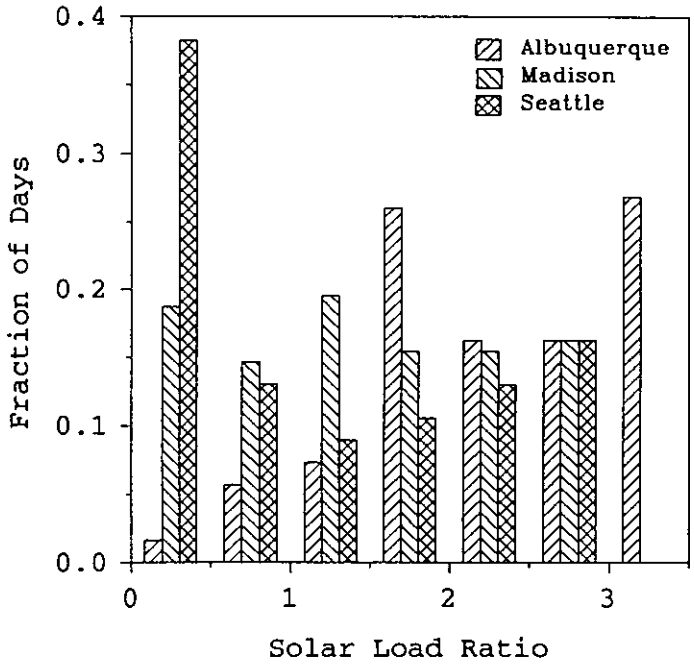

Figure 6. Values of Solar Load Ratio calculated from TMY weather data as determined for the three locations studied.

is apparent from this plot that Seattle is heavily biased toward the low SLR's while Albuquerque and Madison are more evenly distributed. Short 22 has one test day with a SLR of zero and the balance of the test days above 3. It is likely that the introduction of more test days with low SLR's into short 22 would produce better results.

4. EXPERIMENTAL TESTS

To evaluate the practicality of performing a shorted test sequence similar to that described above, a series of experimental tests were conducted using a commercial SDHW system similar to that previously described. The tests were conducted using an experimental apparatus as described in reference 1 with the solar input being provided by a collector loop heater. The test sequence consisted of a 103 hour test period starting with three days at constant irradiance levels of 100, 650, and 900 W/m^2 applied for 14 hours each. The test sequence ended with a fourth no-solar day. Day 1 had a single 50 L draw, and day 2 and 3 had distributed draws of 20 L for each of the 14 hour periods, Figure 4. Typical results obtained from this test are given in table 2.

Table 2: Experimentally Determined Performance Parameters (Short 22)

	AC* (m2)	UC* W/m2K	US W/K	CS (MJ/K)	KL (-)	SC (-)	C (W)
Expected	2.08	7.4	1	0.73	0.1	1	
Measured	1.78	8.24	5.88	1.06	0.09	0.41	11.8

5. CONCLUSION

The best short term test sequence, in terms of long term performance, is Short 22. However, modelled output is higher than the simulated "measured" output at high powers. This was a consistent problem throughout the series of simulations. One of the changes that was made to the later test sequences was to raise the irradiation so that parameters could be fit to conditions producing these very high outputs. This does not appear to have had any effect on the modelled system output. This suggests that perhaps there is a problem in the model itself that leads to such an error.

The best short term test, in terms of parameter predictions, is Short 9. This is based on the assumption that the TRNSYS parameters are correct for this model as well. This should be a good assumption, as the dynamic model is similar to TRNSYS. It should be noted that in the second series of tests, almost all of the test sequences produced fair approximations to the actual parameters. But the three candidates for the best long term performance were actually poor estimates of the actual parameters. This may again suggest that there is a problem in the model, or it may indicate that, due to the nature of the solution of the model, and the fact that all the parameters are estimated together, the assumption that the TRNSYS parameters are correct is not sound. However, the frequency of the appearance of parameters similar to the TRNSYS ones tends to shed some doubt on the latter idea.

It has been seen that it is indeed possible to get good long term performance from the information in a very short test sequence. Preliminary experimental tests indicate that a test sequence can be applied and realistic parameter values identified. Careful attention to the values of the SLR may provide a means to further develop an improved short term test sequence.

6. ACKNOWLEDGEMENTS

The assistance of Mr. Paul Makuch in the set up of the experiments and with the preparation of this document is greatly appreciated.

7. REFERENCES

1. ASHRAE 95-1986, Methods of Testing to Determine Thermal Performance of Packaged Solar Domestic Hot Water heating systems, ASHRAE, New York, N.Y.

2. W. Spirkl; Dynamic SDHW Testing; University of Munich; Journal of Solar Energy Engineering, Transactions of the ASME, 112:98-101.

3. S.A. Klein et al; TRNSYS: A Transient System Simulation Program; Solar Energy Laboratory, Madison, Wisconsin; 1983.

4. W. Spirkl; Dynamic SDHW System Testing Program Manual, (Version 1.11); Ludwig

INVESTIGATIONS ON OPTIMAL TEST DESIGN

Wolfgang Spirkl and Stefan Endres

Ludwig-Maximilians-Universität München
Sektion Physik
Amalienstr. 54
D-8000 München, FRG

1 Introduction

In the frame of a diploma thesis [1], the problem of test sequence optimization was treated. The investigation was based on computer simulations as well as on experiments with a system described in [2].

The main issues of this work are:

- Definition of a function – called the goodness function – describing the amount of information resulting of a measurement.
- Analysis of ways how to compute this function – either in simulation, before the measurement or after the measurement.
- Optimization of test sequences in order to minimize the goodness function.

2 The Goodness Function

The goodness function G is intended to measure the mean prediction error for different measurements with a certain test strategy $\mathcal{T}$. One example for a test strategy is the german DIN proposal [3].

The mean value to compute G is taken over different measurements (and its associated errors), different systems and (at least for outdoor measurements) for different weather conditions.

The prediction is made for a reference sequence containing very different operating conditions; the error is measured by the (unnormalized) objective function defined in the DST method. The reference sequence is designed such that its objective function C is a reasonable measure of the long term mean prediction error averaged over different test reference years.

$$G(\mathcal{T}) = \mathrm{E}_{\{test,weather,system\}}\left[C(\mathbf{p}(\mathcal{T}), ref)\right], \tag{1}$$

where $\mathrm{E}_{\{a,b,\ldots\}}\left[f(a,b,\ldots)\right]$ denotes the expectation value averaged over different values of a, b, ..., $\mathbf{p}(\mathcal{T})$ is the parameter set obtained from the test, and $C(\cdot, ref)$ is the DFIT objective function.

3 Analysis of Ways to Compute the Goodness Function

3.1 Linearization

In the following we refer to the mathematical description in [4] and [5]. Linearizing the objective function in Eq. (1) with regard to **p** yields:

$$G(\mathcal{T}) = G_0 + \mathbf{V}(\mathcal{T})\,\mathbf{H}(ref). \tag{2}$$

Here, **H** is the second derivative of the objective function using a linearized model, i.e. **H** is the Hessian matrix in a linearized theory. It was found that this linearization is a very close approximation of Eq. (1). Hence, the calculation of G may be reduced to the calculation of the covariance matrix **V**.

Using further linearization and an expression simplified compared to [4], **V** is approximated by:

$$\mathbf{V} = \mathrm{E}\left[G_1\,\mathbf{H}(\mathcal{T})^{-1}\right]. \tag{3}$$

Hence, G may be expressed by $G_0(ref)$, the minimum error obtainable with the model for the given reference sequence, $G_1(ref)$, the combined measurement and model error resulting from the test fit, $\mathbf{H}(\mathcal{T})$, the Hessian matrix associated with the test sequence, and $\mathbf{H}(ref)$, the Hessian matrix associated with the reference sequence:

$$G(\mathcal{T}) = G_0 + \mathbf{H}(ref)\,\mathrm{E}_{\{test,weather,system\}}\left[G_1\,\mathbf{H}(\mathcal{T})^{-1}\right]. \tag{4}$$

Like the unnormalized objective function C, the quantities G, G_0 and G_1 are Integrated Quadratic Filtered (IQF) errors, with physical unit $\mathrm{W^2s}$.

The main uncertainty of G – especially for the case of little data – comes from the estimation of the covarianc matrix **V** of the parameters using Eq. (3).

3.2 Estimation *Before* the Measurement

For *off line* optimization of test strategies, a method to calculate G for different test strategies before the individual measurement is required. The results indicate, that G can be computed before the measurement, if a reasonable value of G_1 is available. The Hessian $\mathbf{H}(\mathcal{T})$ may be taken from a simulation of a system similar to the system under test.

3.3 Estimation *During* the Measurement

During the measurement, there might arise the wish to decide on how to proceed the measurement (e.g. with which load) and on when to end it. The next step in a test should be taken such as to decrease G as much as possible. If G is below a certain threshold, the measurement might be stopped.

As the measurements proceeds, the quantities G_1 and $\mathbf{H}(\mathcal{T})$ become more reliable, and hence the estimation of G.

3.4 Estimation *After* the Measurement

There is no principal difference to the estimation procedure above. Endres finds that after a reasonable measurement the estimated value of G is a reliable measure for the information content gained from the test and hence for the prediction error.

4 Optimization of Test Strategies

Finding the optimum test strategy means finding the test strategy $\mathcal{T}$ minimizing G. In the present work [1], a genetic algorithm was used to optimize the test strategy. First results indicate that this procedure might significantly improve test designs. It seems possible to find optimal test strategies for certain conditions, e.g. for a national standard taking into account the class of systems used and the local climate.

5 Conclusions

An important result is, that G can be separated in two factors, the Hessian $\mathbf{H}(ref)$ and the covariance matrix $\mathbf{V}$, and that $\mathbf{V}$ can also be separated in two factors, one describing the variation of the input variables (the Hessian matrix $\mathbf{H}(\mathcal{T})$), and one (G_1) summarizing the measurement errors and model errors. However, large variations generally increase G_1.

Another promising result is, that the special choice of the reference sequence has not too much influence on the result.

There are at least two potential applications of the concept of the goodness function: At first, it could be a figure of merit function for finding an optimal test design $\mathcal{T}$ minimizing $G(\mathcal{T})$, e.g. for finding an optimal test sequence for indoor testing. At second, it might be a criterion for finding an adequate termination time and effective test continuation for outdoor testing, especially for in-situ testing.

6 Nomenclature

Symbol	Units	Meaning
$\mathrm{E}_{\{x\}}[f(x)]$		Expectation value of $f(x)$ averaged over x
G	[W^{2}s]	Goodness Function corresponding to a test sequence $\mathcal{T}$
$\mathbf{H}$		Hessian Matrix
$\mathbf{p}$		Parameter set
$\mathcal{T}$		Test Strategy
$\mathbf{V}$		Covariance Matrix; $V_{ij} = \mathrm{E}[(p_i - \mathrm{E}[p_i])(p_j - \mathrm{E}[p_j]]$

7 References

[1] S. Endres. *Führung von Experimenten zur Ertragsvorhersage für Solaranlagen.* Diplomarbeit, LMU München, 1991.

[2] J. Muschaweck. Dynamic Fitting on Outdoor Data from a Mid-Size SDHW System with Internal Auxiliary Heater. 1991. Contribution to the DSTG Report.

[3] Draft for a standard for testing SDHW systems. May 1990, DIN, Deutsches Institut für Normung, Postfach 1107, D-1000 Berlin 30, FRG.

[4] W. Spirkl. Dynamic SDHW Testing Program Manual (Version 1.18). University of Munich (LMU), FRG, 1991. Available from DIN, E. Memmert, Postfach 1107, D-1000 Berlin 30, FRG.

[5] W. Spirkl. Dynamic SDHW Testing. *J. of Solar Energy Eng., Transactions of the ASME*, **112**:98–101, 1990.

INTEGRATED SOLAR DOMESTIC HOT WATER SYSTEM TEST PROCEDURE – HARDWARE AND SOFTWARE RECOMMENDATIONS

J. Muschaweck

Ludwig-Maximilians-Universität München
Sektion Physik
Amalienstr. 54
D-8000 München, FRG

1 Hardware recommendations

A set of instruments and sensors suitable for solar domestic hot water (SDHW) system testing has been compiled at the Ludwig-Maximilians-University Munich. When the instruments were selected, cost effective solutions that do not increase measurement errors were preferred.

SDHW system testing makes specific demands on instruments and sensors. The recommended set of instruments and sensors meets these demands, has been or is being tested at the Ludwig-Maximilians-University and complies with the specifications of the german draft standard [1].

At current prices, the total cost for the instruments compiled here will be around 18,000 US-$, where the basic equipment, extension for measuring a second thermal power and calibration equipment will cost around 12,000 US-$, 2,500 US-$ and 3,500 US-$, respectively.

In the sequel the recommended instruments and sensors are described briefly.

Irradiance: Standard class 1 pyranometer.

Collector ambient temperature: Fan cooled, double shielded RTD thermometer.

Store ambient temperature: Standard RTD room thermometer.

Wind speed: Cup anemometer.

Fluid temperature: Very small four wire Pt100 RTD in stainless steel tube; fluid mixing device.

Volume flow: Piston ring flow meter or magnetic-inductive flow meter with electrical pulse output.

Electrical power: Commercial electricity meter with electrical pulse output.

Computer: IBM-compatible PC-AT.

Resistance and Voltage: Commercial $6\frac{1}{2}$ digit digital multimeter with IEEE bus interface and scanner.

Digital I/O: Digital output and counter card to be plugged into PC; with pulse debounce circuitry, external galvanic decoupling and external semiconductor relays.

Drawoff control: Commercial solenoid valve controlled by digital I/O card.

A detailed description of this set of instruments, their properties and a list of suppliers is available from the Ludwig-Maximilians-University, Munich.

2 Software recommendations

For the recommended set of instruments, a test version of a data acquisition program (`SDHWTEST 0.1`) is available from the Ludwig-Maximilians-University, Munich, which performs control and measurement for testing solar domestic hot water (SDHW) systems according to the requirements of the german draft standard [1].

In addition to collecting and recording the data from the sensors, `SDHWTEST 0.1`

- performs all necessary calculations,
- produces data files which can be read directly by the DST program package, and
- controls the drawoff by opening and closing valves automatically according to a pattern specified by the user.

If instruments and/or sensors are to be used that differ from the recommendations, a different data acquisition program must be used, or `SDHWTEST 0.1`, which is available in source code, must be adapted.

3 On Measuring the Thermal Energy Drawn From a Hot Water Store

In this section,

- A definition of the *thermal power* P_L drawn from a hot water store is given. It is shown that other definitions may yield an error of several percent.
- A formula is given which makes possible the calculation of P_L from easily measurable quantities.
- The measurement of those quantities and the associated errors are discussed.
- Some important recommendations for testing solar domestic hot water (SDHW) systems result:
  - The pressure conditions in the store during the measurements must comply with the manufacturer's instructions.
  - The thermal time constant of the temperature sensors can lead to large errors and must be taken into account.

3.1 The Problem

Before measuring the thermal power or energy drawn from a hot water store a *definition* of that power or energy must be given and it must be clear how to measure the quantities necessary for the calculation.

The problems that arise in defining this energy result from the temporal shift between the entry of cold water into the store, the heating of this water and the exit of hot water. In detail the following questions need to be answered:

- The volume and mass flow rates at inlet and outlet are different because of the thermal expansion of water. Which flow rate is relevant?
- When the cold water temperature does not remain constant, the notion of *exergy of the store* loses its meaning, and the question rises, *at what time* the cold water temperature T_{in} entering an equation for instantaneous system power should be measured. Which consequences result?

When considering an ideal demand heater without losses, capacity and volume, these questions do not arise. Therefore such an ideal demand heater is used as a simple reference case in the following.

3.2 Definition of the Energy Q_{L} delivered by the store

A drawoff in the interval $I = [t_0, t_1]$ is considered. At the inlet there is a mass flow rate $\dot{m}_{\mathrm{in}}(t)$, the inlet temperature is $T_{\mathrm{in}}(t)$ and the water density is $\varrho(T_{\mathrm{in}})$. At the outlet there are the anologous quantities $\dot{m}_{\mathrm{out}}$, T_{out} and $\varrho(T_{\mathrm{out}})$.

The power $P_D(t)$ delivered by an ideal demand heater is the product of a mass flow rate times the energy necessary to heat one mass unit from inlet temperature T_{in} to outlet temperature T_{out}:

$$P_D(t) = \dot{m}(t)\Big[h\Big(T_{\mathrm{out}}(t)\Big) - h\Big(T_{\mathrm{in}}(t)\Big)\Big] \tag{1}$$

Here the mass flow rate through the demand heater is called $\dot{m}$, and h denotes the the mass specific enthalpy of water. In this demand heater case holds $\dot{m}_{\mathrm{in}} = \dot{m}_{\mathrm{out}}$.

Eqn. 1 is equivalent to

$$P_D(t) = \dot{m}(t)\overline{c_p}(T_{\mathrm{in}}, T_{\mathrm{out}})(T_{\mathrm{out}} - T_{\mathrm{in}}) \tag{2}$$

Here $\overline{c_p}(T_{\mathrm{in}},T_{\mathrm{out}})$ denotes the specific heat of water averaged over the temperature interval $[T_{\mathrm{in}}, T_{\mathrm{out}}]$.

The power P_{L} or energy Q_{L} delivered by a hot water store must be calculated in a similar manner. But the water entering the store remains there for a while, it is then heated (in general) and it is drawn off later. Therefore it must be defined more clearly what is meant by $\dot{m}, T_{\mathrm{in}}$ and T_{out}.

It is stressed that $\dot{m}_{\mathrm{in}}$ and $\dot{m}_{\mathrm{out}}$ are in general *not* equal (nor are $\dot{V}_{\mathrm{in}}$ and $\dot{V}_{\mathrm{out}}$); on the contrary, these quantities may differ up to several percent due to thermal expansion of store *and* water.

The user has water of temperature T_{in} at his disposal and consumes water of temperature T_{out} with a mass flow rate $\dot{m}_{\mathrm{out}}$. The energy $\mathrm{d}Q$ delivered by the store in the time interval $\mathrm{d}t$ is now *defined* as the energy an ideal demand heater would need to heat water with mass $\mathrm{d}m_{\mathrm{out}}$ from T_{in} to T_{out}:

$$\mathrm{d}Q = \overline{c_p}(T_{\mathrm{in}}, T_{\mathrm{out}})(T_{\mathrm{out}} - T_{\mathrm{in}})\mathrm{d}m_{\mathrm{out}} \tag{3}$$

This is consistent with the observation that the user is mainly interested in the amount and temperature of water that flows from his tap. The minimum amount of energy needed and the amount of water fed into the store is a consequence of his hot water demand and the current cold water temperature.

The amount of heat Q_L drawn off in an interval I results as

$$Q_L = \int_I \dot{m}_{out} \overline{c_p}(T_{in}, T_{out})(T_{out} - T_{in}) dt \tag{4}$$

The problem is now: measure $\dot{m}_{out}$, T_{in} and T_{out} with sufficient accuracy and time resolution to calculate Q_L with a certain maximum error ΔQ_L.

Here it is assumed that Q_L should be evaluated with an error of less than two percent.

3.3 Measurement of the Mass Flow Rate $\dot{m}_{out}$

In general it is not possible to measure $\dot{m}_{out}$ directly, because the customary flow meters are volume flow meters. Moreover, it is not a good idea to measure the volume flow at the outlet, because the temperature (and density) in the flow meter is different from the point where the outlet temperature is measured; additionally there may be problems with calcification etc.. The flow rate measurement therefore yields $\dot{V}_{in}$ instead of $\dot{m}_{out}$, in general.

To calculate $\dot{m}_{out}$ from $\dot{V}_{in}$ the store has to be considered in more detail. The store shall have the volume V_S, which depends on the temperature distribution inside the tank. V_S is assumed to change by dV_S during the time interval dt due to thermal expansion of the store material. Then holds:

$$dV_{in} = dV_{out} + dV_S \tag{5}$$

It is assumed that V_S depends approximately linearly on the mean temperature inside the store,

$$V_S \approx (1 + 3\alpha\overline{\theta_S})V_S^0 \tag{6}$$

where α denotes the linear expansion coefficient of the store material. Then the volume change dV_S is given by

$$dV_S = 3\alpha\, d\overline{\theta_S} V_S^0 \approx 3\alpha(T_{out} - T_{in}) dV_{in} \tag{7}$$

Now the mass dm_{out} drawn from the store can be calculated:

$$dm_{out} = \varrho(T_{out}) dV_{in}\Big(1 - 3\alpha(T_{out} - T_{in})\Big) \tag{8}$$

The energy Q_L drawn from the store can now be calculated from the easily measurable quantities $\dot{V}_{in}$, T_{in} and T_{out}:

$$Q_L = \underbrace{\int_I \underbrace{\varrho(T_{out})\dot{V}_{in}\Big(1 - 3\alpha(T_{out} - T_{in})\Big)}_{\dot{m}_{out}} \overline{c_p}(T_{in}, T_{out})(T_{out} - T_{in})\, dt}_{\dot{C}_L} \tag{9}$$

Here $\dot{C}_L$ denotes the thermal capacitance rate that is used by the DST method [2] as input variable.

It is assumed that the pressure of the cold water inlet remains constant during the test.

3.4 Physical Meaning of Eqn. 9

The energy Q_L calculated from Eqn. 9 is the same an ideal demand heater would need to generate the same amount of hot water with the same temperature. The difference between Q_L and the energy input from the sun and/or an auxiliary heater must be attributed to

- heat losses to the store environment,
- energy carryover in the store,
- and mass carryover in the store.

The third item shall be considered in more detail:

The values of the density of water and the expansion coefficient of the store material at $T_{out} = 60\,°C$ and $T_{in} = 10\,°C$ show that the volume of a stainless steel tank[1] changes by approx. 0.3% and the density of water changes by 1.7%. Therefore, the volume change of the store can be neglected, but the density change makes it necessary to calculate the drawoff mass as outlined above.

In general, $\dot{m}_{in} \neq \dot{m}_{out}$ holds during drawoff. The difference is compensated during the heating of the store. When operating in no pressure mode (drawoff valve at the inlet), hot water will drip out of the outlet. When heating the store under pressure, cold water at the bottom will be pushed back into the inlet pipe. If there is a non-return valve, a pressure balance device should be installed which holds the excess water during the heating of the store.

Yet another effect can influence the gain of a SDHW system negatively when it is operated in no pressure mode: the (pressure dependent) forming of bubbles on the surface of an immersed heat exchanger, especially between the fins. It is concluded that SDHW systems must be tested with the pressure conditions recommended by the manufacturer; a no pressure test of a normally pressurized system can lead to an underestimation of the solar fraction of several percent.

The temporal behaviour of the inlet temperature should also be considered. Normally, the inlet temperature will be almost constant. Large changes during the test would mean testing under unrealistic conditions. Moreover, energy could be gained from this temperature change, and the notion of store exergy would lose its meaning. Therefore, the inlet temperature should remain as constant as possible during each coherent system test sequence. This also means, that the inlet pipe should be rinsed for a few minutes before each drawoff with an extra valve.

Also, because of the different mass flow rates at inlet and outlet the ideal demand heater model is not really applicable: there would be a delay of several percent between the

[1] $\alpha = 2 \cdot 10^{-5} K^{-1}$

inlet temperature as function of time and drawoff volume, respectively. When the inlet temperature is constant, this problem does not arise.

3.5 Measuring the Inlet and Outlet Temperature

Here several error sources can be distinguished and must be considered:

1. Common mode errors of T_{in} and T_{out} at constant temperatures.
2. Errors of $(T_{\text{out}} - T_{\text{in}})$ at constant temperatures.
3. Errors of changing temperatures due to thermal inertia of sensors and the flow time of water in the pipes.

Ad 1.: Common mode errors enter the density and heat capacity in Eqn. 9. A consideration of the listed values of these quantities shows that even a common mode error of 10 K yields only an error of 1 % in Q_{L}. Therefore, a common mode error of 1 K can be tolerated.

Ad 2.: Q_{L} is approximately linear in $(T_{\text{out}} - T_{\text{in}})$; therefore the error in temperature measurements should be no greater than 0.1 K.

Ad 3.: The error sources considered up to now are errors of the power P_{L} and do not depend on the temporal behaviour of P_{L}. On the other hand, the errors due to thermal inertia appear only when P_{L} is changing, and they do *not* average out but lead to an underestimation of Q_{L}, in general.

Let us assume that at time t_0 both sensors are at the same temperature. (e.g. store ambient temperature), that the store is fully mixed and now a drawoff with constant mass flow rate $\dot{m}_{\text{out}}$ begins and lasts until t_1, when the drawoff ends. If the sensors have a time constant τ, then the resulting error in Q_{L} is:

$$\frac{\Delta Q_{\text{L}}}{Q_{\text{L}}} \approx -\frac{\tau}{t_1 - t_0} \tag{10}$$

The following recommendations for system testing result:

- The sensors should have low thermal inertia; their time constant should be less than 1 % of an average drawoff time. This can be reached through using thermocouples or small RTD's and avoiding unnecessarily short drawoff intervals (less than 5 minutes).
- The sensors should be mounted close to the tank to avoid long delays in the pipes and to obtain thermal contact between sensors and store.
- If possible, each drawoff should be started with e.g. 30 s of drawoff with reduced flow rate to reduce the power at those times when the error of the temperatures is large.

3.6 Hints for numerical calculation of Q_{L} and $\dot{C}_L$

Because of the fast variation of T_{out} during drawoff Q_{L} and $\dot{C}_L$ should be calculated by the data acquisition system using the instantaneous values of temperatures and flow rate.

It is necessary to be able to calculate $\varrho(T_{\text{out}})$ and $\overline{c_p}(T_{\text{in}}, T_{\text{out}})$ easily from T_{in} and T_{out}. To calculate these quantities quadratic polynomials are sufficient to reach an accuracy of 10^{-3} in the range between 0 °C and 100 °C. The following formulas have been obtained through linear regression from values listed in [3]:

$$\varrho(\theta) = \left(1000.67 - 7.3845 \cdot 10^{-2}\,°\text{C}^{-1}\theta - 3.547 \cdot 10^{-3}\,°\text{C}^{-2}\theta^2\right)\frac{\text{kg}}{\text{m}^3} + \Delta\varrho; \qquad (11)$$

$$|\Delta\varrho| < 0,8\,\frac{\text{kg}}{\text{m}^3} \qquad |\Delta\varrho| < 0,5\,\frac{\text{kg}}{\text{m}^3} \text{ for } \theta > 3\,°\text{C}$$

$$\begin{aligned}\overline{c_p}(T_{\text{in}}, T_{\text{out}}) \;=\; & \Big(4.20028 - 5.048 \cdot 10^{-4}\,°\text{C}^{-1}(\theta_1 + \theta_2) \\ & + 4.097 \cdot 10^{-6}\,°\text{C}^{-2}\Big((\theta_1 + \theta_2)^2 - \theta_1\theta_2\Big)\Big)\frac{\text{kJ}}{\text{kg K}} \qquad (12)\end{aligned}$$

The right side of Eqn. 12 has been cast into a form yielding a minimum number of multiplications.

4 References

[1] Draft for a standard for testing SDHW systems. May 1990, DIN, Deutsches Institut für Normung, Postfach 1107, D-1000 Berlin 30, FRG.

[2] W. Spirkl. Dynamic SDHW Testing Program Manual (Version 1.14). University of Munich (LMU), FRG, 1990.

[3] Robert C. Weast, editor. *Handbook of Chemistry and Physics.* CRC Press, Boca Raton, Florida, 60th edition, 1980.

DYNAMIC FITTING ON OUTDOOR DATA FROM A MID-SIZE SDHW SYSTEM WITH INTERNAL AUXILIARY HEATER

J. Muschaweck

Ludwig-Maximilians-Universität München
Sektion Physik
Amalienstr. 54
D-8000 München, FRG

1 Summary

In the fall of 1988, a SDHW system assembled from commercially available components has been tested at the collector test facility of the Ludwigs-Maximilians-Universität, Munich, Germany. The system (6 m^2 collector area, 300 l store volume, immersed electrical auxiliary heater) is sized for a single family house. During four test sequences, the system has been subjected to different load profiles and different auxiliary set temperatures. Parameters are determined for different combinations of test sequences to assess the validity of the plug flow model for this system; system performance is predicted for the test sequences not used for parameter identification to assess the DST method's predictive capability.

The validity of the plug flow model is confirmed. Performance prediction errors range from 2 % to 10 %. It is found that prediction errors tend to be smaller when the test data show sufficient variability to encompass the system states to be predicted.

2 Experimental Setup

The system is located on the collector test roof of the University of Munich. The store is contained in a small hut on the roof adjacent to the collector array. All sensors are connected to a data acquisition system in the building below.

The piping and the electrical connections are depicted in Fig. 1. The system consists of a store with immersed collector loop heat exchanger and immersed electric auxiliary heater, a collector array and a controller for the collector pump and the auxiliary heater. The system specifications are compiled in Table 1.

For controlling the auxiliary heater, the top store temperature is measured and compared with an adjustable set temperature. A differential on-off controller with adjustable hysteresis is used for the collector loop.

3 Results and Conclusions

For parameter identification and performance prediction, the plug flow model with six parameters (collector area A_C^*, collector losses u_C^*, store capacity C_S, store losses U_S,

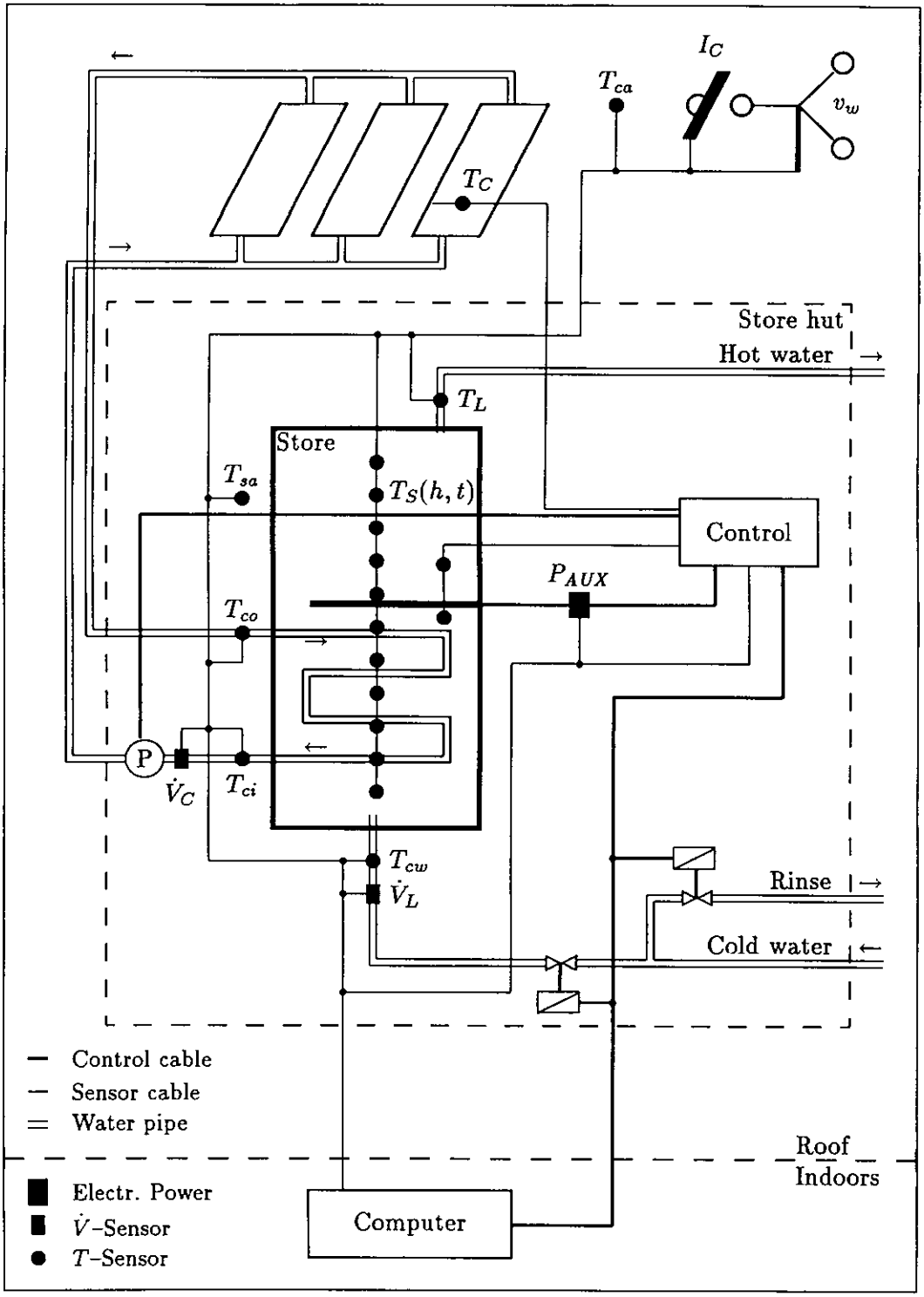

Figure 1: Piping and sensor locations.

Manufacturer:	Viessmann, D–3559 Allendorf/Eder.
Collector:	Type Acredal-s, non concentrating flat plate collector with black aluminum absorber and double glazing.
Area:	$6\,m^2$ (three modules with $2\,m^2$ each).
Optical properties:	$(\alpha\tau)_0 \approx 0.8$ (for vertical irradiation).
Orientation:	45° south.
Heat exchanger:	Immersed stainless steel tube in the lower part of the store.
Surface area:	$1.8\,m^2$.
Store:	Vertical stainless steel cylinder.
Volume:	300 l.
Insulation:	10 cm soft foam.
Auxiliary :	Electrical resistance heater with 4.5 kW, heats approx. 125 l or 40 % of the store.

Table 1: System specifications according to the manufacturer.

auxiliary fraction f_{AUX} and cold water mixing constant D_L) is used. This model is denoted $\mathcal{M}$. Additionally, for one test sequence where wind speed data are available, the wind speed dependence of the collector losses (parameter u_v) is modelled. This model is denoted $\mathcal{M}_w$. In the sequel, the modelling errors and the connections between test data quality and prediction accuracy are assessed.

Data sets are measured for four separate sequences. These sequences, called $\mathcal{S}_1 \ldots \mathcal{S}_4$ differ in load profile and in the auxiliary set temperature (see Table 2).

	Time	T_{set}	Load profile		
			morning	noon	evening
$\mathcal{S}_1$	6.10. – 16.10.88	45 °C	100 l	100 l	100 l
$\mathcal{S}_2$	18.10. – 31.10.88	45 °C	50 l	50 l	100 l
$\mathcal{S}_3$	3.11. – 14.11.88	60 °C	100 l	—	—
$\mathcal{S}_4$	14.11. – 21.11.88	—	—	150 l	150 l

Table 2: The data sets $\mathcal{S}_1 \ldots \mathcal{S}_4$ used for system analysis are characterized by different load profiles and weather conditions.

The first two sequences simulate an average user behaviour. In $\mathcal{S}_3$, the auxiliary set temperature T_{set} and the load flow rate $\dot{C}_L$ are chosen to produce high losses and thus low solar gain, whereas $\mathcal{S}_4$ pursues the opposite: the auxiliary heater is turned off completely, while water heated by the collector loop is drawn off as soon as possible.

3.1 Identification of System Parameters

To determine the parameters for the system models $\mathcal{M}$ and $\mathcal{M}_w$, at first only data from sequence $\mathcal{S}_1$ are used. The low pass filter time constant is set to $\tau = 24\,\mathrm{h}$. Therefore, the value of the objective function $c(\hat{\mathbf{p}})$ approximates the modelling error for daily average system power.

The parameter identification results are compiled in Table 3.

Parameter		Model $\mathcal{M}$	Model $\mathcal{M}_w$
A_C^*	$[\mathrm{m}^2]$	3.27 ± 0.17	3.48 ± 0.06
u_C^*	$[\mathrm{WK}^{-1}\mathrm{m}^{-2}]$	6.67 ± 0.94	6.68 ± 0.31
u_v	$[\mathrm{WsK}^{-1}\mathrm{m}^{-3}]$	0	0.59 ± 0.05
U_S	$[\mathrm{WK}^{-1}]$	6.32 ± 0.80	5.38 ± 0.30
C_S	$[\mathrm{MJK}^{-1}]$	1.17 ± 0.05	1.15 ± 0.01
f_{AUX}	[—]	0.40 ± 0.04	0.44 ± 0.01
D_L	[—]	0.01 ± 0.03	0.00 ± 0.01
$c(\hat{\mathbf{p}})$	[W]	8.2	3.2

Table 3: Results of parameter identification using data set $\mathcal{S}_1$

3.1.1 Interpretation of the Results

1. The parameters are consistent with the specifications of the manufacturer:
   - The effective collector area A_C^* corresponds e.g. to an absorption-transmission product of 0.75 and a heat removal factor of 0.75.
   - The value found for C_S is equal to the heat capacity of 280 l of water, which agrees very well with the specification of 300 l considering the "dead zone" below the heat exchanger coil.
   - The auxiliary fraction f_{AUX} is determined as about 110 l, while being specified as 125 l.
2. The wind speed dependence of the system gain is significant. The parameter u_v can easily be determined, since its standard error is quite small. The introduction of this parameter reduces the modelling error for this sequence by more than one half as well as the standard errors of the remaining parameters. For this data set, the modelling error of $\mathcal{M}$ is mainly due to the wind speed influence on the collector losses.

3. Compared to the average system output power of about 400 W, the modelling error even for model $\mathcal{M}$ is found to be of the same order of magnitude as the measurement error for thermal powers.

3.2 Short Term System Gain Prediction

Accurate long term performance prediction for arbitrary conditions is the goal of the DST method. Here, the prediction accuracy can only be checked for sequences of several weeks. However, from different combinations of the test sequences described in Table 2 the influence of test data quality on performance accuracy can be determined.

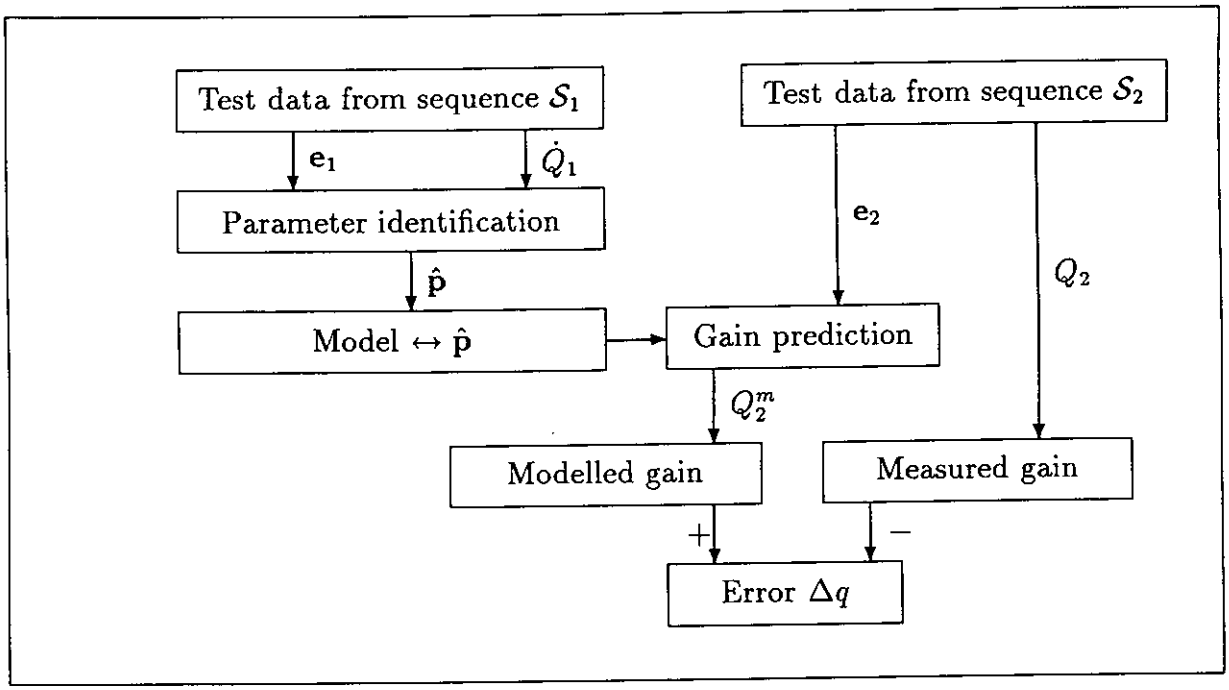

Figure 2: The consideration of different data sets yields conclusions about the accuracy of system gain prediction. In the figure, the parameters gained from test sequence $\mathcal{S}_1$ are used to predict the performance for sequence $\mathcal{S}_2$.

The procedure to perform an experimental check of the prediction accuracy is shown in Fig. 2:

1. From data measured in sequence $\mathcal{S}_1$, parameters $\hat{\mathbf{p}}$ are determined which are optimal for *this* sequence.
2. The measured system gain Q_2 is determined for sequence $\mathcal{S}_2$.
3. The modelled system gain Q_2^m is computed using the input data $\mathbf{e}_2$ from sequence $\mathcal{S}_2$ and the already determined parameters $\hat{\mathbf{p}}$.

4. The resulting relative error

$$\Delta q = \frac{Q_2 - Q_2^m}{Q_2^m}$$

is used as a measure of the prediction error.

Since wind speed data were not available for all sequences, only model $\mathcal{M}$ is used in the sequel.

The measured gain Q_i and the modelled gain Q_i^m,

$$Q_i = \int_{\mathcal{S}_i} \dot{C}_L(T_L - T_{cw})\,dt \qquad Q_i^m = \int_{\mathcal{S}_i} \dot{C}_L(T_S|_{h=1} - T_{cw})\,dt$$

is the thermal energy delivered by the system.

At first, the gain for sequences $\mathcal{S}_2$, $\mathcal{S}_3$ and $\mathcal{S}_4$ is predicted using the parameters determined from sequence $\mathcal{S}_1$ and compared with the respective measured gain. The following values result:

	$\mathcal{S}_2$	$\mathcal{S}_3$	$\mathcal{S}_4$
Q_i^m [MJ]	300	200	40
δq_i	−4 %	−10 %	−10 %

The test conditions for sequence $\mathcal{S}_1$ were similar to $\mathcal{S}_2$, and quite different from $\mathcal{S}_3$ and $\mathcal{S}_4$. The higher relative prediction error for $\mathcal{S}_3$ and $\mathcal{S}_4$ is attributed to this.

- From a ten day sequence with not very variable conditions, it is possible to determine parameters which describe the gain for this system to within a few percent for almost arbitrary conditions.

It is presumed that the remaining prediction error is partly due to a lack of input data variability. In this case, it should be possible to find parameter values that describe sequence $\mathcal{S}_1$ almost equally well while yielding smaller prediction errors for different conditions.

Proceeding as follows, it was attempted to find such parameter values:

1. Parameters are determined which are *simultaneously* optimal for three sequences. This is done for all four possible combinations of sequences.
2. Using these parameter values, the system gain for the respective remaining sequence is predicted.

The resulting values are compiled in Table 4.

Considering that the conditions for sequences $\mathcal{S}_1$ and $\mathcal{S}_2$ were quite similar and that $\mathcal{S}_3$ and $\mathcal{S}_4$ represent extreme conditions, it can be concluded that

Parameters from:	Pred. for:	Q_i [MJ]	δq_i
$\mathcal{S}_1$+$\mathcal{S}_2$+$\mathcal{S}_3$	$\mathcal{S}_4$	40	−10 %
$\mathcal{S}_1$+$\mathcal{S}_2$+$\mathcal{S}_4$	$\mathcal{S}_3$	200	−7 %
$\mathcal{S}_1$+$\mathcal{S}_3$+$\mathcal{S}_4$	$\mathcal{S}_2$	300	+2 %
$\mathcal{S}_2$+$\mathcal{S}_3$+$\mathcal{S}_4$	$\mathcal{S}_1$	250	+2 %

Table 4: Gain prediction errors for different variability of the available input data.

- correct performance prediction will be more likely if the variation of the input data used for testing encompasses the range of conditions for which the performance shall be predicted.

The parameter values which were determined from $\mathcal{S}_1$ only are compared with values that result from using all four sequences (see Table 5). This comparison shows the result of a lack of variability in this case.

Parameter		$\mathcal{S}_1$	$\mathcal{S}_1 \ldots \mathcal{S}_4$
A_C^*	[m^2]	3.27 ± 0.17	3.48 ± 0.10
u_C^*	[WK^{-1}m^{-2}]	6.67 ± 0.94	10.5 ± 0.65
U_S	[WK^{-1}]	6.32 ± 0.80	3.85 ± 0.24
C_S	[MJK^{-1}]	1.17 ± 0.05	1.13 ± 0.02
f_{AUX}	[—]	0.40 ± 0.04	0.47 ± 0.02
D_L	[—]	0.01 ± 0.03	0.03 ± 0.01
$c(\hat{\mathbf{p}})$	[W]	8.2	8.5

Table 5: Parameter identification results from scarce (left) and rich (right) measured data.

Except for the loss coefficients u_C^* and U_S, the parameter values remain almost unchanged. But the distribution of the system losses on collector loop and store changes drastically, when a rich data base is used. From the high value of $r_{23} = -0.79$ for the correlation coefficient of these parameters, it is concluded that the DST method cannot discern well between collector and store losses from $\mathcal{S}_1$ data only. Only sufficient variability of the input data allows correct loss distribution.

The value of the objective function $c(\hat{\mathbf{p}})$ and the performance prediction results show that,

using optimal parameters, the plug flow model describes the daily system gain to within a few percent for a wide range of input data, particularly auxiliary set temperatures and load profiles.

3.3 Assessment of Store Model Validity

The plug flow model makes assumptions on the generation and degradation of stratification which can be checked using experimental data.

For this system, the collector loop does not generate stratification: the immersed heat exchanger heats the bottom part of the store, and natural convection transports heat from the bottom to higher parts of the store. Here, the drawoff is the only mechanism leading to stratification.

However, this generation of stratification is not perfect, as can be seen in Fig. 3. Here, the store is heated to approx. 60 °C during a day of high irradiation and then depleted completely. The inlet and outlet temperatures T_{cw} and T_L are plotted in Fig. 3

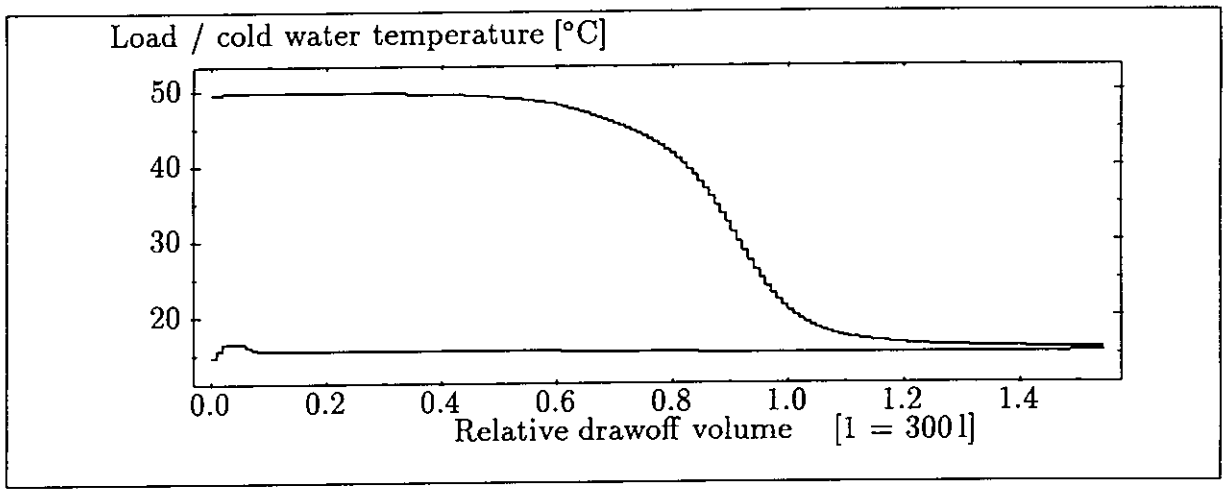

Figure 3: The drawoff temperature curves for depletion of a hot store show the influence of cold water mixing.

For an ideal cold water inlet, a rectangular step response would be expected (neglecting heat conduction). The drop of T_L from $C_L \approx 0.6\,C_S$ on is partly due to the "dead zone" below the heat exchanger. However, the slow approximation of T_L to T_{cw} for $C_L > C_S$ is due to eddy generation at the cold water inlet.

This effect is described by the plug flow model using an additional parameter, the diffusion constant D_L. However, for the data considered here this effect is not very significant, since it is found that $D_L \approx 0$.

4 Nomenclature

Symbol	Unit	Meaning
A_C^*	m^2	Effective collector area
$c(\hat{\mathbf{p}})$	W	Minimum value of objective function
$\dot{C}_L$	WK^{-1}	Load capacitance rate
C_S	MJK^{-1}	Store capacity
Δq		Relative system gain prediction error
D_L		Cold water mixing parameter describing stratification degradation
f_{AUX}		Auxiliary fraction of the store
$\mathcal{M}$		System model without wind speed dependent losses
$\mathcal{M}_w$		System model with wind speed dependent losses
Q_n	MJ	Measured system gain for sequence $\mathcal{S}_n$
Q_n^m	MJ	Modelled system gain for sequence $\mathcal{S}_n$
$\mathcal{S}_n$		n^{th} test sequence
T_{cw}	K	Cold water temperature at store inlet
T_L	K	Load temperature (= store outlet temperature)
T_{set}	K	Auxiliary set temperature
u_C^*	$WK^{-1}m^{-2}$	Effective collector loss coefficient
U_S	WK^{-1}	Store loss coefficient
u_v	$WK^{-1}m^{-3}s$	Parameter describing wind speed dependent collector losses

EXPERIMENTAL INVESTIGATIONS OF SHORT TERM TESTSEQUENCE FOR OUTDOOR TESTING OF SOLAR DOMESTIC HOT WATER SYSTEMS

J. E. Nielsen, A. V. Souproun
Solar Energy Laboratory
Danish Technological Institute
P.O. Box 141
DK-2630 Taastrup
Denmark

1. GENERAL

1.1 Purpose

The purpose of this work is an experimental validation of the short term sequence for outdoor measurements of solar domestic hot water (DHW) systems. Influence of weather conditions on results of the system parameter estimation is also investigated in the present paper.

1.2 Test sequence description

In order to get a sufficient accuracy in estimation of values for the solar DHW system parameters in a short time, the following 3 days sequence was proposed with the load flow rate as given in figure 1. Due to such drawoff profile, each day of this test sequence becomes suitable for estimation of some of the system parameters. And finally, 3 days test sequence can give a good possibility for dynamic fitting of the whole solar DHW system.

Load flowrate should be $0.83\ 10^{-5}$ - $1.67\ 10^{-5}$ m^3/s (0.5-1.0 litres/min) per square

meter of collector's aperture area to achieve good accuracy in both temperature difference and flowrate measurements.

Timetable for drawoffs during 3 days test sequence:

First day:

Single continuous drawoff from 1 am till 18 pm (for preconditioning of the system at the beginning of the test and for keeping collector at low temperatures during a day for better estimation of its area).

Second day:

Four small drawoffs of 50 litres each, at 10, 12, 14 and 16 o'clock.

Third day:

One small drawoff in the morning at 8 am and one large drawoff in the evening (in order to remove all the heated water from the store at the end of test) from 18 till 23 pm.

Figure 1 represents grafic interpretation of load profile for proposed test sequence with the duration of three days.

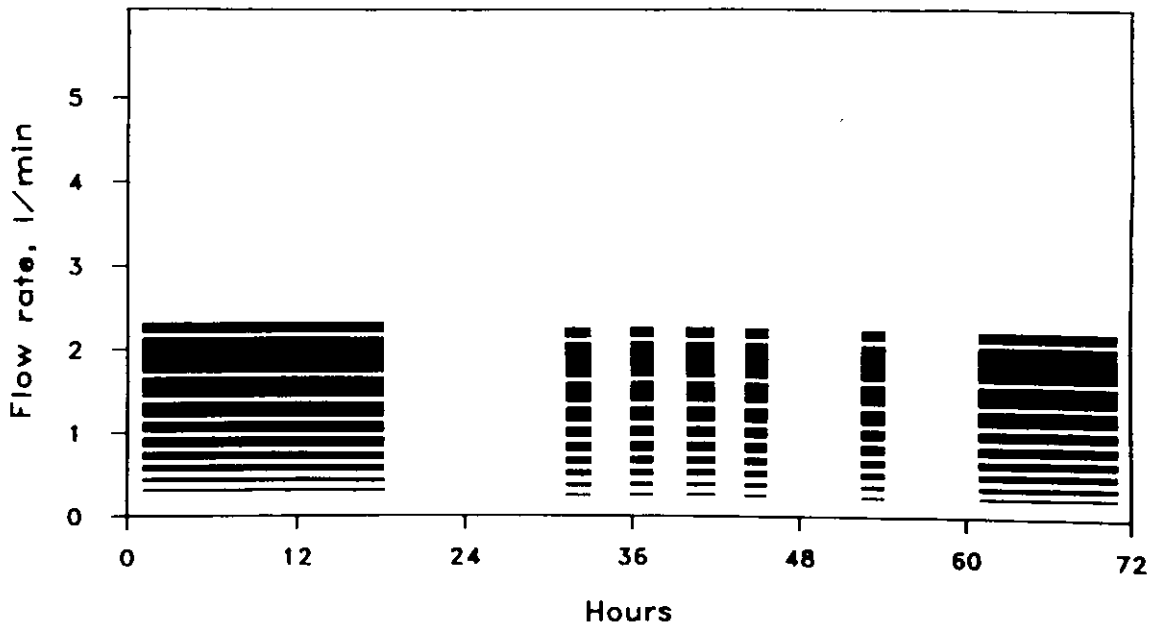

Figure 1: Three days test sequence for dynamic fitting of the solar DHW system.

1.3 Data aquisition system

Data aquisition system consists of IBM personal computer connected to a datalogger. All the channels are scanned every 20 seconds and are stored as 2 minutes mean values on the computer disk. The temperature sensors used are of Pt100 type with an accuracy of 0.1 °C, the flow meters are of the magnetic type with an accuracy of 2%. Measurements of solar irradiance were carried out with a help of Eppley pyranometers separately for diffuse and total radiation. The datalogger is able to control relays for openning and closing of the water valves accordingly to the desired load profile.

1.4 System description

Two different indirect solar DHW systems of remote storage type were measured at the same time and some results of their comparison are presented herein.
Solar collectors of the both systems were mounted on a south-facing roof of the laboratory test building with a slope of 45°. No shading objects were in the neighbourhood of the test building. Stores for the hot water were located vertically in the laboratory room and were connected to the solar collectors by well insulated pipes. During the drawoffs, water in the stores of each system has being replacing by new portion of cold water from the supply system, where it was maintained at constant level of the temperature (around 11 °C).
First system uses a storage tank of the 325 litres volume, which has been provided with the heat exchanger located near the bottom of the store. It has two flat plate collectors with a selective surface on the pipe ribs (sunstrip type) and total aperture area of 4.32 m^2.
Second system comprises one hot water tank (265 liters) with a mantle type heat exchanger for the solar collector loop. The store was supplied with the auxiliary heater and control unit for switching the heater off when certain temperature level in the water tank is reached. Solar collector of this system is a plastic collector consisting of a long hose of a black polypropylene in the insulated box, covered with

a double sheet of polycarbonate with 3.84 m^2 in aperture area. Such a collector works with a relatively low flow rate, resulting in a large difference between inlet and outlet temperatures, and in developing a stratified temperature distribution in the hot water tank.
Both systems are commercially available in Denmark.

1.5 Test method

The dynamic method [1] of the solar DHW system testing, which has been developed at the Ludwig-Maximilians-University (Munich), was used in this work for estimation of the system parameters as well as for short- and long term predictions.
Fitting of the system parameters was carried out with a help of version 1.16, and external collector model was implemented for investigation of the solar collectors in the present work.
The model for wind speed dependence of the collectors was excluded from the program run, since the use of this option is still under discussion.

2. EXPERIMENTAL RESULTS

2.1 Influence of the solar radiation level

In order to estimate correct values of the system parameters, long data series with wide range of weather conditions and load variations are preferable. But it rises a question of selection of the experimental data, because some of them may be insufficient for investigation of the solar DHW systems. First of all, it concerns the solar irradiance level. If the level is too low, calculation may result in some obviously false parameter values, because the fitting procedure needs certain variations of energy transfer.
Dependence of the solar irradiance level on the parameter values was investigated

for the solar collector of the system 1, and some results of such investigation are presented in this paper. Since the solar collectors are the most sensitive to the variations of the solar irradiance among other parts of the solar DHW system, the external model (only for solar collector) was used in the program batch in order to determine the lower admissible level of the solar irradiance during the measurements.

Seven different data series were taken for the same solar collector, and these series differed from each other only by weather conditions. Thus, average value of the solar irradiance in these tests varied from approximately 40 till 200 W/m^2. The results of parameter estimation are plotted in figures 2 and 3. Expected values for this solar collector are given in appendix.

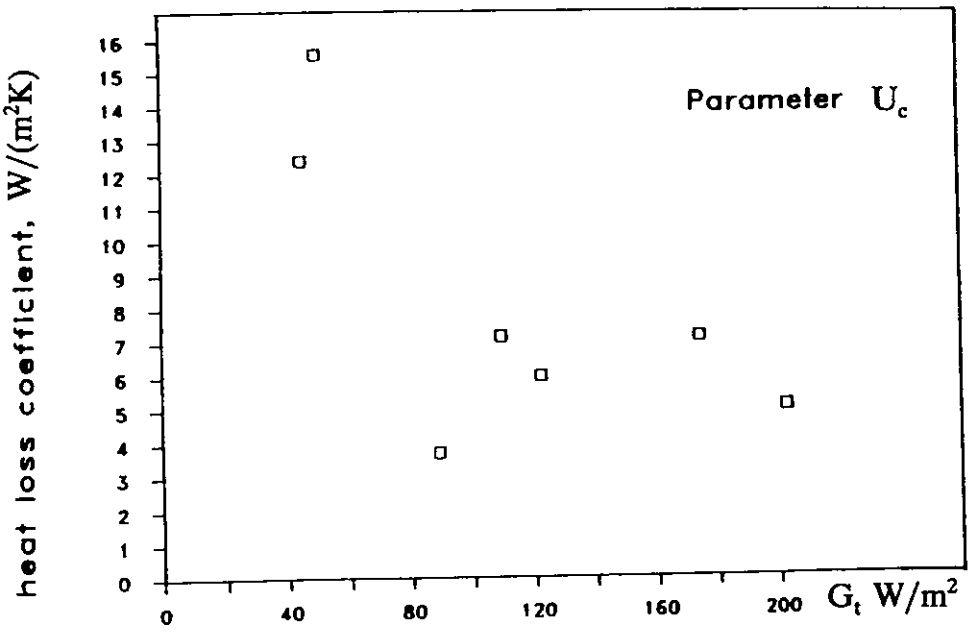

Figure 2: Estimated values of heat loss coefficient for different levels of solar irradiance during the measurements.

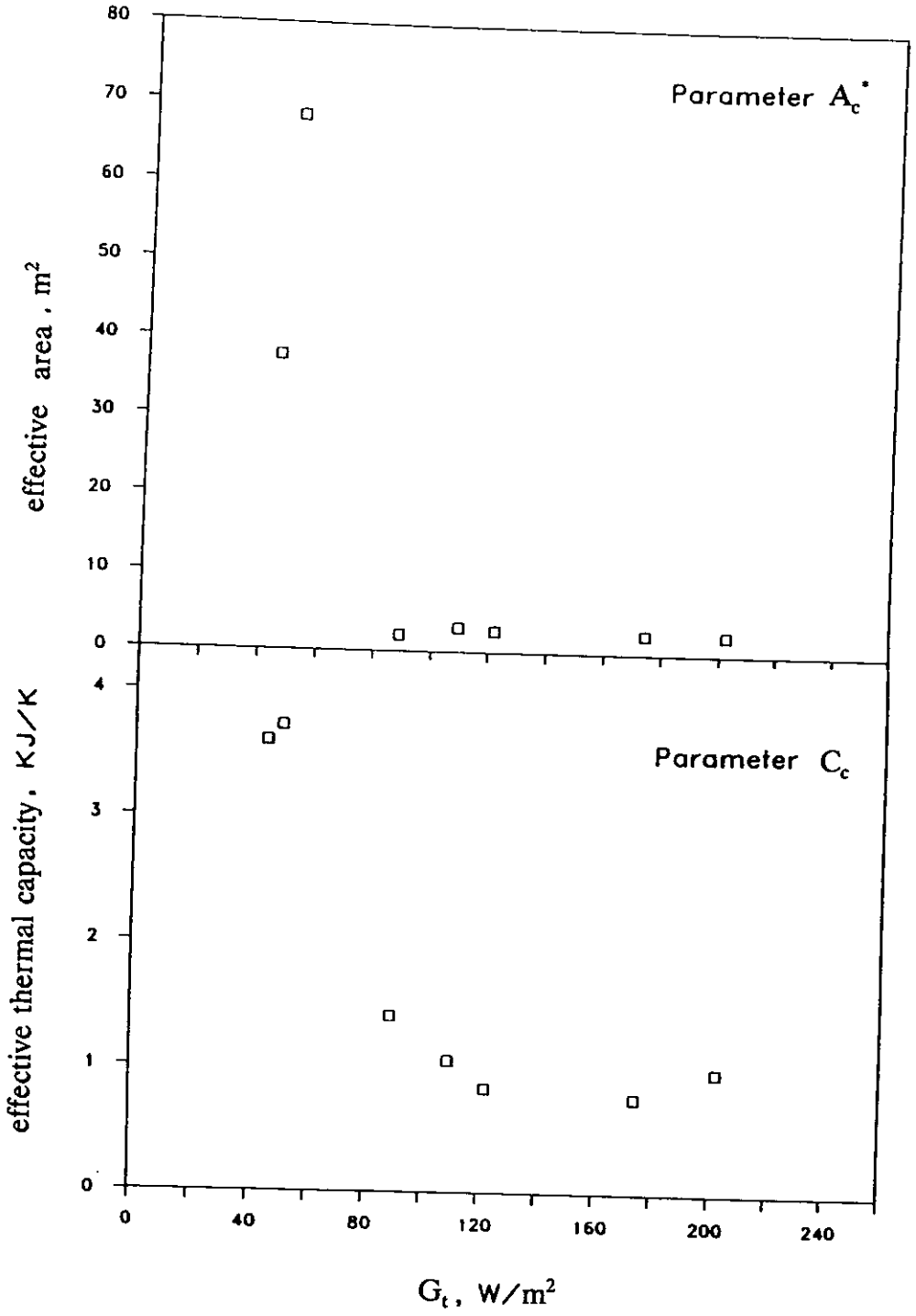

Figure 3: System parameters versus average solar irradiance during the 3 days test.

It is evident that at the levels less than 100 W/m^2 of averaged solar irradiance during the test, values of collector parameters, obtained by DST-method, became totally erroneous for the solar collector tested. As it naturally influences on predicted energy output from the whole solar DHW system, such weather conditions cannot be used for short term outdoor tests with duration of several days only.

2.2 Long term prediction for the Danish Test Reference Year

The annual prediction was made for the both solar DHW systems described above. Solar radiation data from the danish Test Reference Year has been corrected due to the incidence angle modifier. Results of long term prediction for these systems are presented in the table 1.

Table 1: Long term prediction for the typical danish weather.

Characteristics	System 1	System 2
Cold water temperature, °C	10	10
Demanded temperature, °C	45	45
Daily load volume, litres	200	200
Simulation time, days	365	365
Mean solar irradiance, W/m^2	119	119
Ambient temperature, °C	7.94	7.94
Room temperature, °C	20	20
Number of test days	15	12
Energy gain, W	210	178
Fractional system gain	0.618	0.524
Auxiliary consumption	0	0
Effective collector area, m^2	1.76	1.49
Mean load temp. difference, °C	21.6	18.3

From this table it can be seen that the system 1 provides better energy output under the same weather and load conditions. This can be explained by taking into consideration the fact, that the system 1 has bigger and better collector, which indeed

increases solar input to the store. Results presented in this paper show that this dynamic test method [1] can be successfully used for comparison between energy outputs of different solar DHW systems.

It was found out that days with bad weather conditions may lead to unacceptable uncertainces in final results. Such an influence of the weather conditions on the parameter values can be suppressed to a certain level by increasing the duration of outdoor tests. On the other hand, prolongation of the measurements converts them into an expensive and timeconsuming procedure. Because of this, the following investigation was made. Different durations of the measurements (with the proposed 3 days sequences) were used for the assessment of deviation in long term predicting results. Number of days which have been used for carrying out the measurements varied from 3 up to 15.

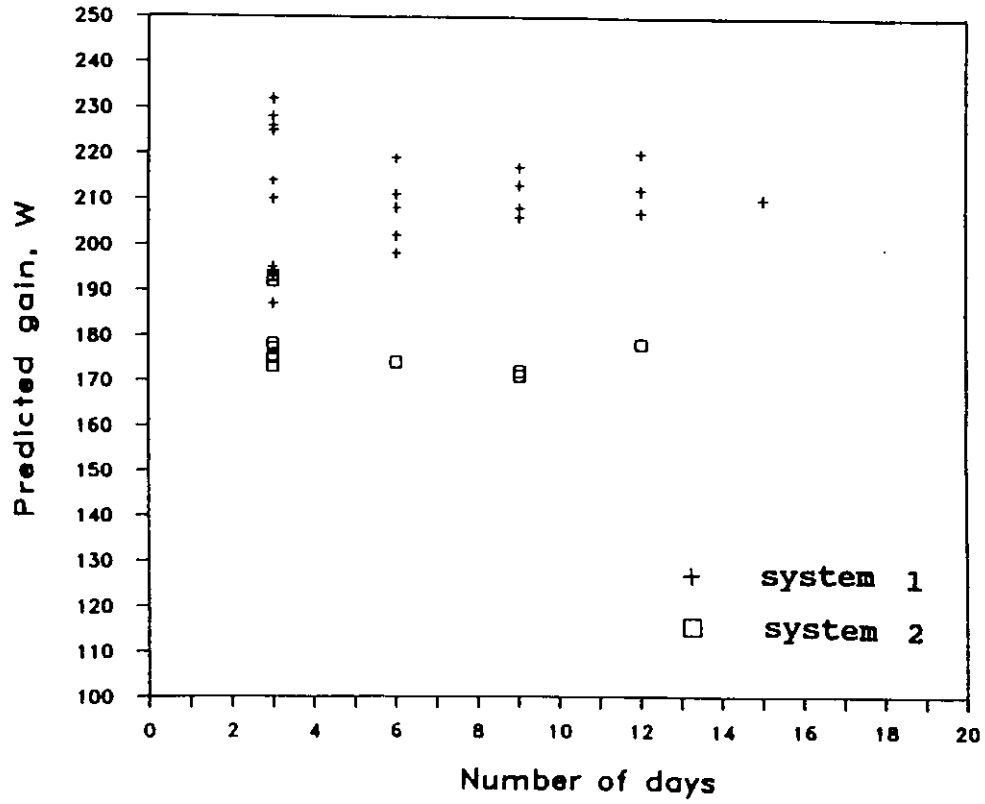

Figure 4: Long term prediction for the both systems based on the measurements of different duration.

These data, plotted in figure 4, show that for 3 days outdoor test on the solar DHW system the deviation of the predicted energy gain is within 11%, while 6 days tests reduce such range to 6%, which may be assumed suitable enough for the systems tested. An analysis of system annual energy gain was made in order to create recommendations for improvement of accuracy of the such prediction. Certain selection of weather conditions may reduce errors in the predicted system output. Thus, deviations in long term prediction may be less then 4% when using only 3 days (with the proposed load profile) of more than 220 W/m^2 in the mean solar irradiance. It was found, that the same accuracy can be provided by using 6 days with the mean solar irradiance of more than 180 W/m^2.

2.3 Results of short term prediction

Prediction of the system energy gain for several tests was made for the system 1. Each test sequence consists of 3 days with the proposed drawoff profile. Measured values of the mean solar irradiance and output energy gain of the system 1 for each test is given in table 2. Table 3 includes results of prediction of the system energy output based on the parameters, which have been estimated from different tests. Comparison between predicted and measured values of the system output can be made based on the data presented in tables 2 and 3, and it is evident, that results of energy prediction are much more closed to the measured values if the same test was used for both the parameter estimation and short term prediction procedures. Table 4 includes parameter values, which have been estimated for the system 1 from different outdoor tests. Expected values of the parameters for the system 1 are: A_s=3.0 m^2, U_c^*=6.0 W m^{-2} K^{-1}, U_s=3.0 W K^{-1}, C_s=1.36 MJ K^{-1}. One can see, that some of the estimated parameters have values which differ from the expected values, but, nevertheless, even such short time tests can give more or less sufficient results in prediction the behaviour of the whole system.

Table 2: Measured values of the mean solar irradiance and energy gain for the

system 1.

Test number (3 days sequence with proposed load profile)	Mean solar irradiance, W/m^2	Measured energy gain, W
1	184.0	478
2	267.3	730
3	97.5	207
4	140.8	420

Table 3: Predicted energy gain based on the system parameters from the different tests.

Test number for energy prediction	Tests used for the parameter estimation				
	1	2	3	4	1+2+3+4
1	476±5.5	469±2.7	398±5.1	452±1.6	478±6.2
2	696±7.7	748±8.7	580±7.8	687±3.4	715±8.3
3	254±3.6	272±0.42	212±3.0	250±1.4	261±4.5
4	378±7.8	476±14	308±5.12	416±3.7	422±8.9

It means, that parameters obtained from the dynamic fitting of the solar DHW systems can not be used separately and only a combination of all the system parameters may present full enough information for prediction of the system output energy under different weather conditions. It is important to note, that change in the operation conditions will influence on the system energy gain, and first of all it concerns annual prediction. So, in order to compare two different solar DHW systems one should use the same load profile for each system tested, and with no doubts, load profile which looks like real user's hot water consumption, is

preferable.

Table 4: Estimated parameter's values for the system 1.

System parameters	Units	Test nr 1	Test nr 2	Test nr 3	Test nr 4	Test nr 1+2+3+4
Effective collector area	m^2	2.441	3.078	2.039	2.653	2.671
Collector heat loss coefficient	$W/(m^2K)$	0.761	10.953	0.215	5.067	3.033
Store loss coefficient	W/K	1.321	2.293	0.438	5.581	6.125
Store thermal capacity	MJ/K	1.472	1.343	0.934	1.273	1.368

The rightside column of the table 4 represents values of the system parameters, which have been obtained by using 12 days with proposed load profile, in the other words, four different tests. These parameters are capable to predict energy output of the solar DHW system with a better accuracy, than the parameters from only 3 days test (see table 3), despite that fact, that the values of such parameters are also sofisticated and they are far away from real figures for the system tested. The only exeption is for the test with low level of the mean solar irradiance (test nr 3), for which prediction is might be much more difficult due to the reduced system heat exchange during these days. It was noticed, that influence of weather conditions (first of all, mean solar irradiance during the test) on the results of parameter fitting and short term prediction is reducing with increasing of the test duration, so it is up to user to decide how many test sequences should be used, depending on the weather conditions. But, our own experience prompts that duration of 6 or 9 days will be good enough for the european countries with a moderate climate, and further improvement of accuracy can not be achieved by increasing testing time.

2.4 Solar load ratio

Since solar load ratio (SLR) was considered to be a usefull characteristic, which could give information about system tests quality, it was implemented with a purpose to show the difference between the test sequences with the proposed load profile (see fig.1) and common used daily load of 200 litres (with four drawoffs of 50 litres in each at 10, 12, 14 and 16 o'clock, accordingly). Frequency of hour values for the system 1 versus decimal logarithm of the solar load ratio was plotted in figure 5.

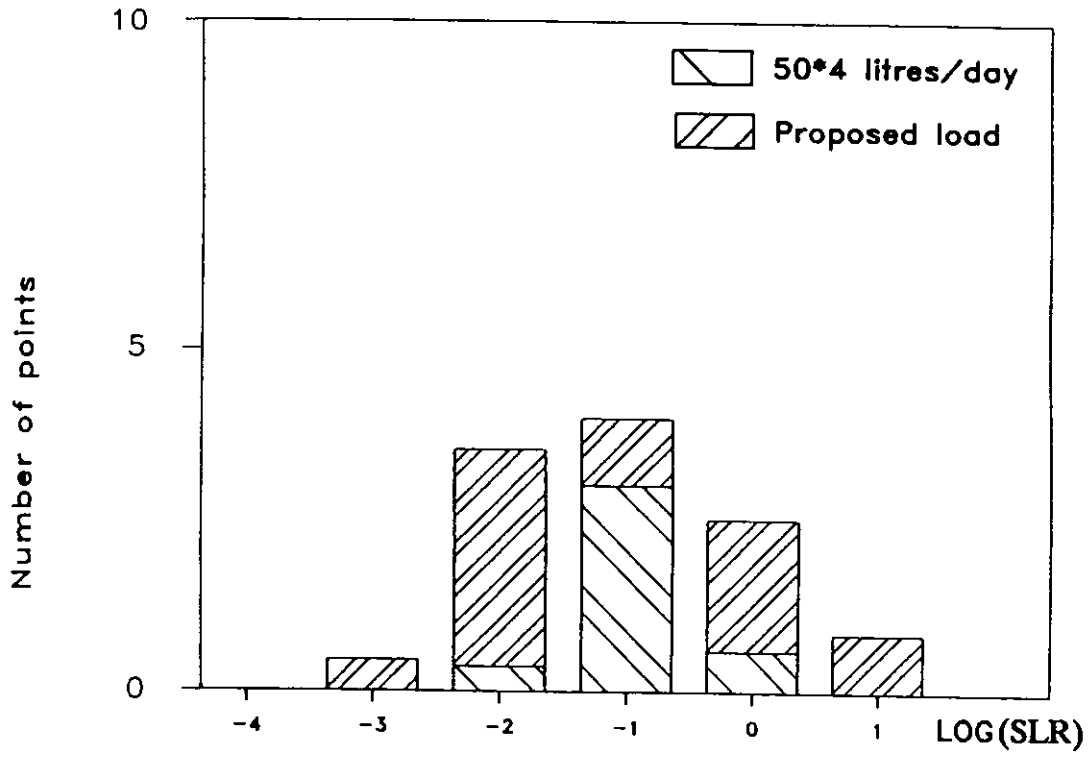

Figure 5: Distribution of the measured points during 3 days test used for the parameter estimation.

It can be easily seen from the fig.5, that proposed load profile for the three days

test sequence gives much more experimental points for the parameter estimation. The distribution of these points is also better even for the same weather conditions, because in a case of the proposed test sequence they cover the whole possible range of values for real solar DHW system.

3. CONCLUSIONS

Short term measurements with duration of only several days may be recommended for dynamic fitting of parameters for solar DHW systems. Proposed drawoff profile for three days test sequence gives enough information about system for prediction its behaviour to another weather conditions with sufficient accuracy. Since solar systems are rather sensitive to solar irradiance level, certain care should be taken in selection of weather conditions for such test. Longer duration of the measurements may release restrictions to the weather conditions and provide the same accuracy in the parameter estimation but for lower levels of solar irradiance during outdoor tests.

NOMENCLATURE

C_c effective thermal capacity of the collector [J/K]
G_t solar irradiance in the collector plane [W/m^2]
T_a ambient temperature [°C]
T_m mean fluid temperature [°C]

REFERENCES

[1] Spirkl W., 'Dynamic Solar Domestic Hot Water Testing', Transac-

tions of the ASME, 112, 1990, PP.98-101.

APPENDIX

Technical characteristics of the solar collector of the system 1 :

Type: BATEC 22 SELECTIVE

Aperture area: 2.16 m^2

Transparent insulation: single glazing, 4 mm glass

Weight: 40.0 kg

Thermal efficiency from indoor stationary test:

$$\eta = 0.78 - 4.2\,(T_m - T_a)/G_t - 0.011\,(T_m - T_a)^2/G_t$$

Expected values of the parameters for the collector of the system 1:

U_c = 5.2 $W/(m^2K)$

A_c^* = 1.68 m^2.

DYNAMIC TESTING WITH MEASURED DATA FROM TWO SMALLER SDHW SYSTEMS

(Progress Report)

Peter Kovács and Per Bergquist
Swedish National Testing and Research Institute (SNTI)
P.O. Box 857, 50115 Borås
Sweden

1. INTRODUCTION

This report describes the work carried out at the Swedish National Testing Institute (SNTI), concerning dynamic fitting based on real system test data.

One objective of the work was to gain experience from practical application of the dynamic testing. Another was to conclude whether the two systems tested were properly modelled by the plug flow model. That is, if the system parameters had good agreement to the physical ones and/or if they could be used for an accurate prediction of the gain of the systems.

Two smaller domestic hot water systems were tested. One, a pumpcirculated system (A) with axilliary heater, was measured during three periods of in all 97 days. The other one, a thermosyphon system (B) without auxiliary heater, was measured during two periods of in all 47 days.

The measurements were made outdoors during summer and autumn 1989 and during spring 1990 at the test site of the Swedish National Testing Institute in Borås, Sweden. The test site is situated about 60 km east of Gothenburg and at a latitude of 57° N.

The results considered are fitted system parameters and short term predictions of measured sequences.

This project relates to project grant 900091-3 from the Swedish Council for Building Research to the Swedish National Testing Institute.

2. DESCRIPTION OF SYSTEM COMPONENTS

2.1. Solar collector

	System A	System B
Absorber type	Flat plate, copper tubes in aluminium fins	Flat plate, copper tubes on aluminium fins
Outer cover	Lowiron glass	Standard glass
Inner cover	Teflon film 0.025 mm	-
Absorber surface	Selective	Selective
Insulation	Mineral wool 70 mm	PUR 20 mm
Aperture area	5.0 m^2	3.93 m^2
Orientation	South, 45°	South, 45°
$\tau\alpha$	0.85	0.86
F_R	0.89	0.88
$Uc(T_c - T_{ca} = 37\ K)$	3.99 W/m^2K	5.96 W/m^2K
Heat capacity	8.4 kJ/m^2K	6.4 kJ/m^2K
Flow rate	0.07 kg/s	-
Fluid	Water/water-glycol	Water

2.2. Heat storage

	System A	System B
Type	Vertical steel cylindre	Horizontal steel cylindre
Storage volume	300 liters	267 liters
Insulation	PUR 40/20 mm	PUR 35 mm
Heat loss coeff. U_S	3.1 W/K	3.6 W/K
Solar loop heat exchanger	Coil at tank bottom	Coil in tank

2.3. Auxiliary heating

	System A	System B
Type	Electric heater at tank top	-
Appr. heated fraction	1/2 of tank	
Max. power	1 kW	

2. 4. Piping and pumps

	System A	System B
Collector inlet piping	11 m isolated plastic pipe Ø 10 mm	0.25 m isolated copper tube Ø 12 mm
Collector outlet piping	- " -	- " -
Heat loss	0.30 W/mK	0.15 W/mK
Heat capacity	0.03 kJ	-
Pump power	50 W	

2.5. Control

	System A	System B
Pump control	Sensors clamped to collector outlet pipe and at tank bottom	- -
Ton	~10 °C	
Toff	~2 °C	

2.6. Summary of system parameters

The system parameters used in the plug-flow model are listed below, their values being calculated from the physical properties of the system.

These values served as initial values at the fitting.

Table 2.1. Calculated system parameters.

	System A	System B
Ac*	3.8 m^2	3.0 m^2
Uc*	7.0 W/m^2K	8.0 W/m^2K
US	3.1 W/K	3.6 W/K
CS	1.30	1.15
D_L	?	?
Sc	0	0
Faux	0.5	-

3. MEASUREMENTS

3.1. General

The tests were made outdoors at the test-site of the SNTI in Borås, Sweden.

Sequences 2-6 (see table 3.2) were designed according to recommendations in an early version of the program manual. The test sequences were chosen so that the system should operate in as wide a temperature range as possible, thus obtaining as de-correlated parameters as possible.

Sequences 11-14 are about the same as for the sequences 2-6. Remaining sequences 15-25, are similar in output, using the same draw off profile all over. These sequences, i. e. sequences 15-25, simulate the systems under normal operation in a one-family house in Sweden.

3.2. Test site

The test site is situated at longitude 58° latitude 13°. Ground reflexion during the measurements was approximately 0.2.

3.3 System loads

The loads used were both continuous draw offs (cont.) and draw off profiles (profile), as given in Table 3.3 for each individual test sequence. The time and load distribution of the load profile is given in Table 3.1.

Table 3.1: The draw off profile.

Time of day	Lead volume (l)
07.00	50
12.00	50
16.00	40
18.00	40
20.00	20
	Σ 200 l/day

3.4 Test periods

The data was collected during summer and autumn 1989 and during spring 1990. The weather was varying from good to bad (see table 3.1). In all, 97 days of measurements were made. The timesteps used were, one hour for sequence 1, one minute for sequences 2-23, and a variable timestep of one hour at non-drawoff and about ten seconds during draw off in sequence 25.

Table 3.2: Measuring period for the test-sequences used.

Sequences	Duration days	April	May	June	July	August	Sept.	Oct.
1	14			x				
2-6	10			x	x			
11-14	10				x	x		
15-16	11					x	x	
17	7						x	
18-20	20						x	x
21-23	16							x
25	42	x	x					

Table 3.3: Main characteristics of the measured sequences.

Sequence	Duration h	Load type	Flow l/min	Weather type	Tcw °C	Tca °C	Tsa °C	Skip h
1	348	Profile	8	Good	-	-	-	25
2	6	Cont.	1	Bad	16	13	23	2
3	45	Cont.	1	Mixed	16	9	18	2
4	49	Cont.	8	Good	16	16	25	17
5	50	Cont.	1	Good	28	18	30	2
6	88	Profile	6	Mixed	19	18	28	2
11	12	Cont.	8	Mixed	16	12	20	2
12	53	Cont.	1	Mixed	18	14	24	2
13	62	Cont.	1	Good	29	15	26	17
14	93	Profile	8	Good	17	9	19	2
15	145	Profile	8	Mixed	16	10	19	5
16	170	Profile	8	Bad	17	10	18	26
17	190	Profile	8	Mixed	15	9	20	22
18	170	Profile	13	Mixed	17	13	25	22
19	190	Profile	13	Good	15	6	21	22
20	190	Profile	16	Bad	14	5	19	22
21	190	Profile	16	Bad	12	7	19	22
22	175	Profile	16	Bad	13	8	19	22
23	95	Profile	16	Bad	12	7	19	23
25	1030	Profile	16	Mixed	15	9	21	21

4. RESULTS

4.1. General

The calculations were made with the standard DFP-model. The calculations have been made without the wind option of the program. We used standard precision and the filter time constant was set to 24 h and C_F to 1E5.

The expected parameter values as given in Table 2.1 served as initial values for the different parameter fitting calculations. Four local minimas were investigated before the final run.

Different skips were used depending on the flowrate and type of load (see table 3.3). All files were preprocessed with SDHWPRE, and thus produced files with extension D3 were used for parameter fitting calculations.

The program packages of the versions 1.13 or 1.14 have been the basic calculation tools in the report. The system parameters have been identified from several sets of data files, both from test sequences designed to give enough system information from short term tests (< 11 days) as well as from data files with a duration of 11-40 days.

The parameters calculated by the DFP-program using the different data file sets are given in Table 4.1-4.3. The parameters are compared to one another and to expected parameters. Standard deviations and large correlation coefficients are listed.

Short term predictions are made for some of the measured sequences using different parameter sets to predict these sequences. Predicted and observed energy gain is listed and the errors in power as well as in temperature are considered.

4.2. Fitted parameter values

Table 4.1: Expected and identified parameters, measurement sequences 2-6.

Pumpcirculated system A

Sequences	AC* m^2	UC* W/m^2	US W/K	CS MJ/K	DL
Expected	3.80	7.03	3.1	1.29	?
2-6	3.34±0.06	9.18±0.78	2.98±1.27	1.10±0.03	0.0±0.05
2.3.5.6	3.05±0.22	6.34±2.66	3.23±1.32	1.06±0.03	0±0.04
2.3.4.6	3.34±0.07	9.82±1.00	2.64±1.87	1.11±0.04	0±0.07

Thermosyphon system B

Sequences	AC* m^2	UC* W/m^2	US W/K	CS MJ/K	DL
Expected	2.99	8.04	3.6	1.15	?
2-6	2.33±0.04	6.98±1.29	4.18±0.91	1.12±0.04	0.06±0.06

Comments

The parameters fitted from sequences 2-6 are well determined, only DL-US showed a strong correlation of -0.78 for system A and UC*-US = -0.75 for system B. Shortening the test had a big influence on the quality of the fit.

These test sequences were designed with the intention to get enough system information from a short term test. It seems possible that the total testing time of ten days could have been shortened even more without bad influence in the results.

Differences between expected and fitted values are here below 30 % .

Table 4.2: Expected and fitted parameter values, mesurement sequences 11-14.

Pumpcirculated system (A) with auxilliary heater

Sequences	AC* m^2	UC* W/m^2	US W/K	CS MJ/K	Faux	DL	Obj. W
Expected	3.80	7.03	3.1	1.29	0.5	?	-
11-14	3.54 ±0.09	7.12 ±0.39	3.18 ±0.34	1.17 ±0.03	0.58 ±0.02	0.022 ±0.014	6.5 -

Thermosyphon system (B), without auxilliary heater

Sequences	AC* m^2	UC* W/m^2	US W/K	CS MJ/K	Faux	DL	Obj. W
Expected	2.99	8.04	3.6	1.15	-	?	-
11-14	2.67 ±0.06	7.61 ±0.40	5.31 ±0.40	1.23 ±0.03	- -	0.08 ±0.03	5.1 -

Comments

The accuracy is clearly improved for both systems compared to table 4.1. Large correlation coefficients changed to Ac*-UC* = 0.73 for system A and AC*-CS = 0.55, AC*-D_L = 0.51 for system B.

Differences between expected and fitted values are below 15 % for system A.There are no big differences between sequences 2-6 and 11-14, just a bit more sun in the latter and a slightly different order of sequences. The conclusion from this would be that it is essential with a proper design of the test sequences.

Table 4.3: "In-situ" measurements, sequences 15-23 system A and sequences 15-16 system B. Notice that from sequence 17 and forth the solar loop of system A uses water/glycol 50/50 as heat transfer fluid.

Pumpcirculated system A, with auxilliary heater

Sequences	AC* m^2	UC* W/m^2	US W/K	CS MJ/K	Faux	DL	Obj. W
Expected	3.80 (?)	7.03	3.1	1.29	0.5	?	-
15-16	3.69 ±0.2	7.74 ±0.84	2.65 ±0.43	1.14 ±0.05	0.58 ±0.02	0.02 ±0.02	5.5 -
18-20	4.65 ±0.32	11.27 ±0.65	2.60 ±0.35	1.01 ±0.03	0.55 ±0.02	0.03 ±0.01	6.9 -
21-23	2.30 ±0.27	4.34 ±1.83	2.50 ±0.69	1.00 ±0.05	0.55 ±0.02	0.02 ±0.02	7.0 -
25	3.14 ±0.10	7.22 ±0.48	2.80 ±0.42	1.14 ±0.02	- -	0.03 ±0.01	7.5 -

Thermosyphon system B, without auxilliary heater

Sequences	AC* m^2	UC* W/m^2	US W/K	CS MJ/K	Faux	DL	Obj. W
Expected	2.99	8.04	3.6	1.45	-	?	
15-16	2.71 ±0.19	6.76 ±0.54	2.11 ±0.77	1.37 ±0.12	0.29 ±0.15	4.33 -	

Comments

The length of these testperiods reaches from 11 days (sequences 15-16) to 42 days (sequence 25). Compared to parameters resulting from specially designed sequences in table 4.2, these parameters are not as well determined. No. 25 is an exception. Large correlation coeffiecients are for system A, AC*UC* = 0.85 and US-DL = 0.70 for all fits and for system B, AC*CS = 0.88 and A*UC* = 0.76. The change in heat transfer fluid could possibly be detected in parameters resulting from sequence 25, but none of 18-20 or 21-23 confirms this.

These sequences could probably not compare to true in-situ measurements, as the load-profile here was the same day after day.The results indicate however that for in-situ testing, at least a months´ measurements are required in order to get a good determination of the parameters.

4.3. Short term prediction

The STP-program was used in combination with the standard fit program DFP. Predicted sequences are No. 1, 16 and 17, using different sets of parameters. In tables 4.4 and 4.5 the different short term predictions are listed along with sequences used for fitting and related errors in the predicted energy gain.

The aim of the predictions is mainly to see how it will influence the result, if the parameters are less accurately determined. It is also interesting to see if predictions are consistent in the respect that predicting periods where water served as heat transfer fluid with parameters resulting from "water/glycol"-periods, should give an underestimation of the output and vice versa.

Table 4.4: Short term predictions for the pumpcirculated system A.

Parameters from sequences	Predicted sequence	System gain (W) predicted	observed
11-14	1	509 ± 11	498
15-16	1	517 ± 15	498
18-20	1	507 ± 11	498
11-14	16	168 ± 11	179
15-16	16	176 ± 14	179
11-14	17	190 ± 12	183
15-16	17	197 ± 14	183
18-20	17	188 ± 1 1	183
21-23	17	167 ± 16	183

Table 4.5: Short term predictions for the thermosyphon system B.

Parameters from sequences	Predicted sequence	System gain (W) predicted	observed
11-14	1	350 ± 9	320
15-16	1	351 ± 9	320

Comments

The errors calculated as $\frac{\text{predicted - observed}}{\text{predicted}}$

are within the statistically calculated errorbands for all predictions but the sequence 1 system B and is below 10 % in all cases. The errors in predicting system A sequence 1 is below 5 %. In sequences 16 and 17 the relative errors become higher because the use of an auxilliary heater reduces the system gain.

If, as suggested, the temperature error is calculated as

$$\frac{\text{predicted - observed}}{\text{(mean load capicitance)} \cdot \text{(mean load temp.difference)}},$$

Also these predictions end up below 5 % error.

Predicting system B sequence 1, is not as successful but still, errors are below 10 %. The predictions are consistent in the respect that the more similar data in fitting and prediction, the better the results. The extreme is 15-16, predicting 16, which yields as excellent a prediction as one could expect.

The results also show a slight reduction in predicted output when parameters estracted from the "water/glycol-system" are used to predict the "water-system" and this was also expected. Somewhat surprising are the results where parameters from sets 18-20 and 21-23 are used to predict 17. Sets 18-20 gave parameter values far from the values received in the other runs. Sets 21-23 gave parameters that were quite uncertain and also the weather during these sequences was bad. Still prediction is made with errors lower than 10 %!

5. CONCLUSIONS

Here the results from fitting and prediction are summarized and discussed.

5.1. Dynamic fitting

The investigations confirmed that short term outdoor tests combined with the dynamic fitting procedure could produce well determined sets of parameters to model the two systems. It was not possible for us to conclude from the parameters and their errors, which one of the two systems that was "best" modelled.

The fitting is sensitive to the initial values given, and expected values should be used in general. The fitting also seems to be quite sensitive to the design of the testsequences at short-term tests made outdoors. This might be a problem if the sun "has to" turn up in the right moments. On the other hand, prediction showed little sensitivity to parameters that were not so good determined.

The expected parameter values are subject to a great deal of uncertainty because of aged collectors and insulations, and the storelosses being calculated and not tested. There fore, the comparisons between fitted and expected values should be made with that background.

5.2. Short term prediction

The STP-runs that were made, all resulted in deviations less than 10 %. The pumpcirculated system A was predicted better than 5 %, concerning temperature error. In general,the predictins showed surprisingly little sensitiity to the differences in the parameter sets. Unfortunately, no predictions of late autumn or early spring sequences were made.

VALIDATION OF THE DYNAMIC SYSTEM TESTING (DST) FOR AN INTEGRATED COLLECTOR STORAGE WITH TRANSPARENT INSULATION MATERIAL (TIM)

A. Wagner, J. Asmussen
Fraunhofer-Institut für Solare Energiesysteme
Oltmannsstraße 22, 7800 Freiburg
Federal Republic of Germany

SUMMARY

A new type of domestic hot water system consisting of a transparently insulated collector storage with an auxiliary continuous-flow gas heater was tested on the institute's outdoor test field, using the DST procedure. By comparing the results of individual measurement series it was found that the desired accuracy of 5 % for the energy output prediction from the measurements was achieved for the integrated collector storage (ICS) with a TIM cover. Thermal losses from subsidiary components (pipe lines, additional heating) have a significant influence on the accuracy of the parameter determination. The results of long-term predictions based on parameters from different measurement series, are essentially the same for equal boundary conditions and the same prediction period.

1. CONSTRUCTION AND EXPERIMENTAL SET-UP

The integrated collector storage used in the experiments, was developed at the Fraunhofer-Institute for Solar Energy Systems (ISE) as part of the research work in the field of transparent insulation [1]. The main component is a cylindrical, stainless steel storage tank (volume 108 l), with a black outer coating serving as the absorber (fig. 1). The TIM cover, which is 5 cm thick, minimizes the thermal losses through the front of the collector and ensures - together with the thermal mass of the system - that freezing cannot occur. Due to this the collector storage can be connected directly to the domestic hot water circuit. For the experiments, the collector storage (1.4 m^2 aperture area) was integrated into a south facing roof with a tilt angle of 45°. For additional heating a temperature-controlled continuous-flow gas heater was connected to the ICS.

2. MEASUREMENT PROCEDURE

The performance of the total system was determined by using a dynamic short time procedure, which was developed within the research project VELS. The DST procedure is intended to be incorporated into the DIN regulations, governing the measurement of solar DHW system performance. The procedure uses optimization routines to determine characteristic parameters for a computer model from measurement series with a pre-defined load profile. With these parameters predictions of the system's energy output can be made for any period of time or location, using simulation calculations. The measurement procedure is described in detail in [2].

3. MEASURMENT RESULTS

In the period from July to September 1990, six measurement series were carried out and analysed [3]. The system efficiency for the individual measurement series was between 35-37 %, with a solar fraction of 76 % to 100 %.

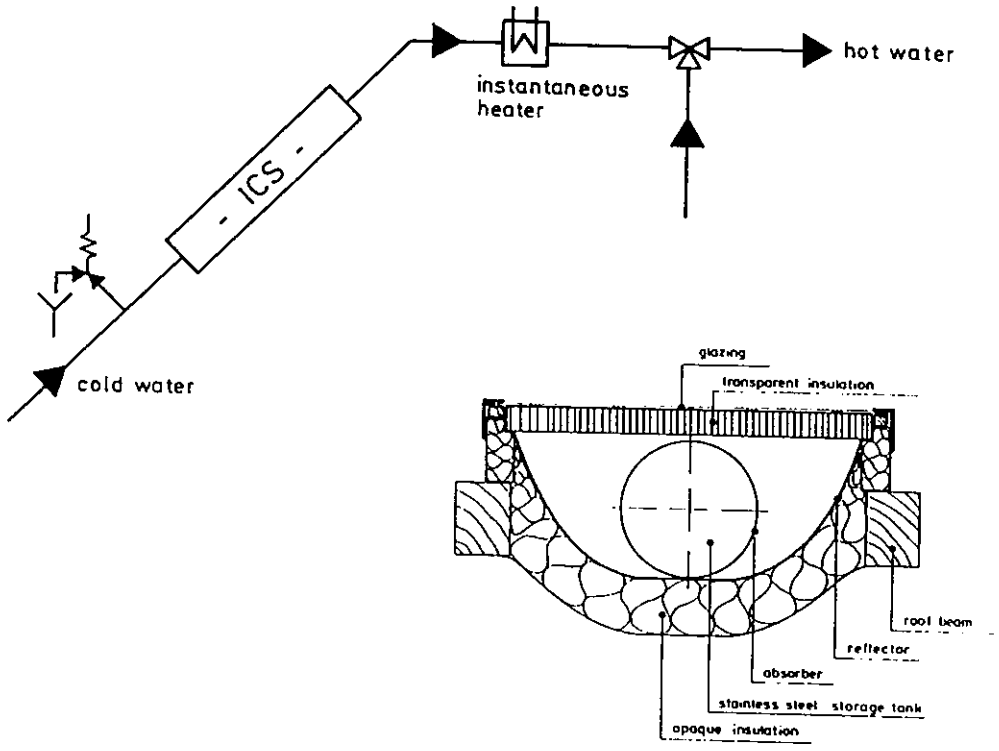

Fig. 1: Cross section through a collector storage and circuit diagram of the complete system

4. ANALYSIS WITH THE DST PROCEDURE

Parameter sets were obtained for each measurement series with the DST procedure. Predictions of the energy output were made by using parameter sets for those measurement sequences, which were not used to determine parameters. In doing so, two separate cases were distinguished: (A) the collector storage itself and (B) the collector storage with the piping and the continuous-flow gas heater connected. However, the auxiliary heater was not operated during the DST tests; its performance was evaluated separately and is not discussed here. The output of the system was determined as the hourly average of the power in Watts. As an alternative, the wind velocity was also taken into consideration in some analyses.

4.1 Model parameters

As an illustration, the parameters determined by the DST procedure from two measurement sequences will be compared with the real system parameters (fig. 2). The total losses, which cannot be attributed individually to the collector and the storage unit in an ICS system, are attributed to the component losses UC* and US in widely differing proportions by the fit programme in the DST procedure. The remaining parameters are of the same order of magnitude as the corresponding real system parameters. In case B, the thermal losses from the piping and the connected components have a strong influence on the loss parameters US* and US.

case	sequence	AC* (m^2)	UC* (W/m^2K)	US(W/K)	CS (MJ/K)	DL (-)
A	2	0.94	0.00	3.06	0.35	0.085
	3	1.12	2.50	3.06	0.35	0.077
B	2	1.11	7.53	2.86	0.37	0.042
	6	0.86	0.44	3.48	0.38	0.027
real system parameters		1.4	2.4	3.3	0.43	-

NOMENCLATURE

AC*	= effective collector area	(m^2)
UC*	= equivalent collector heat loss factor	(W/m^2K)
US	= heat loss coefficient of the store	(W/K)
CS	= thermal capacity of the store	(MJ)
DL	= mixing constant	(-)

Table 1: Comparison of the DST parameters with the real system parameters

4.2 Short-term prediction (STP)

Judging by the results obtained so far, the DST procedure predicts the energy output with an accuracy of ± 5 % on the basis of a short measurement period of 8 days. This is not only valid for the collector storage itself (case A), but also for the whole ICS system investigated here, comprising the collector storage and the continuous-flow heater with piping connected to it (case B). In one case, in which the load profile was considerably lower than the pre-defined DST load profile, the predicted energy output deviated from the real value by ± 7 % (case A) and ± 13 % (case B). The wind velocity had only little influence on the predicted energy output for wind speeds between 2 and 4 ms^{-1}.
The variance of the input data is significant for the prediction. The duration of the measurement series only plays a role when there is insufficient variance in the data from a short measurement series. In order to make a better assessment of a measurement series, it would be useful to include the solar fraction and the system efficiency value in the results, as for the long term predictions.

4.3 Long term prediction (LPT)

Long term predictions using different parameter sets were made for cases A and B with the Test Reference Year of Freiburg. The conditions assumed were a total daily load of 53 l or 80 l at a temperature of 45 °C, withdrawn at three times each day. The LTP programme determines the system output P_{net} in Watts, the solar fraction f and the system efficiency A_s over the whole prediction period. The DST version 1.15 cannot take the wind data into account for the LTP programme.

The deviation in the solar fractions between predictions based on different parameter sets is only slight in case B (fig. 3). Only when parameters from the series with the lower load profile were used, the resulting f, A_s and P_{net} are somewhat lower. To get a usual dimensionless efficiency value, the efficiency value A_s, which is given in m^2 has to be devided by the aperture area.

LTP RESULTS FOR AN INTEGRATED COLLECTOR STORAGE (1.4 qm absorber area) case B (whole system; auxiliary heating off)						
daily demand at 45 °C	80 liter			53 liter		
parameter sets	f (-)	A_s (m^2)	P_{net} (W)	f (-)	A_s (m^2)	P_{net} (W)
SQ12R	0.474 ± 0.021	0.485 ± 0.022	64.3 ± 2.9	0.512 ± 0.031	0.349 ± 0.021	46.3 ± 2.8
SQ1R	0.457 ± 0.028	0.469 ± 0.028	62.1 ± 3.8	0.498 ± 0.047	0.340 ± 0.032	45.1 ± 4.3
SQ2R	0.476 ± 0.034	0.487 ± 0.035	64.6 ± 4.6	0.514 ± 0.046	0.351 ± 0.032	46.5 ± 4.2
SQ6R	0.471 ± 0.033	0.482 ± 0.034	63.9 ± 4.5	0.522 ± 0.050	0.356 ± 0.034	47.2 ± 4.5

Table 2: Long term prediction with the Test Reference Year of Freiburg for different parameter sets from case B

The results of a long term prognosis for a collector storage module without the connected components (case A) are described in detail in a DIN report [4]. With a daily load of 100 l (water temperature 45 °C, withdrawn at three times each day), a solar fraction of 48 % with a system efficiency of 44 % was calculated.

REFERENCES

[1] Ch. Schmidt, A Goetzberger, J. Schmid
Test results and evaluation of integrated collector storage systems with transparent insulation, Solar Energy 41 (5), pp. 487-494, 1988

[2] W. Schöllkopf
Bestimmung der Leistungsfähigkeit von Solaranlagen zur Warmwassererwärmung, DIN-Entwurf, LMU München, 1990

[3] J. Asmussen
Experimentelle Untersuchung eines neuartigen Kollektorsystems zur solaren Brauchwassererwärmung unter Berücksichtigung der Nachheizung, Diplomarbeit an der TU Braunschweig (Lehrstuhl für Raumflugtechnik und Reaktortechnik), 1990

[4] J. Asmussen
Prüfbericht nach DIN-Entwurf - Solaranlagentest - für einen TWD-Speicherkollektor FhG-ISE, Freiburg, Mai 1991

DIFFERENT SDHW SYSTEM TESTING USING DYNAMIC METHOD

C.Arkar,S.Medved and P.Novak
Faculty for Mechanical Engineering, University of Ljubljana
Murnikova 2, 61000 Ljubljana
Slovenia

1. INTRODUCTION

Two years ago we got a copy of dynamic method for solar system testing [1, 2] on our Faculty for mechanical Engineering in Ljubljana. Comparing other existing methods we had known was this dynamic method very simple and practical to use - simple short term measurements and automatic calculation. We have therefore decided to evaluate this method with measurements of four simple SDHW systems [4, 6].

2. SYSTEMS MEASUREMENTS

2.1. Systems description

We have worked with the dynamic method version 1.14 [3]. The measurements were made at the outdoor test loop of the Laboratory for Heating, Sanitary and Solar Technology of our Faculty in Ljubljana. Three termosiphon systems (A,B,C) and one integrated collector storage (ICS) were tested. The characteristics of this systems are:

Table 1: Characteristics of measured systems

system	collector area	storage volume
	Ac (m^2)	V_{HS} (m^3)
A	2	0.096
B	2	0.120
C	1.44	0.080
ICS	1	0.050

All termosiphon systems had a solar collector of the same manufacturer, but they are of different size. They are all titled to an angle of 30 degrees. System A and B are distinguished by their heat storage or better said by their heat exchanger. System A had the external jacked heat exchanger and system B had a coil heat exchanger. This two heat storages are insulated with 5 cm insulation with thermal conductivity 0.04 W/mK. System C had no heat exchanger. Heat storage of system C was practically uninsulated - only tin cover. System ICS had a black painted heat storage, insulated with 1 cm Transparent Insulation Material. The cover was made of acrylic glass with pyramidic shape and aperture area of 1 m^2.

2.2. Experimental results

We have made four to five measurement sequences for each system. The length of this sequences is between two and six days. The load has been various. On the basis of measurements we obtained following parameter values.

Table 2: Parameter values and objective function for four measured systems

System		System A	System B	System C	System ICS
param	Units				
Ac*	m^2	1.04	0.871	0.565	0.337
uc*	W/m^2K	8.66	1.99	0.825	0
Cs	MJ/K	0.416	0.319	0.426	0.166
Us	W/K	2.324	3.788	6.924	1.934
D_L	-	0.027	0.517	0.057	0.585
Sc	-	0.269	0.065	0.002	
C(p)	W	7.56	8.97	24.59	2.38

The wind speed was also measured but this data by system modeling weren't used as we weren't able or we didn't know how to make LTPP with such system model.

Systems were not previous tested by any other method, so that we don't have comparative results.

We can only compare systems between each other.
Comparing the values for collector loop, the values for Ac* are good but there are quite big differences by uc* .
If we compare store heat capacity, we can see that system B had smaller capacity than system A despite bigger heat storage volume. It was shown that heat storage of system B have large death volume.
Comparing store heat loses, we can find the largest number by system C. As it was said this storage was uninsulated.
The objective function is the biggest by system C. The measurements on this system were stopped after 11 days because of the problems with the system.

3. SYSTEMS PERFORMANCE PREDICTION

3.1. Short term performance prediction

An additional check of this models was made with short term performance prediction (STPP). Two sequences for each system were chosen. Next figures show the results of these analyses: the values of measured and predicted mean load power P_L of analyzed measurement sequence. This sequences were checked with system model made with all sequences.

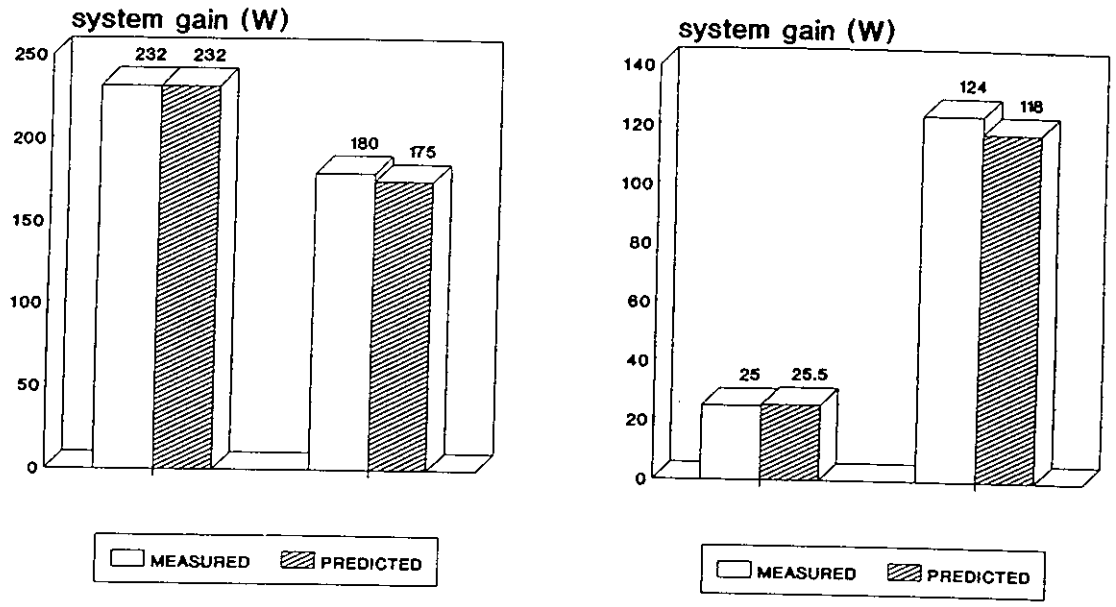

Figure 1: Measured and predicted solar gain for system A and system B in observed sequences

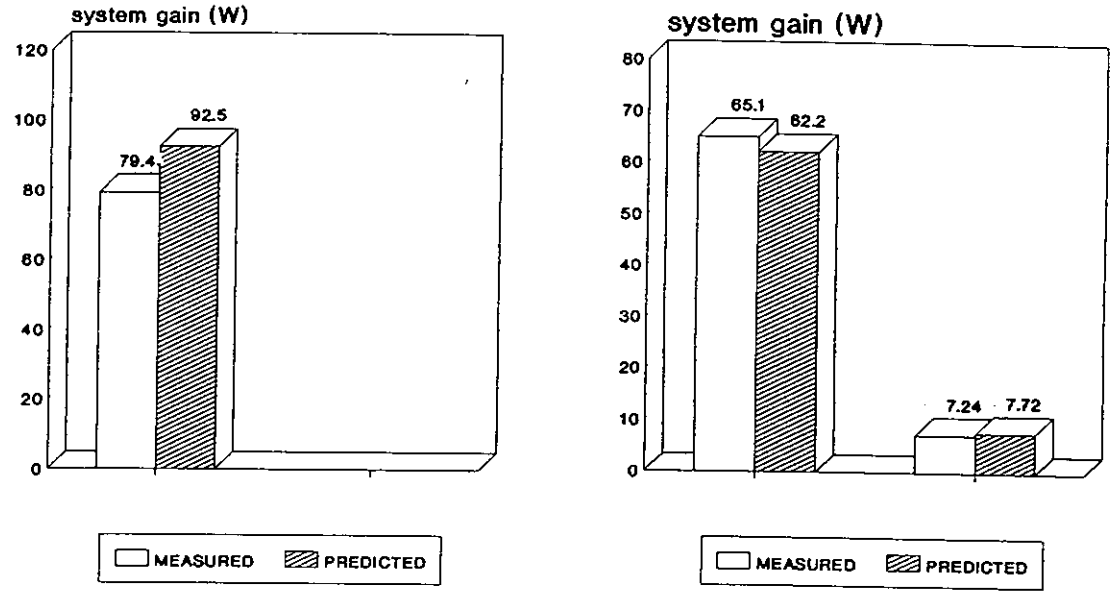

Figure 2: Measured and predicted solar gain for system C and system ICS in observed sequences

Results show good agreement between measured and predicted gain. The only exception is system C, where the objective function already clearly indicates inadequate performance of the system.

3.2. Long term performance prediction

On the basis of the system models, we carried out long term performance prediction (LTPP) for two different places - for Ljubljana, SLO and Split, CRO. Ljubljana is an industrial city with a continental climate and Split is a touristic city at the Adriatic coast with a mediterranean climate. For LTPP meteorological data and load profile is required. We used test reference year for Ljubljana and real year for Split. The following load profile was defined:

Table 3: Load profile

daily load draw off volume		1 volume of heat storage
draw off profile:	from 6 to 7	33%
	from 12 to 13	33%
	from 18 to 19	33%
required temperature of hot water		45°C
temperature of cold water inlet		15°C

Next figure shows the values for fractional system gain (f) and solar efficiency divided by the collector area (As/Ac) for Ljubljana (Lj) and Split (St).

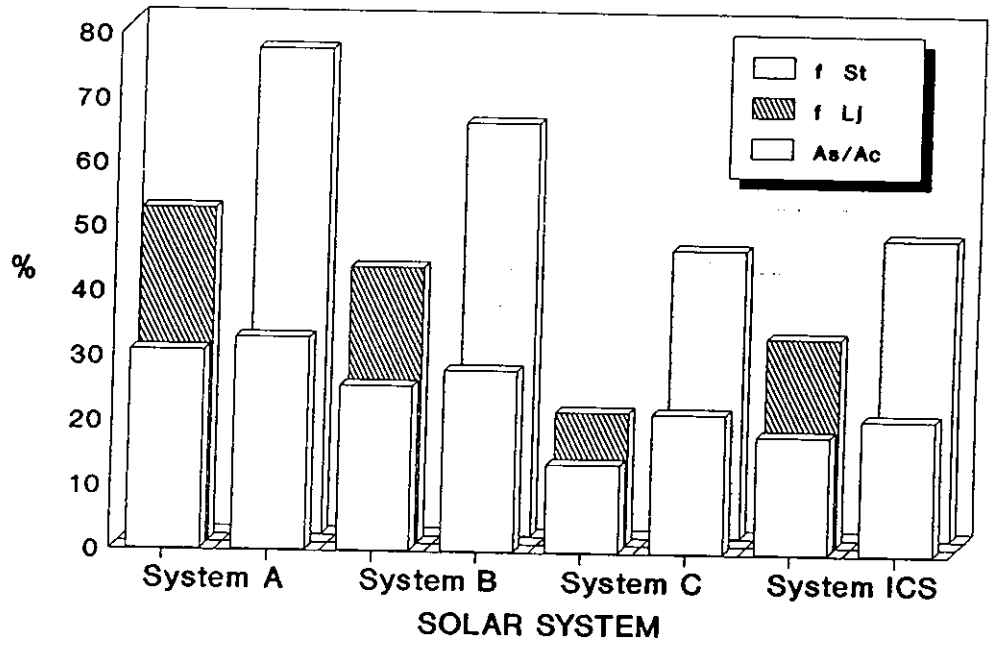

Figure 3: Long term performance prediction of the measured systems

Such a big difference in fractional system gain is because Split has much higher average ambient temperature and yearly average daily insulation than Ljubljana.

3.3. Working out the system model

System models which are presented in this paper were obtained after several fit procedures, and they are distinguished from the models got after the first run. Some of parameters are changing a lot and objective function is decreasing with every further run. On next pictures there is presented how the parameter values change and how this influence on results of STPP and LTPP. The analyze is made for system A.

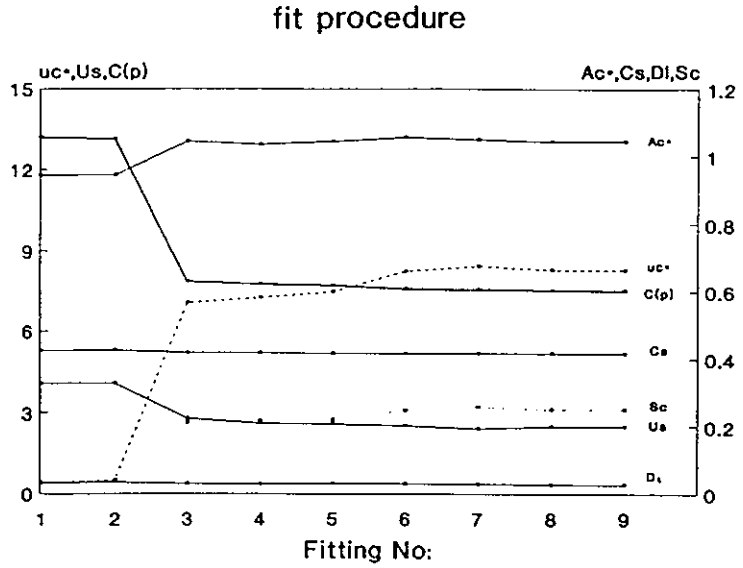

Figure 4: Differences in system model

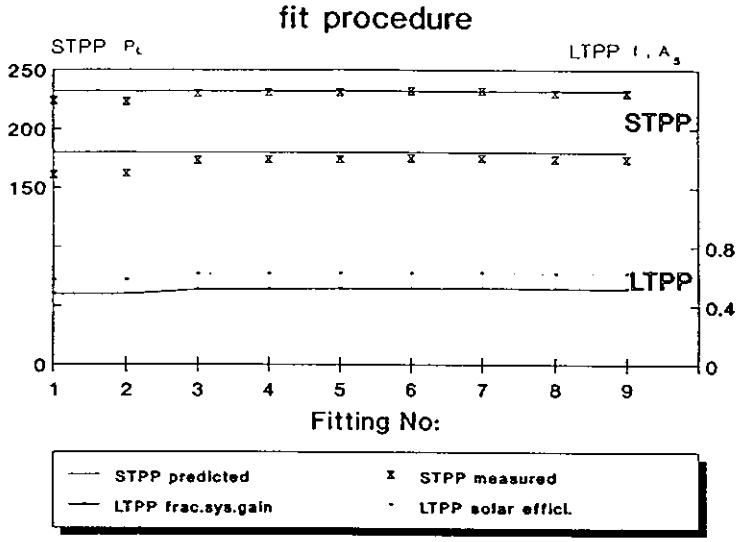

Figure 5: STPP and LTPP with different models

4. CONCLUSIONS

The practical application of the dynamic method by which four simple SDHW systems were tested confirmed all the advantages of this method: simple and short

term measurements, automatic calculations and long term performance prediction and a sufficiently precise system model despite the small number of measured variables. The short term performance prediction is particularly useful in verifying the suitability of the system models. A smaller problem might occur when a lot measurement sequences or more TRY want to be used because a free memory on floppy disk for this files is limited and it is quite small. The last analyze shows big differences in system models if more fit procedures are used. The fit error generally decrease. If the last model is the right one means that a lot of computation time is needed to get the right model. But generally this dynamic method is good.

NOMENCLATURE

V_{HS}	Storage volume	m^3

REFERENCES

[1] Spirkl W., 'Dynamische Vermesung von Solaranlagen zur Warmwasser-bereitung, Disertation',L-M. University, Munich, 1989

[2] Spirkl W., 'Dynamic solar domestic hot water testing', Transactions of the ASME, J. S. En. Enginee., Vol. 112, 1990, 98-101

[3] Spirkl W., 'Dynamic SDHW system testing, Program manual, Version 1.14', L.-M. University, Munich, 1990

[4] Arkar C., 'Kakovost solarnih sistemov , Diploma work' , University of Ljubljana, Ljubljana, 1990

[5] Arkar C., 'Dinamicna metoda za testiranje sistemov za pripravo tople potrosne vode', Sunceva energija, Vol.11 No.1-2, Rijeka, 1990, 47-51

[6] Arkar C.,Medved S.,Novak P., 'Dynamic method for solar system testing - measurement results and long term performance prediction of different SDHW systems', Solar World Congress, Vol.2 Part I, Denver, 1991, 1380 - 1384

DEVELOPMENT OF AN *IN SITU* SHORT-TERM TEST PROCEDURE FOR SOLAR DOMESTIC HOT WATER HEATING SYSTEMS

J.-M. SUTER, M. BOLSINGER†, M. GSTIR†
Paul Scherrer Institute (PSI)
Laboratory for Energy and Process Technology
CH-5232 Villigen PSI
Switzerland

†On leave from the Fachhochschule Aalen, D-7080 Aalen, Germany

1. INTRODUCTION

1.1 *In situ* testing in the normal operation mode of the tested system

In Switzerland, the interest for system tests is mainly concentrated on *in situ* testing, since most systems sold are tightly integrated into the buildings after adaptation to the local conditions. There is no series production of complete systems in the factory. So, the interest for laboratory tests and performance prediction under standard climate and demand conditions is low, at least up to now.

To increase the purchaser's confidence in the performance of a solar heating system, a cheap procedure based on measurements performed *in situ* in the normal operation mode of the system should be available for the prediction of the yearly energy balance and, in particular, for that of the yearly auxiliary energy consumption. The measurement period required should be short and the measurements themselves as simple as possible. For example, intrusive temperature measurements within the store should be avoided

and the whole data acquisition and evaluation should proceed automatically. These ideas on *in situ* short-term system testing have been formulated some time ago by the Swiss Professional Association of Solar Energy Firms (SOFAS), which assigned four goals to such a procedure: (i) quality control, (ii) comparison between design and real data (especially the actual heat load), (iii) stimulation of owner's confidence in solar energy technology, and (iv) improvement of the experience level of designers and installers of solar energy systems. SOFAS set a relative accuracy target of $\pm 10\%$ for the yearly auxiliary energy consumption prediction [1, 2].

Two Swiss research programmes coordinated and partly supported by the Swiss Federal Office of Energy are dealing with the development of *in situ* test procedures: (i) a national programme operated by SOFAS, focusing on combined solar space heating and hot water systems; (ii) a programme at Paul Scherrer Institute (PSI) about solar domestic hot water (SDHW) heating systems, within the framework of the IEA Dynamic Systems Testing Group (DSTG). The present text only reports on PSI activities.

1.2 Objective of developments at Paul Scherrer Institute

The main difference between laboratory and *in situ* testing lies in the degree of freedom when choosing the test sequence. In the lab, many input variables like, e.g, the hot water withdrawal sequence and the cold and hot water temperatures may be chosen freely. On the contrary, in the case of *in situ* testing the only free option is the length of the measurement period as the variations of the input variables are induced by weather and users. The main objective of our work at PSI was the identification of a criterion which might be used by the automatic data acquisition unit to stop the measurements at the optimal moment, i.e. as soon as the yearly energy balance may be predicted accurately enough from the recorded data. This criterion search was done with a SDHW heating system of great similarity to the system assumed by the University of Munich when developing Model P [3].

Originally, the investigation of the applicability limit of this model as well as of the ability of the dynamic system test procedure to detect system failures were also planned. Systems with more exotic configurations and a lot of non optimal design features or even failures should have been included in the study. However, it turned out that the development of the appropriate criterion for terminating an *in situ* test required a lot of effort and the analysis of these systems was postponed.

2. DESCRIPTION OF THE INVESTIGATED SDHW SYSTEM

Because of limited ressources, we could not perform new measurements for the DSTG programme. We processed existing data of our previous monitoring campaign on 29 commercially built solar systems of the first period of active solar technology in Switzerland. The systems monitored were operated in the normal mode, the users living in the houses during the measurements. The monitoring units ran for one to three years. See, e.g., [4, 5].

The PSI contribution to the DSTG programme is based on data from System #12 [6] installed 1977 in a single family house with doctor's practice in the City of Winterthur (latitude 47°30' N, longitude 8°40' E, altitude 425 m). For the monitoring period, 4 persons were living in the building. They used hot water mainly in the morning, at noon and in the evening. The local climate is characterized by a sunny summer and mild winter, however with poor insolation from November to February.

System #12 has been designed for solar domestic hot water heating and swimming pool heating (Fig. 1). However, in the period of interest (August 1981 to July 1982) it was operated as a pure domestic hot water heating system, the pool heating being out of operation. Moreover, the loop installed on the load side to keep the hot water distribution lines warm was continuously out of operation (valve closed by hand) in this

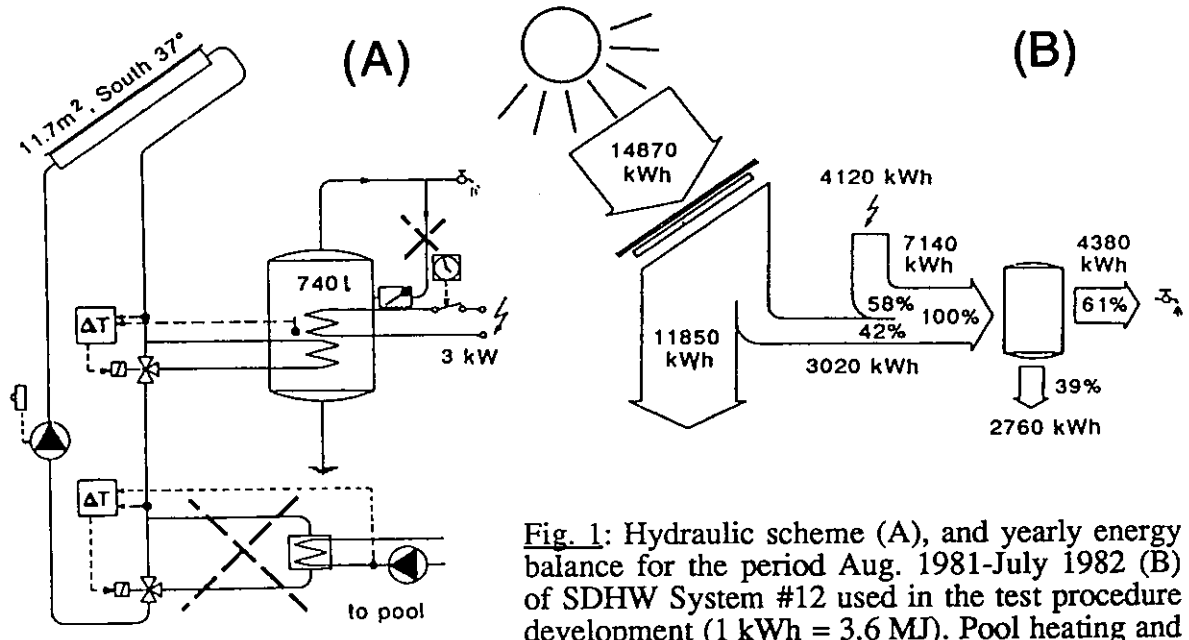

Fig. 1: Hydraulic scheme (A), and yearly energy balance for the period Aug. 1981-July 1982 (B) of SDHW System #12 used in the test procedure development (1 kWh = 3.6 MJ). Pool heating and hot water circulation return line were out of operation at that time [6].

period. In a previous period (not reported here) it had been found that the heat consumption by this circulation loop was even higher than the hot water load itself!

As an overview, Fig. 1B gives the energy balance of System #12 in the period of interest for the present analysis. It was measured according to Section 3, some gaps due to monitoring failures being filled by extrapolation. Both collector and storage efficiencies are much lower than what may be achieved with today's state of the art.

System #12 has 3 flat plate, non selective collectors with 3.88 m^2 aperture area each. The double polycarbonate glazings has reinforcements connecting the two glazings together creating air filled channels in the slope line (Fig. 2). Collector azimuth is +2°, its tilt angle 37°. The horizon is free, except for Eastern azimuths where sunrise is delayed by about one hour (Fig. 3).

The water storage tank is in vertical position (diameter ~0.7 m, height ~2 m) with a total volume of 740 l, the insulation thickness being 10 cm. A coil heat exchanger is mounted at the bottom of the tank. The electrical auxiliary heater has a nominal power of 3 kW and is turned off by a clock at daylight time as well as in the evening (heating only with off-peak electricity). It is located at ~2/5 from the bottom of the vessel, yielding an auxiliary heated volume of ~440 l and a solar-only heated volume of ~300 l. No construction drawing of the tank is available any longer.

The collector pump with 90 W nominal electrical power is controlled by a daylight sensor (Fig. 1). The two bypass valves connecting the collector loop to the domestic hot

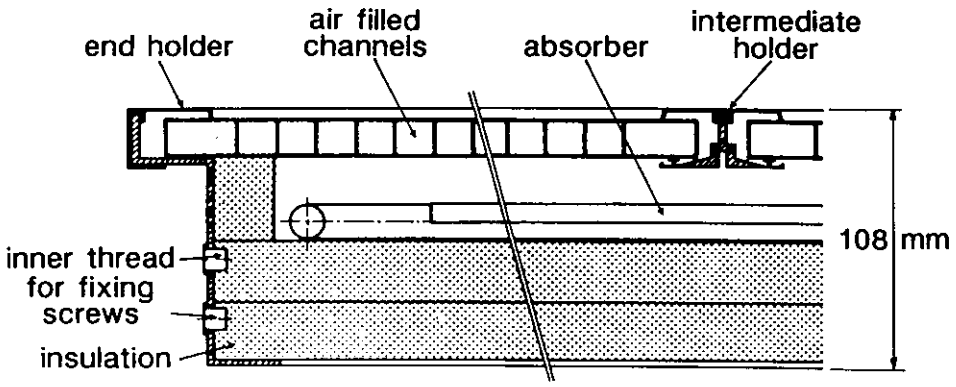

Fig. 2: Collector cross section perpendicular to the channels of the polycarbonate double glazing. The channels axes are slope lines of the collector glazing.

water storage vessel and to the swimming pool are controlled by temperature differences. A manual switch selects either the domestic hot water bypass valve, or the swimming pool bypass valve, or both. For the monitoring period reported, the switch was permanently set in the domestic hot water position.

The expected system parameters are displayed in Table 3, Section 5.1. They were obtained as follows:

- A collector of the same type as in System #12 was tested according to the Swiss collector test procedure [7, 8]. The equivalent usual collector parameters are η_0=0.58, and $F'U_L$=3.9 W/m²K at small temperature difference collector/ambient. The expected effective collector area, A_C^*, is accordingly 0.58 x 11.7 x 0.66 = 4.5 m². The last factor, 0.66, accounts for the unknown average incident angle modifier arising from the complicated glazing geometry. The effective absorption transmission product ($\alpha\tau$) is also unknown. We estimate it to 0.7, leading to u_C^* ~ (3.9+0.1)/0.7 = 5.7 W/m²K. The term 0.1 accounts for the collector loop heat losses.

- The expected loss coefficient of the store is estimated from monthly measured losses amounting to 216 kWh/month at a temperature difference of ~40 K between the store and its surrounding. Thus, U_S ~ 7.5 W/K. The store thermal capacity C_S ~ 3.1 MJ/K is calculated from the water volume, 740 l. Similarly, one gets an auxiliary heated

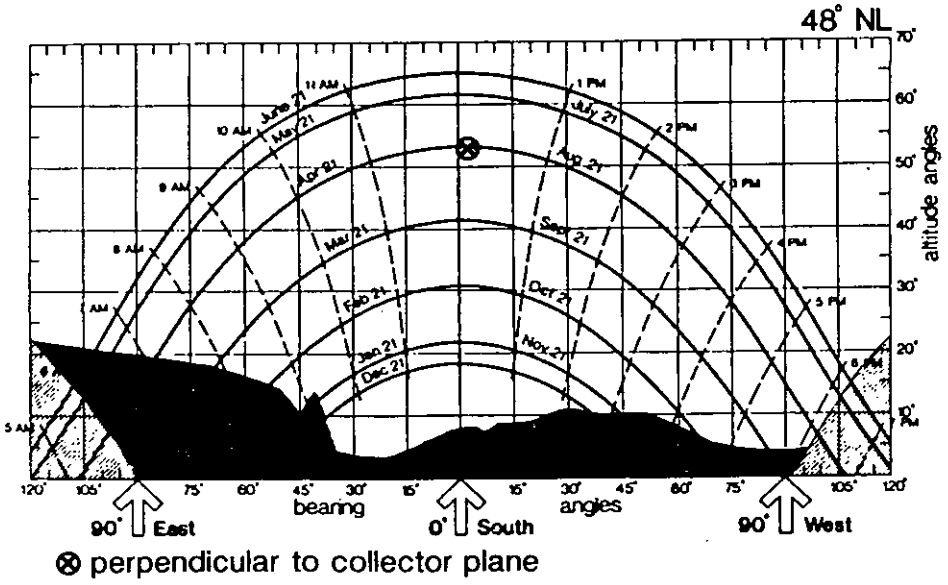

Fig. 3: Sun trajectory and horizon viewed by the collectors

fraction, f_{aux}, of about 60%. Finally, there is no indication allowing to guess the draw-off mixing parameter, D_L.

3. DATA MONITORING AND ON-LINE PREPROCESSING

Like all systems of the monitoring campaign, System #12 has been monitored in the normal mode of operation, the hot water users living in the house. No action was taken to influence the hot water withdrawal. The location of measuring sensors are indicated in Fig. 4. There are more sensors than required by dynamic fitting. This turned out to be an advantage for the present study. The aim of the monitoring campaign was the recording of the long-term energy balance and of averaged or integrated values of variables characterizing system operation like operation temperatures, run time, etc. Additionally, information was gained about system dynamics and controls.

There are three limitations in the recorded data:

- The flow meters were water counters based on the turbine principle. They could not detect small hot water draw-off rates. Their nominal size was adjusted to match the

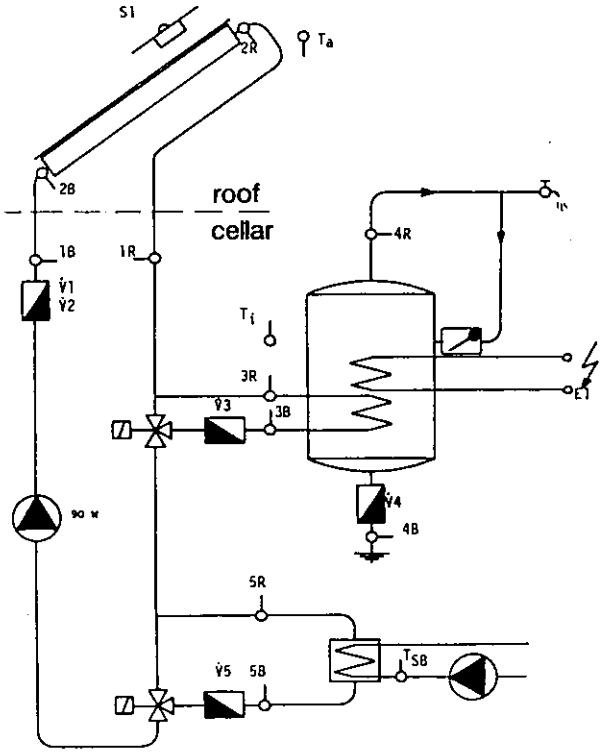

Fig. 4: Location of measuring sensors for System #12

highest load encountered.

- A more serious limitation arises from data representation on the audio tape cassette used to transfer the monitored data from the acquisition unit to the main frame computer for further processing. One single cassette had to be able to contain data from one whole month. Consequently, there was an on-line preprocessing in the data acquisition unit itself. It was made in such a way that no bias was introduced into the long-term system behaviour recorded. Some smoothing was done as explained below.

  The monitoring cycle time was 1 min. From the measured flow within 1 min and from instantaneous temperature measurements, the heat power was calculated each minute. However, the time resolution of the data recorded on the cassette, the so-called "monitoring interval", was mostly longer than 1 min. Switches in the data acquisition unit allowed its selection. For System #12 they were set to 1 hour for the period investigated. So, for each output channel, 60 values were grouped by integration or averaging to give a single one on the cassette.

  Care was taken to get the properly averaged operation temperatures by eliminating the temperature values recorded in the absence of flow in the corresponding pipe. (However, if there was no flow at all for the whole "monitoring interval", all temperature values were retained to calculate an average pipe temperature as additional information.)

- The recorded data generally included heat power, temperature and solar irradiation values, but no flow rate. Hence, we had to recalculate the capacitance rate required by the computer programme for dynamic fitting, from the heat power and the two corresponding operation temperatures. The accuracy of that calculation is limited as all data recorded on the audio cassette were 2-digits integers because of limited cassette capacity. Before recording, the decimal part had been truncated and the remainder carried over to the next "monitoring interval" (to avoid long-term bias). Hence, the resolution in the temperature data available is 1 K.

Summarizing, the on-line preprocessing which differs on principle from the preprocessing needed for dynamic fitting, smoothed the observed system dynamics and introduced some additional numerical noise. However, there was no bias in the long-term integrated or averaged values. The data could be successfully used in the search for *in situ* test sequences leading to accurate long-term energy balance prediction

(Section 5.2), but some aspects of our study have to be examined more precisely using further data involving the full dynamical information about the system behaviour. See our conclusions in Section 6.

4. DESCRIPTION OF THE DYNAMIC FITTING PROCEDURE

4.1 Methodology

As long-term monitoring data were available over extended periods covering nearly one year, the accuracy of the long-term performance prediction by means of the dynamic system test procedure could be easily checked by direct comparison of measured and predicted values. For this purpose, we successively extracted a dozen of test sequences from the monitored data according to various criteria (Section 4.2), used them for system parameters identification, and calculated the corresponding system energy balance over long periods of the year. Additionally, we compared the identified parameter values to the expected ones.

For system energy balance prediction, the programme STP was used. For the period considered, both measured and predicted values of the average net system power, $\overline{P}_{net}$, are printed out, together with the standard deviation of the predicted one. The comparison of measurement and prediction is a check of performance prediction accuracy.

The absolute magnitude for this accuracy check is set by the yearly average load power, $\overline{P}_L$. Fig. 1 indicates $\overline{P}_L = 4380$ kWh/a = 500 W. In Switzerland, the auxiliary energy consumption in a SDHW system usually is about 50% of the hot water heat load. Hence, the 10% accuracy goal set by SOFAS for the prediction of the yearly auxiliary energy consumption corresponds to about **25 W** for System #12.

The incident angle modifier of System #12 double glazing is unknown. We set it to 1 for the whole analysis. Due to the fact that the collectors are South facing, the error introduced in this way was expected to be small, according to the experience of the University of Munich with flat plate collectors.

Details of the analysis may be found elsewhere [9, 10].

4.2 The successive development steps of the test procedure

Table 1 gives an overview of the test sequences considered. Additionally, Table 2 indicates the skip time for each sequence. This quantity was determined according to the procedure supplied in Program Version 1.13. Nearly two years later, the more sophisticated plotting tool supplied with Version 1.17 indicated that the skip time should have had to be chosen somewhat longer for several sequences (compare, e.g, L1 with L1', ..., L4 with L4', in Table 2). However, it has not been possible to repeat the whole analysis. The non optimal choice of the skip time reduces somewhat the accuracy of the predictions.

We began with 4 long sequences, L1 to L4, distributed over spring to autumn. We had initially no idea about the test sequence length required. In a separate analysis not reported here, we showed that the longest ones, L2 and L3, may be shortened to about one month without loss of prediction accuracy.

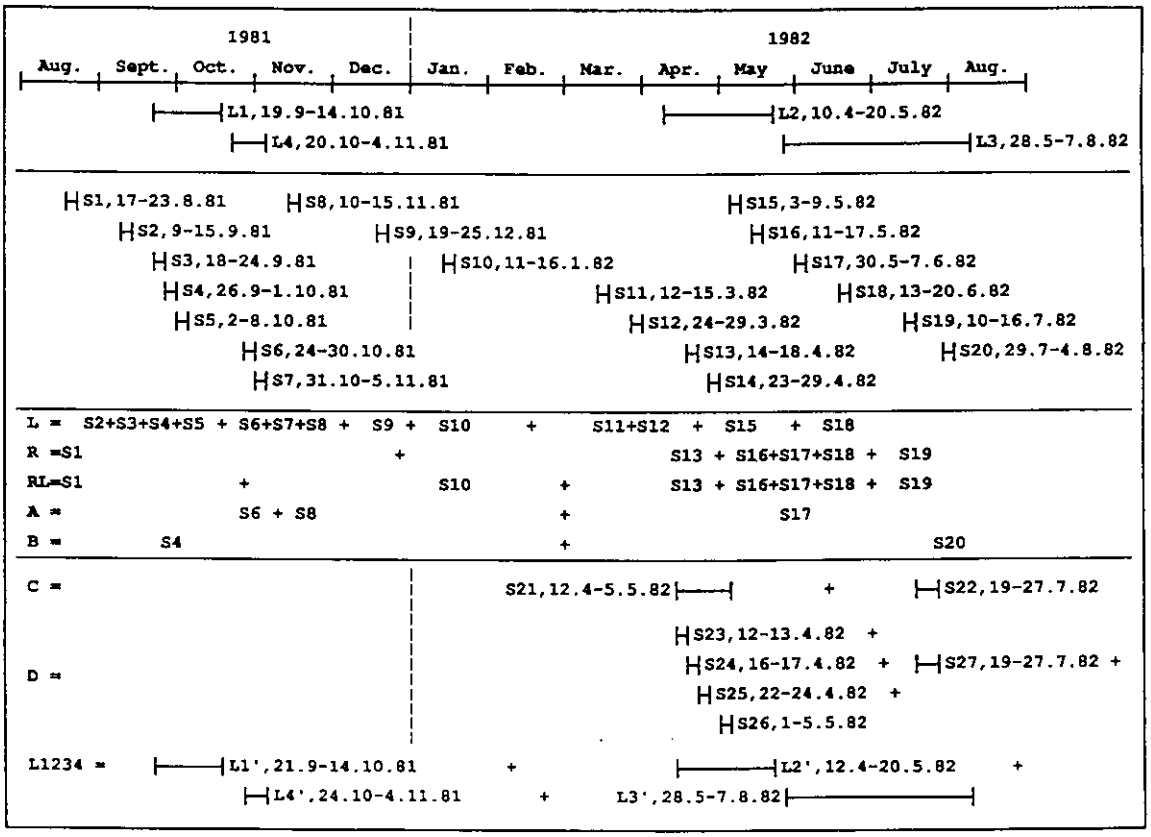

Table 1: Overview of the test sequences successively selected in the course of the present study.

It turned out that a seasonal bias occurs in the long-term performance prediction using system parameters identified from L1, L2 or L4. The observed seasonal bias is not satisfactory. Following DSTG participants' experience, we selected one composite test sequence, S, made of 20 short subsequences, S1 to S20, of 3 to 7 days each. S1 to S20 were chosen in such a way that approximately equal numbers of days with {low load(Q_L), low irradiation(H_t)}, {low Q_L, high H_t}, {high Q_L, low H_t} and {high Q_L/high H_t} respectively are encountered in the composite sequence. To match this condition, S1 to S20 had to be distributed over the whole year, i.e. S is no short-term test sequence any longer. This step in the procedure development must be understood as a feasibility study. The result was positive: The largest part of the seasonal bias disappeared.

We then looked for short test sequences grouped as much as possible in one single season, however, without loss of prediction accuracy in comparison to the composite sequence S. A selection criterion was needed. It was found that the Solar Load Ratio (SLR) may be a good indicator. Its definition and the considerations having led to its identification are given elsewhere in the present DSTG report [11].

In order to check the choice of the SLR as indicator, we selected among the subsequences S1 to S20 those ones leading to small SLR values, i.e. to a SLR histogram having only the leftmost classes filled (composite test sequence L). Similarly, we defined a further composite test sequence, R, by selection of the subsequences leading

#	h	#	h	#	h	#	h
L1	73	S1	61	S11	87	S21	96
L2	145	S2	73	S12	63	S22	432
L3	146	S3	62	S13	74	S23	96
L4	97	S4	81	S14	45	S24	96
L1'	120	S5	61	S15	50	S25	96
L2'	200	S6	63	S16	76	S26	96
L3'	150	S7	61	S17	50	S27	144
L4'	200	S8	72	S18	98		
		S9	78	S19	50		
		S10	82	S20	77		

Table 2: Skip time (hours) for each test sequence or subsequence listed in Table 1.

to large SLR values. As expected, both L and R led to a seasonal bias in performance prediction. We then added the winter subsequence S10 to spring/summer test sequence R, getting sequence RL. In this way, the seasonal bias was removed.

Becoming confident in the indicator's choice, we looked for shorter sequences on the basis of SLR histograms. Sequence A includes only 20 days (plus additional days at the beginning of each subsequence, as required by the respective skip times), whereas sequence RL had 40 days. Sequence B is still shorter and includes 11 days. Accuracy considerations led us to retain the typical length of 20 days for the next development steps.

The composite sequence A includes data from June and October-November. This is not realistic for short-term testing in practice. Therefore, we looked again at the available spring/summer data and selected among them, independently of S1 to S20, 33 days leading to a SLR histogram similar to that of sequence A. This led to the composite sequence C. Sequence D was obtained from sequence C by reducing the number of days considered to 21, all histogram classes being filled with an equal number of days, 3.

Finally, the University of Munich checked our results, and defined composite test sequence L1234 by simultaneously considering L1, L2, L3 and L4 for parameter identification, however, after partial extension of the skip times according to Program Version 1.17.

4.3 Features common to all development steps

The whole analysis was done with Program Version 1.13. In order to get full compatibility of all results, we avoided the use of subsequent versions which became available in the course of our developments. The standard P-model supplied was used. The selected options were:

Model,Aux,On
Model,DrawOffMix,On
Model,LoadHeatExchanger,Off
Model,SolarStratification,Off
Model,WindCollector,Off

So, 6 system parameters had to be fitted: A_C^*, u_C^*, U_S, C_S, f_{aux} and D_L. The number of local minima searched for was 5 (default value), and the filter time constant 24 hours. No parameter got any fixed value before fitting. All data were preprocessed using successively the programmes SDHWPRE and SDHWP of the dynamic fitting package.

5. RESULTS

5.1 System parameters

Table 3 gives an overview of the fitted parameter values with their standard deviation, together with the expected parameters. It was not possible to include the corresponding cross-correlation coefficient matrices into the present report. Their most important features are refered to in the text.

#	A_C^* m^2	u_C^* W/m^2K	U_S W/K	C_S MJ/K	f_{aux} -	D_L -
Expected	4.5	5.7	7.5	3.1	0.60	?
L1	12.1 ± 0.7	15.9 ± 0.4	7.3 ± 0.5	3.6 ± 0.2	0.73 ± 0.02	0.05 ± 0.03
L2	4.8 ± 0.3	7.7 ± 0.6	6.4 ± 0.4	3.6 ± 0.2	0.72 ± 0.01	0.05 ± 0.02
L3	8.3 ± 1.0	11.0 ± 0.8	7.4 ± 0.8	5.0 ± 0.5	0.79 ± 0.04	0.04 ± 0.07
L4	4.3 ± 0.6	10.7 ± 1.0	7.6 ± 0.5	2.4 ± 0.1	0.71 ± 0.02	0.01 ± 0.01
S=[S1-S20]	11.3 ± 0.9	13.6 ± 0.5	6.9 ± 0.4	3.2 ± 0.1	0.74 ± 0.02	0.06 ± 0.02
L	10.9 ± 1.3	14.5 ± 0.7	7.7 ± 0.5	2.9 ± 0.1	0.72 ± 0.02	0.02 ± 0.01
R	8.3 ± 0.6	13.9 ± 0.4	2.5 ± 0.5	2.8 ± 0.1	0.83 ± 0.03	0.14 ± 0.05
RL	11.3 ± 1.4	13.6 ± 0.6	5.7 ± 0.7	3.6 ± 0.2	0.74 ± 0.04	0.09 ± 0.04
A	9.9 ± 1.1	11.5 ± 0.6	7.8 ± 0.6	2.8 ± 0.2	0.77 ± 0.03	0.04 ± 0.02
B	4.0 ± 2.0	4.9 ± 7.3	8.2 ± 1.2	3.5 ± 0.2	0.69 ± 0.06	0.00 ± 0.08
C	5.0 ± 0.4	8.2 ± 0.7	6.8 ± 0.4	3.0 ± 0.1	0.72 ± 0.01	0.01 ± 0.01
D	4.6 ± 0.5	7.0 ± 1.1	7.2 ± 0.4	2.8 ± 0.2	0.73 ± 0.02	0.01 ± 0.01
L1234	4.3 ± 0.2	4.9 ± 0.5	9.2 ± 0.2	4.3 ± 0.1	0.75 ± 0.01	0.00 ± 0.02

Table 3: Expected and fitted system parameter values with standard deviations

Generally, the predicted values are not satisfactory. They differ from the expected ones and vary significantly from one test sequence to the other. As expected, the largest standard deviation is observed for the shortest sequence, B (11 days). Conversely, the smallest one is obtained for the longest sequence, L1234 (147 days). It has to be mentioned that the expected parameter values are also subject to discussion. The incident angle modifier of the collectors as well as the exact storage tank geometry are unknown. The expected values indicated for A_C^*, C_S and f_{aux} are thus uncertain.

Some of the predicted parameters may be strongly correlated. Which ones are correlated, depends on the test sequence. Especially, A_C^* and u_C^* systematically have cross-correlation coefficients near to 1. It seems that the available data have not enough variability, and that the daily irradiation be correlated to the daily mean temperature difference between collector and ambient. This trend, confirmed by plots of daily values, is typical for *in situ* data recorded in the normal system operation mode.

However, the University of Munich showed by grouping L1 through L4 to the very long test sequence L1234 that the expected parameter values may indeed be approached if the test sequence is long enough, i.e. if enough information is available from the input data for parameter identification. Clearly, the on-line preprocessing applied to our data at monitoring time, as mentioned in Section 3, negatively influences the parameter identification. So, no conclusion can be drawn from the parameter identification part of our study, except that realistic parameters may indeed be identified even *in situ* in the normal system operation mode. Different data including the full system dynamics are required to determine the length of the test sequence needed and the related accuracy limit of parameter identification. Let us recall that system parameter identification *per se* was not the primary purpose of our investigations (see Section 1.2).

5.2 Ability to accurately predict the long-term energy balance

In this section, we present the results corresponding to the main objective of our work, defined in Section 1.2. As described in Sections 4.1 and 4.2, we checked the ability to accurately predict the long-term energy balance by comparing measured and predicted values of the average net system power, $\overline{P}_{net}$, for various sequences using parameter values obtained from different test sequences. (Obviously, the $\overline{P}_{net}$ prediction error has to be nearly zero if the energy balance is calculated for the sequence just having been used for parameter identification. Otherwise, the Model P or the number of system parameters fitted is not adequate, as indicated in Part A of present DSTG Final Report.)

5.2.1 First steps with Sequences L1 to L4 and composite sequence S

The first prediction accuracy checks, based on sequences L1 to L4, led to the observation of a seasonal bias (Table 4 and Fig. 5). Large $\overline{P}_{net}$ prediction errors of 24 to 76 W are observed when the energy balance is calculated for a sequence using parameters from a sequence in a different season. Conversely, small $\overline{P}_{net}$ prediction errors of 6 to 22 W occur when both sequences belong to the same season. However, no seasonal bias is observed using parameters from L3, the longest sequence selected. In this case, the observed $\overline{P}_{net}$ prediction errors of 6 to 11 W for the 3 sequences L1, L2 and L4 are all acceptable.

In the next step, the composite all-year-round test sequence S was used for parameter identification. The $\overline{P}_{net}$ prediction errors calculated for L1 through L4 lie between 14 and 32 W. $\overline{P}_{net}$ is overestimated in autumn and underestimated in spring/summer, the amplitude of the error being no longer dependent on the season. Clearly, one crucial factor governing the accuracy of the energy balance prediction is the distribution of the main input variables "heat load" and "irradiation" within the test sequence; the daily values of these quantities were used to select the data for composite sequence S (see Section 4.2). If in the test sequence these variables cover the whole range of values encountered in a year, then, for any period, the input variables vary within the input variable range of the test sequence and no extrapolation is made when calculating the energy balance.

Sequence for parameter identification	Sequence for energy balance prediction			
	L1	L2	L3	L4
L1 (Sept.9-Oct.14)	(0 W)	-53 W	-27 W	+12 W
L2 (Apr.10-May 20)	+24 W	(-1 W)	+6 W	+51 W
L3 (May 28-Aug.7)	+11 W	-6 W	(0 W)	+11 W
L4 (Oct.20-Nov.4)	-22 W	-76 W	-41 W	(+4 W)

Table 4: Prediction error (= predicted value – measured one) for the average net system power, $\overline{P}_{net}$. The seasonal bias is obvious.

Hence, test sequences may be selected in spring and summer, but not in autumn or winter. Very low irradiation values typical for winter time may be namely encountered also in spring or summer, whereas the very high ones typical for spring and summer are not observed in autumn and winter.

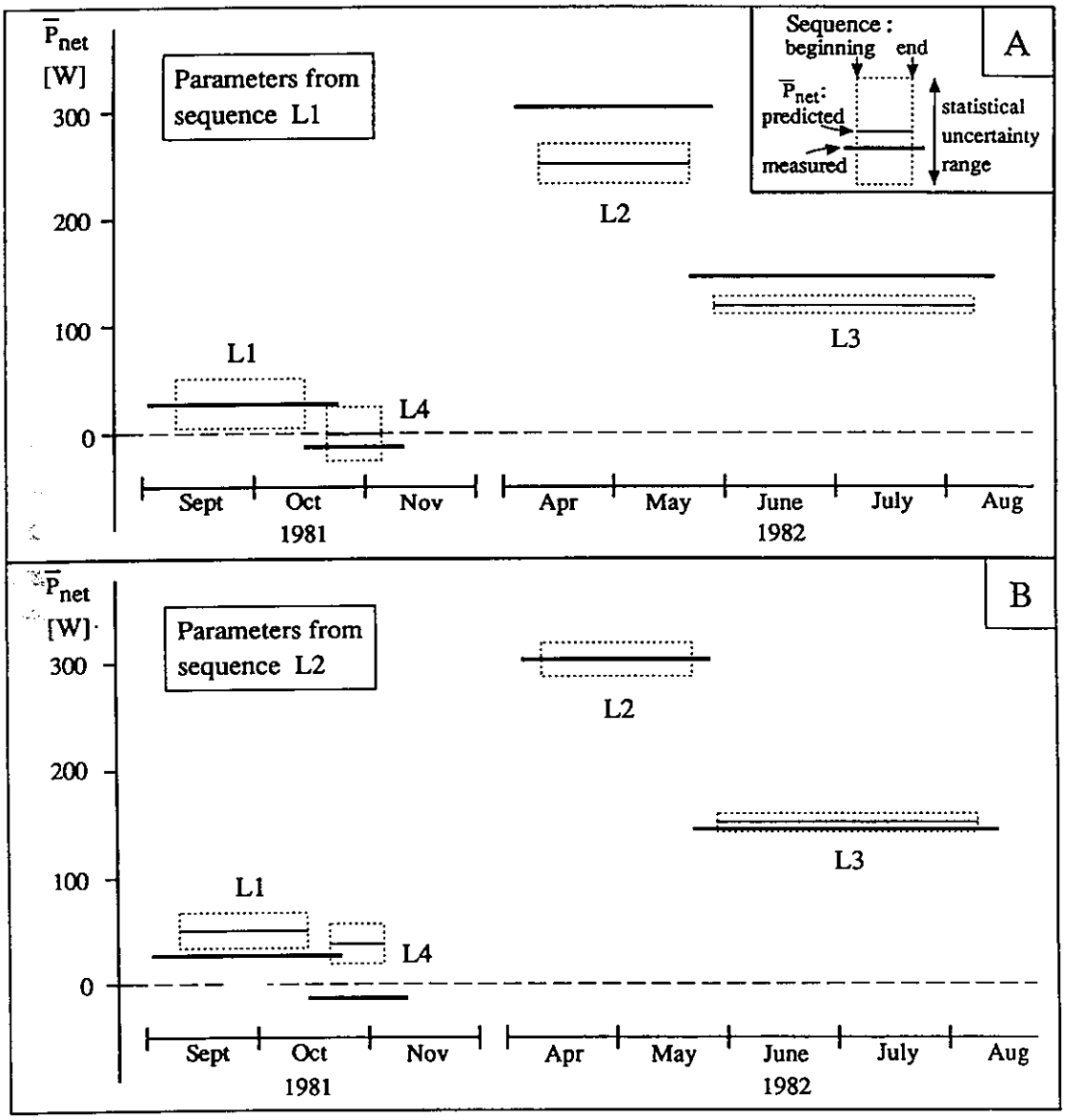

Fig. 5: Measured and predicted $\overline{P}_{net}$ with standard deviation, for parameters identified using test sequence L1 (Fig. 5A) or L2 (Fig.5B). This representation shows the sequence length, the seasonal dependence of $\overline{P}_{net}$ as well as the $\overline{P}_{net}$ prediction error for each sequence. Sunny periods have a positive $\overline{P}_{net}$, periods with winter conditions a negative one.

5.2.2 Getting confident in the solar load ratio

The next test sequence considered, the composite one called L (Table 1), is made of 13 short sequences from the composite sequence S, all having small values of the Solar Load Ratio (SLR, or H_tA_C/Q_L) : $-1 < \text{Log}(H_tA_C/Q_L) < 1$. As indicated in Table 5 and confirmed by further results not displayed, $\overline{P}_{net}$ deduced from parameters obtained with L is underestimated in spring and summer (sequences L2 and L3) and slightly overestimated in autumn and winter (sequences L1, L4, S8, S9 and S10).

As expected, just the contrary happens with the composite sequence R made of 6 short sequences from the composite sequence S all having large SLR-values: $0.25 < \text{Log}(H_tA_C/Q_L) < 2.25$. For the winter sequences, large $\overline{P}_{net}$ prediction errors are observed, the (negative) $\overline{P}_{net}$ beeing overestimated, whereas the spring/summer sequences lead to acceptable prediction errors (Table 5).

Hence, both sequences L and R just show the seasonal bias expected from the SLR-range covered.

Sequence for parameter identification	Sequence for energy balance prediction						
	L1	L2	L3	L4	S8	S9	S10
L(-1<Log SLR<1)	+14	-33	-21	+23	+20	+10	+14
R(0.25<Log SLR<2.25)	+46	-9	+12	+82	+51	+94	+102
RL(-1<Log SLR<2.25)	+41	-1	+3	+63	+21	+22	+19
A(-0.5<Log SLR<1.5)	+18	+4	0	+20	+12	-5	-4
B(-0.25<Log SLR<1.25)	+20	+13	+9	+47	+33	+3	+6
C(-0.1<Log SLR<1.25)	+31	+5	+4	+55	+39	+23	+30
D(-0.1<Log SLR<1.25)	+28	+11	+7	+51	+38	+18	+26

Table 5: Prediction error for $\overline{P}_{net}$ (= predicted value – measured one), in W, obtained using parameters from various sequences, for the long sequences L1-L4 and for the winter short sequences with the poorest solar irradiation, S8-S10

The results for the composite test sequence RL obtained by adding short sequence S10 to sequence R indicate that the parameters deduced from RL predict the winter energy balance as accurate as those from sequence L (Table 5). Thus, the addition of S10 to R, which significantly extended the SLR-range on the left side, removed the largest part of the seasonal bias characterizing sequence R.

It may seem strange to solar energy specialists that the winter energy balance be so important. Let us recall that in Switzerland SDHW heating systems have a typical

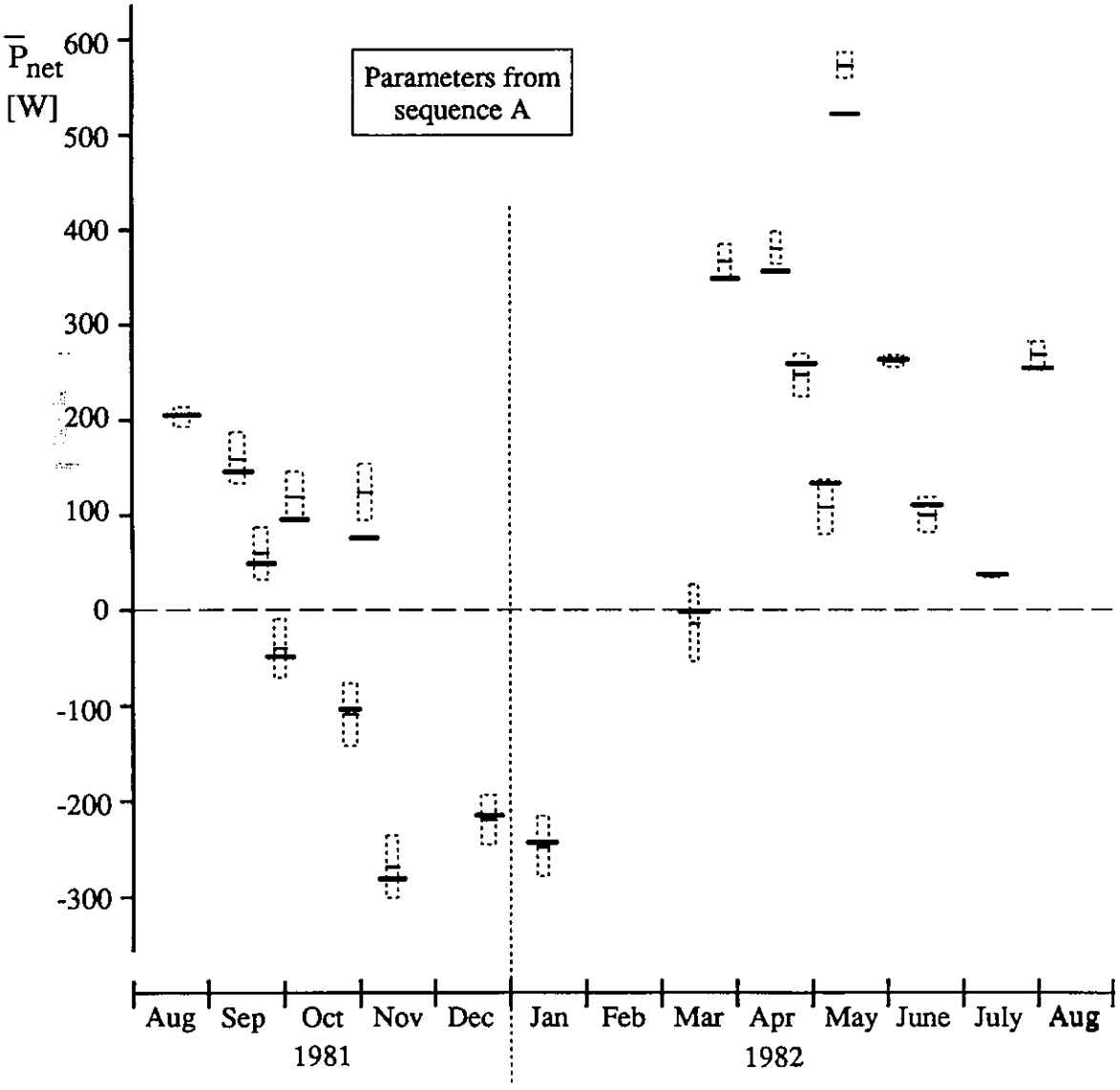

Fig. 6: Measured and predicted $\bar{P}_{net}$ with standard deviation, for parameters identified using test sequence A. See also Fig. 5.

yearly solar fraction of 50 to 60%. Hence, the yearly auxiliary energy consumption is of the same order of magnitude as the yearly collector heat output and has to be predicted as accurately as the latter.

5.2.3 Test sequence optimization for practical use

The influence of test sequence length was investigated using composite test sequences A and B which both cover nearly the same optimal SLR-range (Table 5). B, however, has only half the number of days of A. The $\overline{P}_{net}$ prediction error is quite acceptable for A (Fig. 6), and somewhat larger for B. However, the standard deviation of $\overline{P}_{net}$ is much too large for sequence B, ±60 to ±80 W, compared to ±10 to ±30 W for sequence A. Sequence B is too short (11 days).

For composite sequence C, we selected spring/summer data according to the practical selection rules described in [11], from as short as possible a period. For System #12 with auxiliary heating only during the night, the selection rules only involve system design features. For the lower SLR-range limit, the withdrawal volume was assumed to be equal to the auxiliary heated part of the storage tank (440 l); assuming a demand temperature of 50 °C and a mains temperature of 10 °C, a daily load of 21 kWh/d is obtained. With the daily irradiation of 1.5 kWh/m²d, one gets $\text{Log}(H_t A_C/Q_L) > -0.078$. For the upper SLR-range limit, the withdrawal volume was assumed to be 5 times smaller (90 l, i.e. 20% of the auxiliary heated storage volume) and the irradiation 4

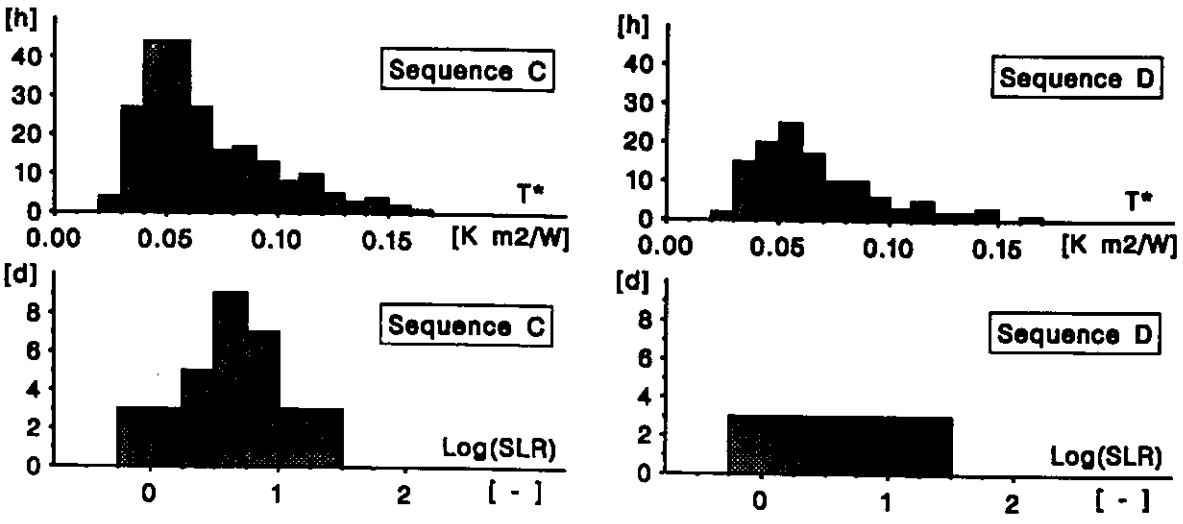

Fig. 7: Histograms of $T^*=(T_C-T_{CA})/G_t$ (hourly values) and $\text{Log}(H_t A_C/Q_L)$ (daily values) for test sequences C and D

times higher (6 kWh/m²d). For System #12, the latter value is large enough to heat up 300 l of water from 10 to 50 °C in one day (14 kWh/d, rounded to 20 kWh/d to compensate for the store losses). The collectors have an efficiency of 29% at the corresponding operation temperature. One gets then $Log(H_t A_C/Q_L) < 1.22$ from these data. Hence, the extent of the required SLR-range is a factor 20 (Fig. 7). This is less than the SLR-range of sequence A (2 decades).

The $\overline{P}_{net}$ prediction errors observed with parameters from sequence C, 4 to 55 W for L1-L4 are comparable to those given by sequence RL, the SLR-range of which extends over 3 decades, but the standard deviation of $\overline{P}_{net}$ is smaller, ± 8 to ± 18 W instead of ± 10 to ± 40 W for RL. Sequence C includes data from April/May (24 days) which have been supplemented by a 9 days period in July with four days of very bad weather ($H_t < 1.5$ kWh/m²d). This is a realistic short term test sequence applicable in practice. On the contrary, sequence RL includes winter, spring and summer data, an unrealistic combination in practice.

5.2.4 Final checks

Coming back to the long sequences L1 to L4, we calculated their SLR-histograms (Fig. 8). For autumn sequences L1 and L6, Log(SLR)-values above 1 are missing and this explains the underestimation of $\overline{P}_{net}$ in spring/summer when using the parameters identified with L1 or L4 (Table 4). Conversely, only one negative Log(SLR)-value is

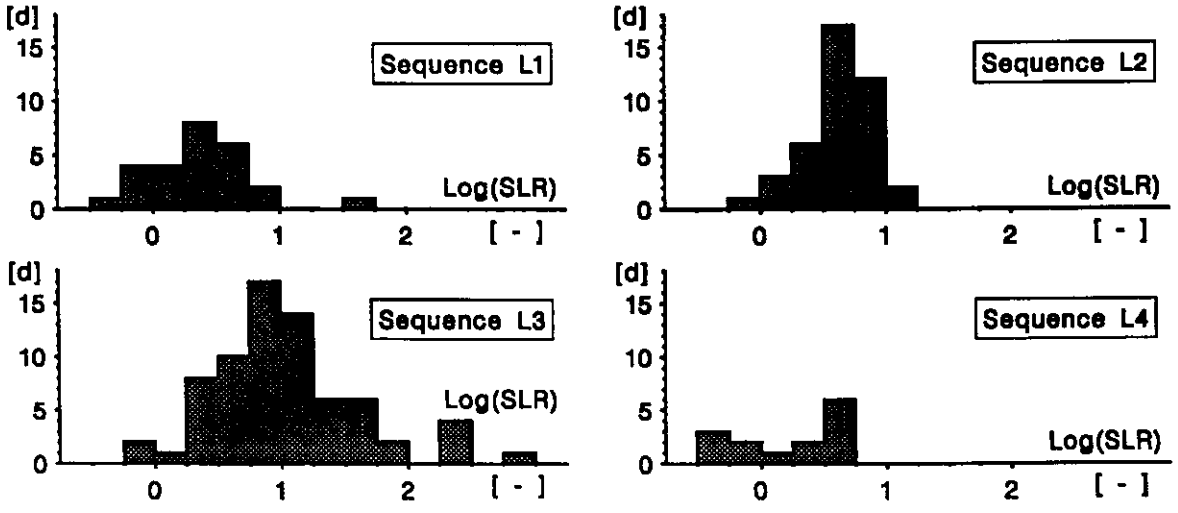

Fig. 8: SLR-histograms for the long test sequences L1 to L4

present in the histogram of sequence L2. This accounts for the overestimation of the $\overline{P}_{net}$ in autumn when using parameters from sequence L2 (Table 4). Sequence L3 without seasonal bias has an unnecessary high number of high SLR-days. However, it includes more days with negative Log(SLR)-value than sequence L2. These are especially the July days with very bad weather. Hence, the correlation between the presence or the absence of seasonal bias and the SLR-histograms is confirmed by the analysis of sequences L1 to L4.

The last test sequence D considered was obtained from composite sequence C by taking out single days in order to get an equal number of days, 3, in each SLR-class in the histogram (Fig. 7). Class width is 0.25 in the logarithmic scale. The total number of days involved in sequence D is 21 (C: 33). The observed $\overline{P}_{net}$ prediction errors are improved by about 10% in comparison to sequence C: The larger errors are reduced, the smaller ones enhanced. The standard deviation of $\overline{P}_{net}$ remains unchanged. The progress introduced by taking out single days from sequence C is thus questionable. Because of the gaps created, the construction of sequence D from the original data is much more complicated than for sequence C. Let us recall that each subsequence included requires a skip time and corresponding additional data not mentioned in the extent of the sequences indicated by Table 1. If further studies show that a homogeneously filled SLR-histogram is a real advantage for short-term testing, the complicated sequence construction could also be avoided by modifying the fit programme. The skip process should be also possible for single days in the main body of a test sequence, whereas at the present time only initial days of a sequence may be skipped.

Fig. 7 also includes hourly histograms of $T^*=(T_C-T_{CA})/G_t$, the variable which determines the collector efficiency. As indicated in Fig. 4, the collector operation temperature and the collector heat output were also available from the original data base. We used this fact to check whether T^*-histograms have to be involved parallely to SLR-histograms when selecting the test sequence. It turned out that this is not necessary. The conditions imposed in order to get an optimal SLR-histogram are more restrictive than for T^*-histograms. Good T^*-histograms are characterized by the typical shape indicated in Fig. 7. The whole T^*-range from the leftmost values (giving a high collector efficiency) to the rightmost ones (corresponding to nearly stagnation and strongly reduced heat output) is covered even if the corresponding SLR-histogram is unacceptable. Hence, intrusive measurements to get the collector heat output and its operation temperature may indeed be avoided even in *in situ* measurements.

6. CONCLUSIONS

The ability to accurately predict the long-term energy balance has been studied in details using data from a one year monitoring period for System #12 in the normal operation mode. The system parameters have been identified from various test sequences including also composite ones with data from all seasons. Then, the energy balance has been calculated for periods different from those used for parameter identification.

In several cases, an unacceptable seasonal bias in the predicted energy balance has been observed. In other cases, the seasonal bias was not present. Rules governing its presence or absence were identified. They include the use of daily histograms of the logarithm of the solar load ratio (SLR) defined as the ratio of the total irradiation of the collector array to the hot-water heat load. The relevant SLR-range to be covered in optimal test sequences is determined from design features of System #12 according to a procedure described elsewhere [11]. In a future application of this data selection criterion to *in situ* testing in practice, SLR-histograms could be calculated already at monitoring time, allowing for automatic stop of the monitoring process when enough data have been recorded.

Due to an unfavourable preprocessing having occured already at monitoring time, the hourly data available for System #12 do not reflect the full dynamics of system behaviour. This was a major disadvantage in our analysis. So, the time related aspects of our conclusions as, e.g., the minimum length of the required test sequence are questionable and should be reexamined in further studies on the basis of really dynamical data. We suppose that the test period may be significantly shortened in comparison to the sequences we used.

In our study, we assumed that the (unknown) incident angle modifier of the collectors be equal to 1. Experience from other DSTG participants showed that such an approximation is of minor importance for south facing flat plate collectors with a tilt angle nearly equal to the local latitude. The collectors involved in our study had similar azimuth and tilt angle, but a much more complicated glazing structure. Despite the latter fact, it seems from our study that the effect of the neglected incident angle modifier be of second order as well.

Finally, we examined the feasibility of the correct determination of the physical system parameters by the fit programme under *in situ* testing conditions in the normal operation

mode of the system. This turned out to be a much more difficult challenge than the ability to accurately predict the long-term energy balance. Even unrealistic system parameters identified from some test sequence fulfilling the SLR-histogram condition may be used for accurate long-term prediction. However, the proper identification of the physical system parameters requires the full dynamical information on the system not available in our data. Therefore, in our case, only a very long test sequence (147 days) allowed for somewhat satisfactory, physically meaningful parameter values.

NOMENCLATURE (Additions to the general nomenclature)

A_C collector array aperture [m^2]

$\overline{P}_{net}$ average net system power = power delivered to the load – auxiliary power, averaged over the sequence which the energy balance is calculated for [W]

H_t daily solar irradiation in the collector plane [kWh/m^2d]

Q_L heat delivered daily to the load [kWh/d]

Log decimal logarithm

SLR solar load ratio = H_tA_C/Q_L [dimensionless]

T_C collector temperature = mean fluid temperature in the collector [K]

T^* parameter determining the collector efficiency, $T^* = (T_C - T_{CA})/G_t$ [$K\ m^2/W$]

$F'U_L$ collector thermal loss factor, obtained by collector testing [W/m^2K]

η_0 collector optical efficiency, obtained by collector testing [dimensionless]

REFERENCES

[1] B. Schläpfer, P. Schneiter, *Kurztestmethode für Sonnenenergieanlagen. Schlussbericht über das Vorprojekt Nov. 1985 bis Mai 1986*
Swiss Professional Association of Solar Energy Firms (SOFAS), May 1986 (in German)

[2] *Summary of National Approaches to Short-Term Testing of Solar Domestic Hot Water Systems*
Report no. T.3.E.1 of the Solar Heating and Cooling Programme of the International Energy Agency (IEA), December 1987, Chapter 2.10, pages 40-42

[3] Volume A of the present DSTG Final Report, Chapter 2.2.2 *Description of the solar domestic hot water system model.*

[4] J. Habegger, *Solare Wassererwärmungsanlagen (Schlussbericht)*
EIR Würenlingen, January 1984 (in German)

[5] J.-M. Suter, P. Kesselring, *Measurements of performance and efficiency of solar energy systems*
Proceedings of the ISES Silver Jubilee Congress, Atlanta (USA), May 1979, pages 1435-1439

[6] M. Rauber, *Sonnenenergieanlage Frick, Winterthur. Schlussbericht über die Messungen an einer Sonnenenergie-Warmwasseraufbereitungsanlage im Schweizer Mittelland*
TM-33-83-4, EIR Würenlingen, 1983 (in German)

[7] Swiss Standard SN 165 001/1, *Methods of Testing to Determine Thermal Performance of Solar Collectors. Part 1: Covered Collectors Using Liquids as Heat Transfer Fluids*
Swiss Association for Standardization, Zurich, 1984 (in German and French)

[8] P. Kesselring, J.-M. Suter, *The EIR method for collector testing*
Appendix A of report *Results and analyses of IEA round robin testing*, IEA Solar Heating and Cooling Programme, Task III *Performance Testing of Solar Collectors*, KFA Jülich ed., Dec. 1979

[9] M. Gstir, *Erprobung und Weiterentwicklung einer Kurztestmethode für solare Wassererwärmungsanlagen. Praktikumsbericht*
TM-51-90-15, PSI Villigen, 1990 (in German)

[10] M. Bolsinger, *Erprobung und Weiterentwicklung einer Kurztestmethode für solare Wassererwärmungsanlagen. Praktikumsbericht*
TM-51-91-07, PSI Villigen, 1991 (in German)

[11] J.-M. Suter, *The Solar Load Ratio, an Indicator for the Ability of a Test Sequence to allow for Subsequent Accurate Prediction of the Annual System Performance*
Contribution to the present DSTG report, Volume A.

DYNAMIC FITTING WITH IN-SITU MEASURED DATA FROM THE LARGE MALUNG SYSTEM

Bengt Perers
Vattenfall Utveckling AB
c/o Miljökonsulterna
P.O. Box 154, 61124 Nyköping
Sweden

1. INTRODUCTION

The IEA-DSTG method has been tested with in-situ data from a large solar domestic hot water and heating system for 125 flats with 600 m^2 flat plate collectors and 100 m^3 short term storage. The annual solar fraction is presently limited to about 10% to avoid dumping of energy in the summer.

Before the collector field was installed off-peak electricity via the 100 m3 storage was used as the only heat source. The electric boiler is now used as auxiliary heater. The heating system in the houses was already from the beginning designed for low temperature operation. This was done to minimize the size of the pressurised storage. The low temperature heating system is an advantage also for the solar energy system.

Figure 1 shows a drawing of the system with measurement points indicated. The solar heating system was added afterwards. This gives a quite complicated system lay-out.

A prototype pit seasonal storage is under test in Malung. If the test is successful the storage and collector field can be expanded to a seasonal storage system with a high solar fraction.

The latitude of Malung is 61°N. This evaluation was limited to a period from April to October to avoid data with snow cover on the collectors. Hourly data from 1989 were used for the test. The measurements were made by the Royal Institute of Technology in Stockholm according to the specifications in the IEA SHAC Task VI reporting format for Solar Energy Systems [1].

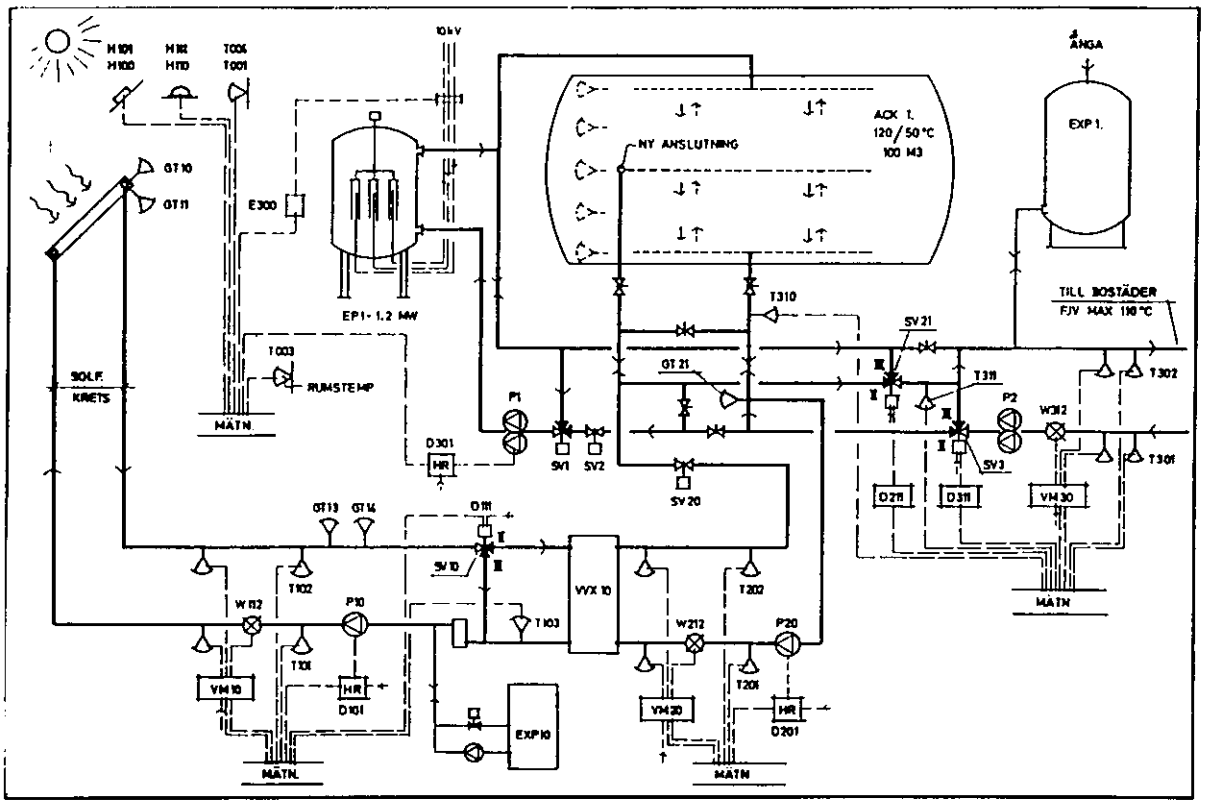

Figure 1: The Malung system with measurement sensor location. The storage is placed outdoors.

The system is a combined hot water and heating system whereas the DFP model is a pure SDHW system model. The return temperature T301 from the district heating network was used as cold water (mains) temperature and the forward flow in the district heating network W312 was used as load flow. T302 was used as forward temperature to the load.

The detailed requirements of the IEA-DSTG method were not known at the time of the measurements. The load side forward temperature is measured after the mixing valve. This means that information is lost for the DFP model. Therefore parameter values that differ somewhat from the system design data could be expected.

Moreover, two operating modes for the auxiliary are present due to the large seasonal variation in the heating load. For summer operation, only the upper half of the storage is heated by auxiliary. During the rest of the year, the whole storage can be heated by the auxiliary. A seasonal variation in f_{aux} could be expected.

All the data have been reprocessed with the IEA-DSTG program version 1.17 for this

report. Monthly data sets of hourly mean values have been used. These have been checked with the SDHWP routine and also with efficiency and input-output diagrams on hourly and daily basis. Except for a long data gap in July and a location dependent inaccuracy in outdoor ambient temperature measurements no errors were found in the database.

2. RESULTS

When looking at the residuals as function of time the IEA-DSTG method gives results very close (± 10%) to the measured net power output P_{net} (= P_L - P_{aux}); see Figures 2a and 2b. The large negative peaks in P_{net} involve the off-peak boiler with a maximum power of 1 MW.

The negative time is the skip time used to estimate the initial state of the storage. The first 8 days (192 hours) in each monthly data set are skipped from parameter identification. This period is still required for the program to identify the internal state of the storage before the fit procedure starts.

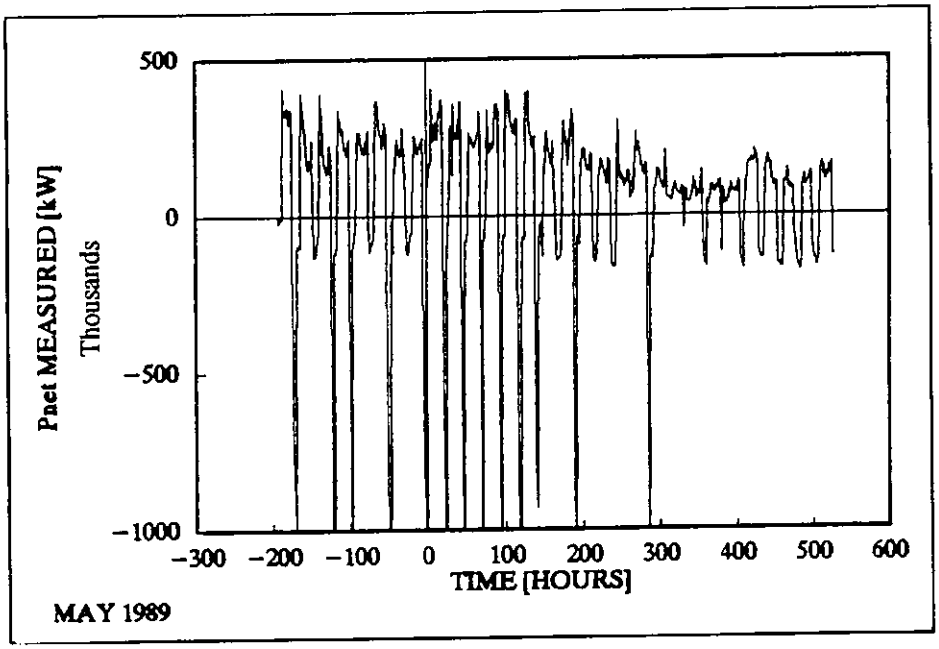

Figure 2a: Measured net system power as a function of time for May 1989.

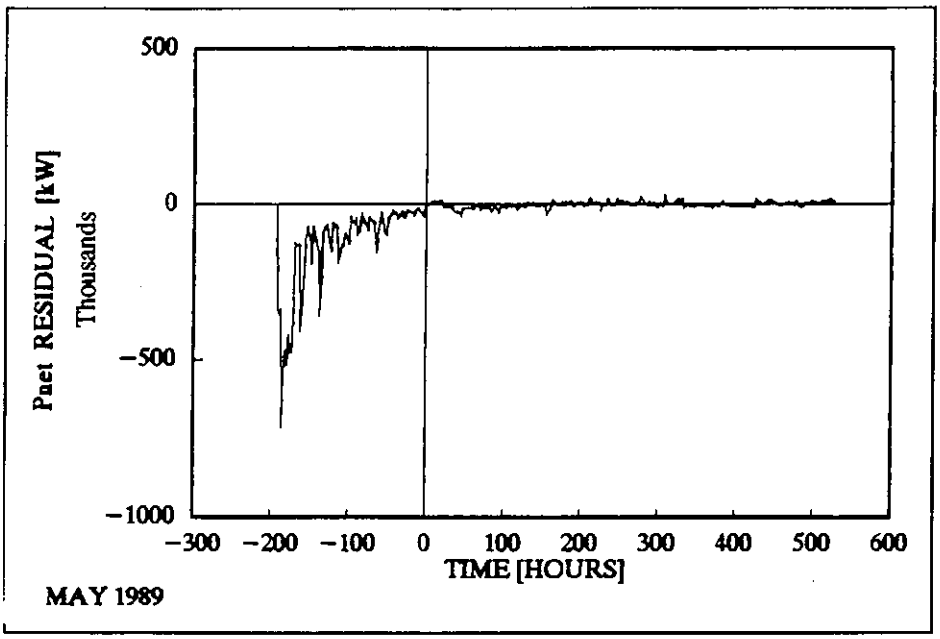

Figure 2b: Residual as a function of time for May 1989.

The absolute parameter values derived with the program are of the correct magnitude, but they are not as close as one would expect from the very good model fit in Figure 2b. The parameter values for 192 hours skip time are given in Table 1 together with the expected values.

Table 1: Comparison of parameter values month by month derived with the DFP program for the Malung system; skip time = 192 h, filter time = 24 h.

test period	A_C^* [m^2]	u_C^* [W/m^2K]	U_S [W/K]	C_S [MJ/K]	f_{aux} [-]	D_L [-]	S_C [-]	Obj. [W]
expected	420	3	75	400	0.5	-	-	
April	133	4.0	90	2180	0.79	0.12	0.0	8660
May	235	3.4	65	1720	0.88	0.08	0.15	2840
June	1310	12.9	15	1150	0.88	3.83	0.03	4250
July	491	9.3	47	915	0.46	5.00	2.55	1790
August	326	9.6	292	684	0.96	0.02	0.67	6470
September	303	4.6	163	981	0.97	0.03	0.13	3750
October	235	3.3	25	2050	0.83	0.05	0.06	2670

Some comments should be given to the parameter values. The systematic seasonal effects which can be seen in Table 1 can be correlated to the large change in heating load during the period. Moreover, two operating modes for the auxiliary heater are involved which should influence the stratification parameters and the auxiliary fraction of the storage f_{aux}. The overestimation of the storage capacity can be due to the mixing valve before the forward load temperature sensor. This probably gives a too low top storage temperature in the fit program. It should also be pointed out that the net solar contribution which is modelled by the IEA-DSTG program is the difference between a large load and a large auxiliary in this case. This leads to a limited accuracy in this parameter, especially for the autumn and spring when the solar fraction is low.

3. SOLAR LOAD RATIO

The daily Solar Load Ratio has been shown to be a good indicator for how representative the data set is for the long term operation. Daily values for each month has been sorted and plotted in Figures 3a and 3b. The distribution for the whole period from April to October is also given.

The distribution in the Solar Load Ratio diagram (Figures 3a and 3b) is dependent on the sizing of the collector area compared to the load. In this case May, August and September have distributions close to the seasonal distribution. The other months have distributions that are peaked towards the low range (April and October) and towards the high range (June and July) as could be expected due to the variation of the heating load and insolation.

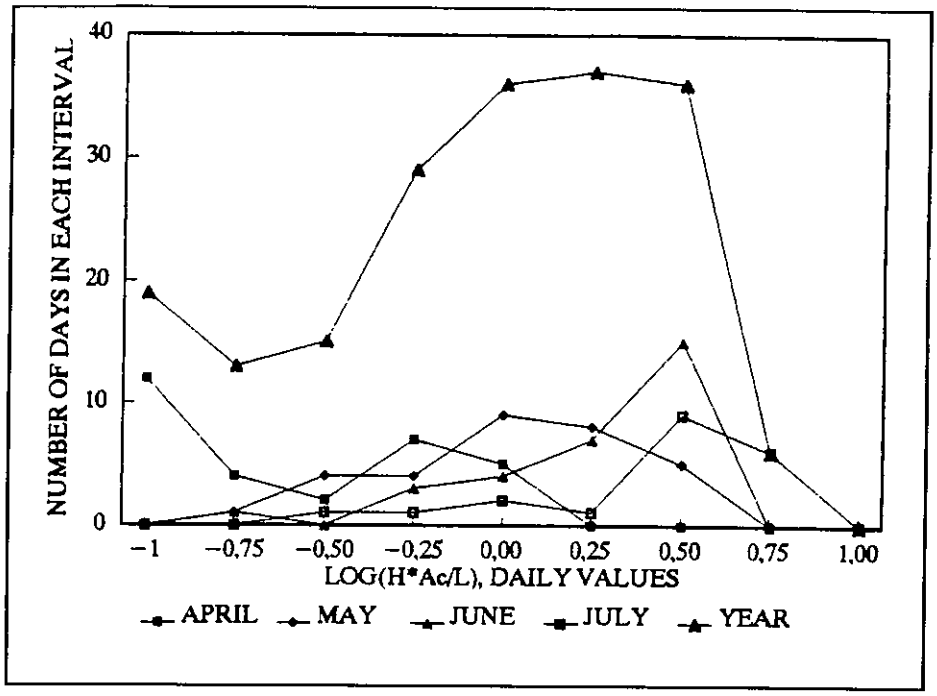

Figure 3a: The distribution of Solar Load Ratio month by month from April to July. The distribution for the whole period April-October is also given.

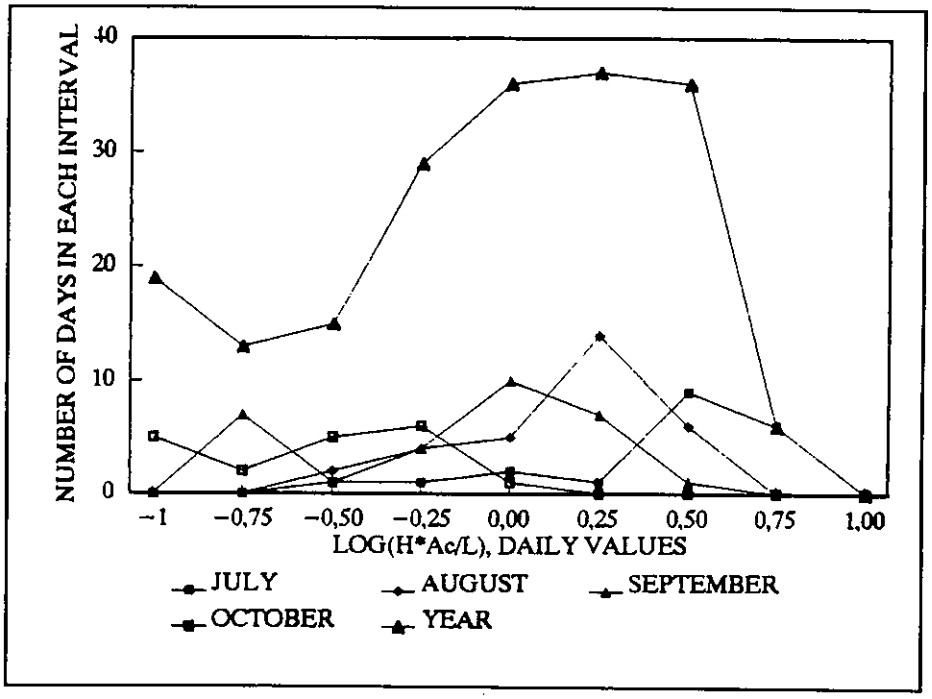

Figure 3b: The distribution of Solar Load Ratio month by month from July to October. The distribution for the whole period April-October is also given.

4. LONG TERM PREDICTION

To give an indication of the long term accuracy of the DSTG method in this case the monthly and seasonal sum of P_{net}, measured and modelled, has been plotted in Figure 4. Two bars are given for the model fit, one with parameters from the same month and one with parameters from May, with a good solar load ratio distribution.

Due to data gaps mainly in July it was not possible to run the whole period in one run with the LTPP program. Instead the fit program (DFP) output data has been summed for each month, excluding the data from the skip time.

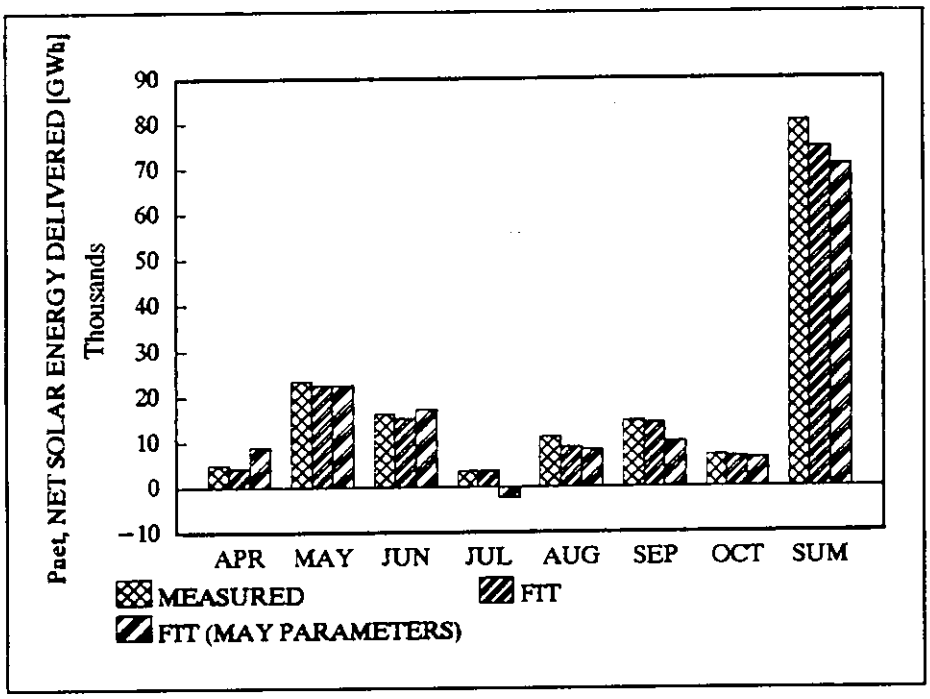

Figure 4: Check of the long term prediction accuracy of the DSTG method for the Malung system.

It can be seen that the accuracy is in the range ± 15% for the seasonal prediction also when using parameters from a single month (May). For the individual months, the difference between measurement and model is larger as can be expected from the difference in system type and sensor location compared to the IEA-DSTG specification. The low values for July are due to a long data gap.

5. LESSONS LEARNED

5.1 Ambient temperature measurements

The data check in the program SDHWP is very useful. No errors were found for the data presented. But one lesson learned was that the method does not warn you for all mistakes in the input data.

A good fit and near expected parameter values were achieved also with a completely wrong storage ambient temperature. The indoor temperature in the heating central was used by mistake for the tank ambient temperature. In spite of this the fit was very good and the parameter values were near the expected values!

The outdoor temperature sensor was also checked. It was placed close to the tank facing north but on a wall which was heated by reflected light from the tank aluminium enclosure. A temperature difference of up to 8°C was observed for 1 hour mean values on days with high insolation between this sensor and the meteorological station in Malung [2].

At the Studsvik Solar Testfield, investigations have been made with different ambient temperature sensor designs and locations. It was found that a location in the shadow behind the collector is almost as good as a reference sensor with forced ventilation [3].

Standard radiation shielding with natural ventilation can give very large errors (5-10°C), especially at low wind speeds and high insolation levels. (This can for example result in an apparent wind speed dependency in the collector performance).

As this IEA-DSTG method is aiming at DHW systems which have comparatively low ambient to operating temperature differences the accuracy of the ambient temperature measurement plays a significant role to give reliable model parameters.

5.2 Solar radiation measurements

When using all day solar radiation data it becomes much more important with the sampling frequency and the pyranometer mounting than for standard collector testing at near normal incidence and with stable irradiation.

Just from geometrical effects, the measurement error of a pyranometer which is not exactly

parallel to the collector plane can well exceed the advantage of a first class pyranometer. A 2° error gives a measurement error of almost 5% at 50 degree incidence angle. One degree corresponds to a slope of 1.8 mm for a 100 mm length.

The sampling frequency for the pyranometers is very important when using outdoor data with rapidly changing solar radiation. A sampling interval of less than 6 seconds is used by the Swedish Meteorological and Hydrological Institute (SMHI) for their solar radiation network. A comparison, between a Kipp & Zonen solar integrator and a high class measurement system with a too long sampling interval of 120 seconds showed that a random error in hourly mean values of ± 10% can occur for hours with variable cloudiness. For 10 minute mean values for example the sampling frequency will be even more important.

6. CONCLUSIONS

The test with Malung data clearly shows that the IEA-DSTG method has the potential to be used also for large systems and for in-situ measurements. The IEA-DSTG method gives a good model fit but the derived parameter values differ quite much from the expected values. The difference in parameter values could be expected due to the difference in actual system design compared to the P model and the difference in load forward temperature measurements compared to the specifications for the IEA-DST method. Also the time resolution of one hour in the data was too low according to the recommendations.

Placing and radiation shielding of ambient temperature sensors should be done with great care. Measurement errors of 5 - 10°C may easily occur otherwise.

Further work is required to add options in the program for systems with a combination of domestic hot water and heating load.

REFERENCES

[1] Chandrashekar, M. and K.M. Vanoli.
Data Collection and Performance Reporting - Specification for Solar Energy Projects. Document: IEA SH&C Task VI - 2. 1986.

[2] Personal communication with Sven Erik Persson VVS.
Planering Falun, Sweden.

[3] Booster Mirrors for Large Solar Collector Fields.
Studsvik Report to be published.

DYNAMIC SOLAR COLLECTOR PERFORMANCE TESTING

J. Muschaweck

Ludwig-Maximilians-Universität München
Sektion Physik
Amalienstr. 54
D-8000 München, FRG

(The following paper has been submitted to Solar Energy Materials & Solar Cells)

1 Abstract

A dynamic solar collector model in conjunction with a dynamic parameter identification and performance prediction method is presented. It promises to make possible solar collector (loop) testing under instationary outdoor meteorological conditions, variable inlet temperature and variable volume flow rate. Measurements for three test sequences were made outdoors under instationary conditions on a 6 sq. meter flat plate collector array with double glazing. A multi-node model with three parameters (effective area, effective loss coefficient and thermal capacity) is used. Collector parameters are determined for one sequence and the collector performance is then predicted for the remaining two sequences using the same model with the already determined parameters. The error of predicting the temperature difference across the collector, averaged over a sequence, is found to lie at or below 0.2 K. A computer program package providing the parameter identification and performance prediction algorithms as well as the collector model is available.

2 Introduction

Several countries have developed standards for solar collector performance testing [1, 2, 3]. Collector performance test methods use a parametrized model and some sort of parameter identification method to match the model as closely as possible to some set of measured data points. For flat plate collectors, the optical efficiency (and possibly its angular dependence) and the thermal loss coefficient (possibly as linear function of the difference between ambient and inlet temperature) are commonly determined.

Within stationary models, the inertia of the collector is neglected. For steady-state conditions (constant inlet and ambient temperature, wind speed, irradiance and fluid flow rate), the thermal capacity of the collector has no effect on its performance; therefore, stationary methods require steady-state or quasi-steady-state conditions for each data point.

For outdoor measurements, steady-state conditions are often difficult to obtain. This makes collector tests more expensive: Either an indoor test facility must be used or one

has to wait until steady-state conditions occur. Also, collectors usually do not at all operate under steady-state conditions. Thus, steady state test conditions are not typical of normal operation.

A test method that incorporates dynamic collector properties not only yields more information about the collector, but makes collector testing easier to perform experimentally. Thus, testing is made less expensive, while the model and the computation procedures will be more complex. However, the model and the computation procedure must be developed only once, while experimental expense must be made for each test.

For most solar system layout tools, e.g. f-Chart [4] or TRNSYS [5], parameters that describe dynamic collector properties are "nuisance" parameters [6]: they are only used to reduce modelling errors to a level where the more important parameters can be easily determined. However, TRNSYS could easily be extended by a dynamic collector model.

Some dynamic models have already been proposed. Wang, Xu and Meng [7] propose an approach using filter methods and a second-order differential equation. They show that the stationary collector parameters can be determined with sufficient accuracy even for days with strongly varying irradiance. Emery and Rogers developed the British collector test standard [8] that allows slow variations of the ambient temperature and uses the collector step response to model the influence of varying irradiance. However, [7, 8] require constant inlet temperature and constant flow rate during the test.

Perers et al. [9] apply multilinear regression methods to one hour average values. They report good agreement between measurement and their one node model for constant flow rate, constant inlet temperature but strongly varying irradiance.

The method outlined below allows arbitrary variations of irradiance, ambient temperature, inlet temperature and fluid flow rate during the test and thus puts no principal restrictions on the test sequence. The multi-node model used in this paper is a first approach and has been validated only for a certain type of flat plate collectors. But the parameter identification and performance prediction method used here is not restricted to a specific model: it can be (and has been) used with different and/or more complex models.

3 The Method

The parameter identification method used in this paper has been developed by Spirkl [10] as a short term test method for solar domestic hot water (SDHW) systems. The same method is used in this paper in conjunction with a collector model instead of the SDHW system model.

The method is outlined shortly in the sequel.

A system is exposed to input data $\mathbf{e}(t)$ as function of time. The internal system state $\mathbf{z}(t)$ is described by a differential equation

$$\dot{\mathbf{z}} = \mathbf{f}(\mathbf{z}(t), \mathbf{p}, \mathbf{e}(t)) \tag{1}$$

and a set of parameters $\mathbf{p}$. The vector $\mathbf{z}(t)$ itself is, in general, not accessible to measurement and its measurement is not needed[1].

For given input data $\mathbf{e}(t)$, due to Eqn. 1 the scalar modelled system output $P_{mod}(\mathbf{p}, t)$ as function of time depends solely – and not necessarily linearly – on the parameters $\mathbf{p}$. $P_{mod}(\mathbf{p}, t)$ is compared to the measured system output $P_{exp}(t)$ yielding the residual $r(t) = P_{mod}(\mathbf{p}, t) - P_{exp}(t)$ (the modelling error) and its cosine transform $\{\widetilde{r}_\nu | \nu = -\infty \ldots -1, 0, 1, \ldots \infty\}$.

Before the RMS modelling error $c(\mathbf{p})$ over the interval $I = [0, t_f]$ is computed, the residual is subjected to a lowpass filter $\{F_\nu\}$ with time constant τ_F:

$$c(\mathbf{p}) = \left[\sum_\nu F_\nu |\widetilde{r}_\nu|^2 \frac{1}{t_f} \right]^{\frac{1}{2}}, \qquad \text{with} \quad F_\nu = \exp\left(-\nu^2 \left(\frac{\tau_F}{t_f} \right)^2 \right). \tag{2}$$

The low pass filter was introduced by Spirkl [10] to minimize the impact of transient modelling and measurement errors that cancel within a short period of time while retaining a maximum amount of information.

The parameters $\mathbf{p}$ are then varied until $c(\mathbf{p})$ reaches a minimum $c(\hat{\mathbf{p}})$ for a certain parameter set $\hat{\mathbf{p}}$. The minimum search algorithm is capable of handling local minima due to nonlinear dependence of $P_{mod}(\mathbf{p}, t)$ on $\mathbf{p}$.

The same model together with the optimal parameter set $\hat{\mathbf{p}}$ can then be used in a dynamic simulation program (e.g. TRNSYS) to perform simulations for the system under test for arbitrary conditions. This approach has several advantages: It avoids entirely the problem of parameter interpretation when transferring test results to simulation and layout programs, and the parameter covariance matrix estimated by the minimum search algorithm yields a performance prediction error estimate that is based on experimental data.

A computer program package providing the parameter identification and performance prediction algorithms, and an interface to external models with the model used here as a source code example is available from [11].

4 The Model

At first, the model used in this paper extends the Hottel-Whillier-Bliss equation [12] to a dynamic one node model. Second, several nodes are connected in series to form a multi-node model.

In the one node model, the collector is assumed to be of uniform temperature $T \equiv \mathbf{z}(t)$. The instantaneous collector power $P_{mod} = \dot{C}_f(T - T_{in})$ is the modelled system output.

[1] In general, z may also be a function of two variables (e.g. a temperature as function of location and time) instead of a vector function of one variable. Then, a partial differential equation is used instead of Eqn. 1

The differential equation governing the system state T is

$$C_C \frac{\mathrm{d}T}{\mathrm{d}t} = A_C'[G_t - u_C^*(T - T_a)] - \underbrace{\dot{C}_f(T - T_{in})}_{P_{mod}} \tag{3}$$

The parameters to be determined are $\mathbf{p} = (A_C', u_C^*, C_C)$. The input data $\mathbf{e}(t)$ to be measured are $\mathbf{e}(t) = (G_t, T_a, \dot{C}_f, T_{in}, T_{out})$. No intrusive measurements need to be made.

For stationary conditions, the left side of eqn. 3 becomes zero. Then, neglecting pipes, A_C' can be interpreted as $A_C' = F'(\alpha\tau)A_C$, where F' is the collector efficiency factor as defined in [12].

Eqn. 3 is solved analytically for each timestep.

This model neglects many properties of a real collector: For a real collector, the fluid flow time leads to a delayed response of the outlet temperature to sudden changes of irradiance and inlet temperature which cannot be reproduced by a one node model.

Furthermore, the collector efficiency as function of capacitance rate for stationary conditions differs from the behaviour of a dispersed system: For the one node model presented here and a dispersed system, the respective collector flow factors F_1'' and F_∞'' as defined by [12] will be

$$F_1'' = \frac{S}{S+1}, \qquad F_\infty'' = S\left(1 - \exp\left(\frac{-1}{S}\right)\right), \qquad \text{with } S = \frac{\dot{C}_f}{A_C' u_C^*}. \tag{4}$$

F_1'' and F_∞'' are equal for very high or very small flow rates but differ up to 0.13 for $S \approx 1$; this would lead to an under- or overestimation of the collector efficiency if the collector were used with S different from the test.

Also, the dependence of the collector losses on ambient temperature and inlet temperature is much more complex for a real collector, and the wind speed dependence of the collector losses has been neglected as well as incidence angle effects. Many more modelling errors could be mentioned. But, compared to neglecting the collector capacity entirely, these are all second-order effects *when the collector is subjected to instationary conditions*.

However, in order to resolve some of the inconsistencies that result from neglecting that collectors are dispersed systems, the one node model described above has been extended to a N-node model by connecting N collector nodes in series where each is assigned $1/N$ of the total effective area and $1/N$ of the total effective capacity. In the sequel, a 30-node model is used[2].

This model can easily be extended; the parameter identification method is not restricted to a specific model, a certain number of parameters, a certain set of measured input data or linear dependence of the system output on the parameters.

[2]The difference between F_{30}'' and F_∞'' is negligible.

Table 1: The three test sequences $\mathcal{S}_1$, $\mathcal{S}_2$ and $\mathcal{S}_3$ are characterized by their respective length, weather and average collector array output power.

Sequence	Length	Cloud Cover	T_a	$\overline{P_{exp}(t)}$	$\overline{G_t}$
$\mathcal{S}_1$	288 hr	Clear, partly cloudy and overcast days	10...22 °C	275W	153W
$\mathcal{S}_2$	239 hr	Partly cloudy and overcast days	8...19 °C	162W	91W
$\mathcal{S}_3$	36 hr	Clear with few clouds	11...23 °C	571W	259W

5 The Experiment

Measurements were made on an array of three parallel connected flat plate collectors with double glazing and an aperture of $2m^2$ each. The collector array was connected via insulated pipes to an adjacent 300l store with an immersed heat exchanger coil. The sensors for T_{in} and T_{out}were located at the heat exchanger inlet and outlet. Water with 30% ethylene glycol was used as heat transfer fluid. The measured quantities were recorded as five minute averages of T_a, G_t, T_{in}, T_{out} and $\dot{C}_f$; the collector power $P_{exp}(t)$ was calculated instantaneously online and recorded as five minute averages also.

The measurements on the collector loop were made outdoors in Munich, Germany during three sequences $\mathcal{S}_1$, $\mathcal{S}_2$ and $\mathcal{S}_3$. The sequences are characterized in Table 1. During the experiment, the collector loop was operated according to the recommendations of the manufacturer, i.e. the collector loop circulation pump was switched on and off by a temperature difference control system. Hot water was drawn from the store almost every day, up to three times per day. For sequence $\mathcal{S}_3$, ambient, inlet and outlet temperatures, irradiance, capacitance rate, and collector power are plotted in Fig. 1. The capacitance rate for sequence $\mathcal{S}_1$ is depicted in Fig. 2.

As can be seen from these plots, all system input variables are highly instationary. The meteorological variables cannot be influenced, the flow rate changes according to fluid viscosity and operation times of the pump, and the inlet temperature usually rises slowly when the store is heated and drops suddenly when cold water enters the store during drawoffs.

6 Parameter identification and performance prediction

The collector parameters $\hat{\mathbf{p}} = (A'_C, u^*_C, C_C)$ are first determined for each sequence separately, then all three sequences are used simultaneously.

The algorithm requires setting of the filter time constant τ_F and a skip time for each data set.

The time constant τ_F is chosen as 1 hr, which proves to dampen dynamic errors sufficiently

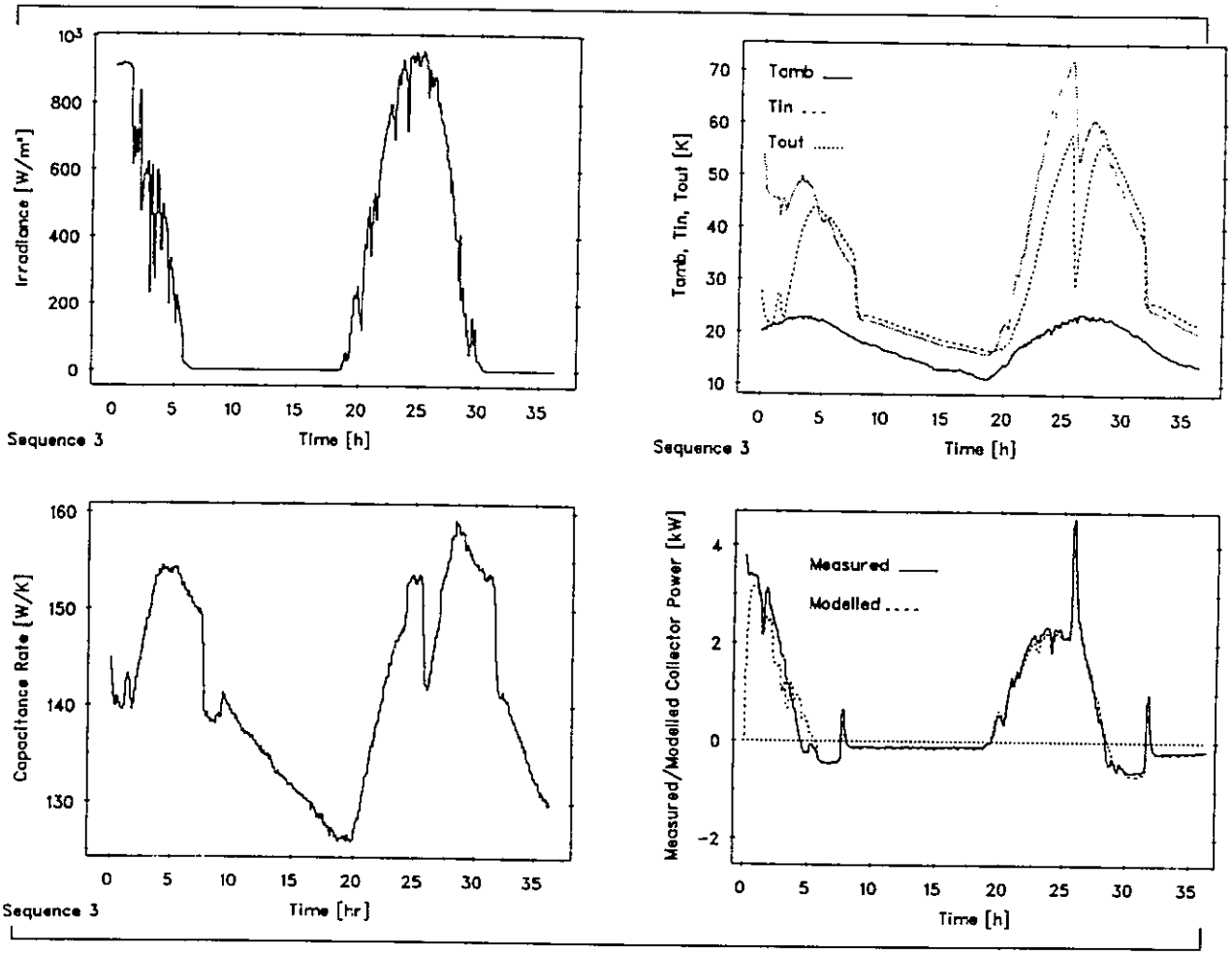

Figure 1: For sequence S_3, the input and output variables are plotted. The top left picture shows the irradiance G_t (almost no clouds were present). In the top right plot, T_a, T_{in} and T_{out} show the slow rise and fast drop of collector inlet and outlet temperature. The bottom left plot shows the change of the capacitance rate due to changing fluid viscosity. However, since $S \approx 4$ during pump operation, F'' and thus collector efficiency remain almost unaffected by this flow rate change. The bottom right plot shows the collector power. The solid line represents measured values; dashed is the modelled power using the optimal parameters shown in Table 2. The spikes at 8 hr, 26 hr and 32 hr are due to the sudden drop of the inlet temperature during drawoff.

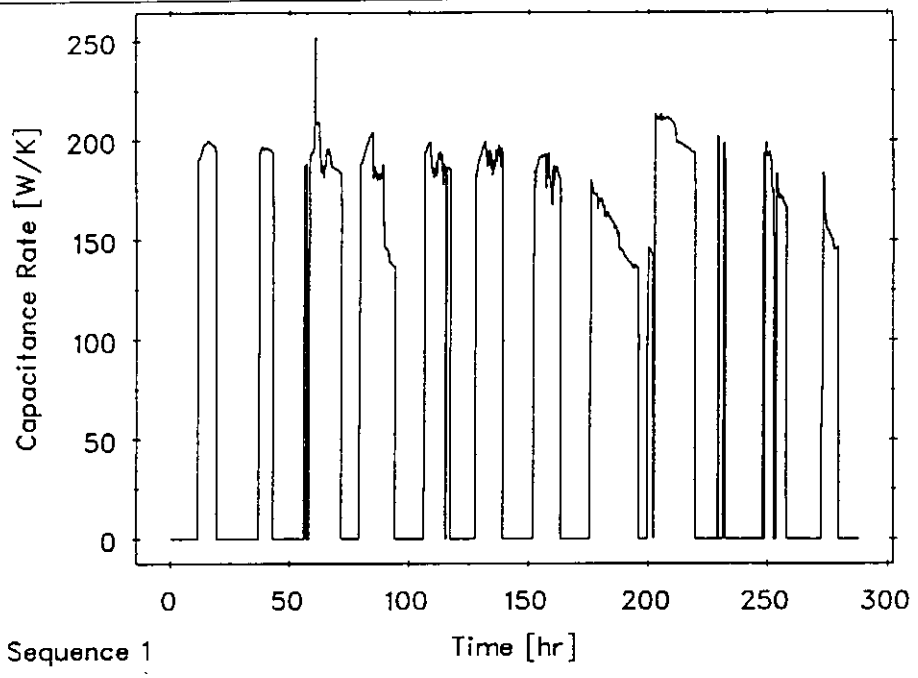

Figure 2: The plot of the capacitance rate for sequence $\mathcal{S}_1$ shows the operation of the collector loop controller: the pump is switched on and off frequently.

while retaining sufficient information. The selection of τ_F is somewhat arbitrary, but the algorithm is not very sensitive to changes as long as τ_F is of the order of several time constants of the collector.

During the skip time, the system state is modelled but the modelling error is not taken into account for the determination of the objective function $c(\mathbf{p})$. The skip time should be chosen as several times an estimated system time constant in order to avoid errors due to the arbitrary setting of the modelled initial system state. For sequences $\mathcal{S}_1$ and $\mathcal{S}_2$, a skip time of 6.6 hr is chosen, which is more than sufficient to let the initial system state fade out even for $\dot{C}_f = 0$. For $\mathcal{S}_3$, a skip time of 1.7 hr is used.

The fit results for the 30-node model are listed in Table 2. Here, the optimal parameter values appear together with their standard error estimates and $c(\hat{\mathbf{p}})$. The respective value of $c(\hat{\mathbf{p}})$ approximates the average hourly RMS modelling error. The values of $c(\hat{\mathbf{p}})/A_C$ remain below 3% of the maximum irradiance. In the top three lines of Table 2, each dataset is used separately. The parameter values for different sequences agree within two or three standard deviations, except for C_C, where the error estimates are too low. Below, using all three sequences *simultaneously* for parameter identification makes the results more reliable. (For the definition of $c(\mathbf{p})$ for several sequences simultaneously see [10].)

As an experimental check of the method's predictive capability, parameters $\hat{\mathbf{p}}$ determined using data from one sequence are used to predict the collector performance for the input conditions of another sequence.

As a measure of deviation between measurement and prediction, ΔT_{out} (the error of predicting the outlet temperature T_{out}) is preferred to the relative or absolute error of delivered energy.

To compute the prediction error ΔT_{out} for an interval I, the difference between measured

Table 2: The results of the parameter identification include parameter values, standard deviations for each parameter and the modelling error $c(\hat{\mathbf{p}})$. First, each dataset is used separately; then, all datasets are used simultaneously.

Parameter	A_C'	u_C^*	C_C	$c(\hat{\mathbf{p}})$	$c(\hat{\mathbf{p}})/A_C$
Unit	[m²]	[Wm^{-2}K^{-1}]	[kJ/K]	[W]	[Wm^{-2}]
Sequence $\mathcal{S}_1$	3.96 ±0.05	8.74 ±0.17	81.7 ±3.5	85	14.2
Sequence $\mathcal{S}_2$	3.74 ±0.06	7.83 ±0.26	46.3 ±3.8	71	11.8
Sequence $\mathcal{S}_3$	4.40 ±0.17	9.40 ±0.49	106 ±15.2	170	28.3
Sequence $\mathcal{S}_1$,$\mathcal{S}_2$,$\mathcal{S}_3$	4.01 ±0.03	8.78 ±0.08	84.0 ±0.8	91	15.2

Table 3: Parameters are determined using data from one test sequence, then the performance is predicted for the two remaining sequences. The prediction errors (expressed as average collector output temperature error ΔT_{out}) compiled here show the feasibility of accurate performance prediction from nonstationary test data.

Prediction error ΔT_{out}			
Parameters from seq.	Prediction for sequence		
	$\mathcal{S}_1$	$\mathcal{S}_2$	$\mathcal{S}_3$
$\mathcal{S}_1$	—	−0.21K	−0.21K
$\mathcal{S}_2$	+0.03K	—	−0.06K
$\mathcal{S}_3$	−0.06K	−0.20K	—

and predicted outlet temperature is weighted by the capacitance rate:

$$\Delta T_{out} = \frac{\int_I (T_{out} - T)\dot{C}_f \mathrm{d}t}{\int_I \dot{C}_f \mathrm{d}t} \tag{5}$$

The performance prediction results are compiled in Table 3. The prediction error ΔT_{out} ranges from 0.05K to 0.27K (which is close to the sensor accuracy of 0.1K) even when the parameters are determined from sequence $\mathcal{S}_3$ with a length of less than two days. Compared to the $\dot{C}_f$-weighted mean absolute temperature difference across the collector (ranging from 3K for $\mathcal{S}_2$ to 6K for $\mathcal{S}_3$), a relative prediction error between 1% and 8% results.

The difficulties in determining the parameter C_C presumably result from the large timestep of the experimental data (5 min) and from the crude way of modelling the thermal capacity of the collector. Since the model used here differs from a real collector in many ways, parameters cannot be assigned a straightforward physical meaning; this applies especially to C_C. However, the performance prediction error is hardly affected by the exact value of C_C: If A_C' and u_C^* are taken as fitted for $\mathcal{S}_2$ and C_C is set to 80kJ/K

instead of 46.3kJ/K, an error of $\Delta T_{out} = 0.04$K instead of $\Delta T_{out} = 0.03$K results for prediction of S_1.

7 Conclusions

- A method is presented which makes possible collector testing under instationary conditions (inlet and ambient temperature, irradiance and fluid flow rate).
- The parameters found in the test can be used directly by simulation programs using the same model. In principle, the same approach is possible for other system components. Thus, component test results could be used directly for system simulation.
- With the three parameter multi-node model used here, accurate performance prediction for a double glazed collector for arbitrary conditions is possible from a short term test (less than two days) provided sufficient input data variability.
- The collector model used here can easily be extended by introducing new parameters and (possibly) additional input quantities without making changes to the parameter identification algorithm; the modelled collector power may depend nonlinearly on the parameter values.
- The method can be used for testing a collector array in situ (including pipes, if desired) during normal operation. E.g. for liability claims, the performance can then be predicted for test reference year conditions.
- Further investigations are necessary: The method should be checked for other collectors, and more detailed models should be developed and tested in order to account for collector performance dependence on e.g. wind speed, turbulence, incidence angle and fluid flow time.

8 Acknowledgements

The author wishes to thank Dr. W. Spirkl and Professor Dr. R. Sizmann.

This work has been supported by the German Minister for Research and Technology, grant nr. 0328101C.

9 Nomenclature

Quantity	Unit	Meaning
$(\alpha\tau)$	[ ]	Effective absorptance-transmittance product.
A_C	[m^2]	Absorber area.
A'_C	[m^2]	Effective collector area.
C_C	[J/K]	Effective thermal collector capacity.
$\dot{C}_f$	[W/K]	Capacitance rate through the collector.

$c(\mathbf{p})$		Function measuring the modelling error (same unit as P_{exp}).
$\mathbf{e}(t)$		Input data (to be measured).
F_ν	[ ]	Low pass filter weights.
F''_N	[ ]	Collector efficiency factor for N nodes.
G_t	[$\mathrm{Wm^{-2}}$]	Irradiance onto the collector plane .
$\mathbf{p}$		Vector of model parameters.
$\hat{\mathbf{p}}$		Value of $\mathbf{p}$ for which $c(\mathbf{p})$ reaches its minimum.
$P_{exp}(t)$	[W]	Experimentally measured system output.
$P_{mod}(\mathbf{p}, t)$	[W]	Modelled system output.
$r(t)$		Residual (modelling error as function of time).
$\widetilde{r}_\nu$		Cosine transform coefficients of $r(t)$.
τ_F	[s]	Time constant for low pass filter weights $\{F_\nu\}$.
T	[°C]	Modelled collector temperature (uniform within one node).
T_a	[°C]	Collector ambient temperature.
T_{in}	[°C]	Measured collector inlet temperature.
T_{out}	[°C]	Measured collector outlet temperature.
ΔT_{out}	[K]	Difference between predicted and measured collector temperature, weighted by $\dot{C}_f$.
S	[ ]	Dimensionless fluid flow rate.
$\mathcal{S}_\mathbf{k}$		Test sequence k (k=1,2,3).
u_C^*	[$\mathrm{WK^{-1}m^{-2}}$]	Effective collector loss coefficient.
$\mathbf{z}(t)$		Modelled internal system state (not to be measured).

10 References

[1] ASHRAE 93-1986. Methods of Testing to Determine the Thermal Performance of Solar Collectors. 1986.

[2] DIN 4757, Teil 4, Sonnenkollektoren, Bestimmung von Wirkungsgrad, Wärmekapazität und Druckabfall. Beuth Verlag, Berlin, 1982.

[3] J.E. Nielsen and O. Ravn. Performance Testing of Domestic Hot Water and Space Heating Solar Systems. Technical Report, Danish Solar Energy Testing Laboratory, Technological Institute, 1985.

[4] F-Chart 4.2. Solar Energy Laboratory, University of Wisconsin, Madison, USA, 1985. EES Report 50.

[5] S.A. Klein, W.A. Beckman, and P.I. Cooper. TRNSYS: A Transient System Simulation Program, Version 12.2. Solar Energy Laboratory, Madison Wisconsin, 1988.

[6] J.P. Norton. *An Introduction to Identification.* Academic Press, 1986.

[7] X.A. Wang, Y.F. Xu, and X.Y.Meng. A Filter Method for Transient Testing of Collector Performance. *Solar Energy*, **38**:125–134, 1987.

[8] M. Emery and B.A. Rogers. On a Solar Collector Thermal Performance Test Method for Use in Variable Conditions. *Solar Energy*, **33**:117–123, 1984.

[9] B. Perers and H. Walletun. Dynamic Collector Models for One Hour Time Step Derived from Measured Outdoor Data. In *Proceedings of the ISES Solar World Congress 1991 Denver*, 1991.

[10] W. Spirkl. Dynamic SDHW Testing. *J. of Solar Energy Eng., Transactions of the ASME*, **112**:98–101, 1990.

[11] W. Spirkl. Dynamic SDHW Testing Program Manual (Version 1.19). Available from DIN, Postfach 1107, D-1000 Berlin 30, FRG, 1992.

[12] J.A. Duffie and W.A. Beckman. *Solar Engineering of Thermal Processes.* John Wiley & Sons, New York, 1983.

DYNAMIC FITTING ON MEASURED DATA FROM A LARGE SOLAR COLLECTOR FIELD

A. V. Souproun, J. E. Nielsen
Solar Energy Laboratory
Danish Technological Institute
P.O. Box 141
DK-2630 Taastrup
Denmark

1. GENERAL

Since large solar collector fields became more spread, investigations of such solar energy plants arise some topical problems. Precise indoor laboratory tests cannot be carried out for such plants due to their dimensions and because of this, only in-situ experimental results may be available for the large fields of solar collectors. Experimental data for the solar energy plant, located near the town of Ry, were treated with a purpose of parameter's estimation. Test method chosen based upon a procedure for dynamic fitting of parameters for different solar domestic hot water systems [1], but a flexibility of software, which has been developed at the Ludwig-Maximilians-University of Munich (Germany), allows using of external models for this a batch of programmes. Such a model for the solar collectors was applied in the present work. Since the solar collectors of the Ry heating system were supplied with the double glazing, an influence of the wind speed during the measurements on the

thermal efficiency curve may be ignored, therefore a simple collector model comprising only a first order heat loss coefficient was used in order to estimate the collector field parameters.

2. SYSTEM DESCRIPTION

Ry collector array represents Denmark's largest solar energy system. Solar collector field of 3267 m^2 in the total area was intended to supplement the town's existing coal fired plant. Ry is a town of apromixately 3000 people and has more than 1300 householders connected to its district heating plant. Solar collector field was designed to produce 1270 MWh, that is approximatelly 4% of Ry's total heating yield. It was expected, that application of such solar collector field would save the enviroment the burning of about 200 tons of coal per year. Solar energy plant consists of 242 flat plate solar collectors of sunstrip type (TEKNOTERM HT). Apperture area of each solar collector is 12.5 m^2. Solar collectors are connected to the main coal fired plant with the isolated pipes of 0.139 m diameter, installed directly in the earth. Total length of all the connecting pipes between the solar collectors and a heat exchanger makes up more than 600 m. Additionally, collector field comprises 200 m of the manifolds between the solar collectors themselves. Heat transfer liquid is heated in the solar collector field by solar energy and then pumped through the heat exchanger as soon as heat transfer fluid temperature at the outlet of the pilot solar collector exceeds 40 °C. In the heat exchanger solar heat is transferred to the plant return water, pre-heating it prior to its entering the boiler.

3. MEASUREMENTS

Data were collected each four minutes during two summer months of the current year. Two in-situ measurement periods (22.7-27.7 and 29.7-17.8) with the total

duration of 26 days were used for the parameter fitting. Measured parameters are:

solar irradience,
temperature of the ambient air,
flow of the heat transfer liquid,
outlet and inlet temperatures,
output energy from the collector field.

In this work we tried to use as wide range of the working temperatures as it was possible due to the operating conditions restricted by the automatical control of the collector loop. Fig.1 can give a certain imagination of the temperature distribution during this period of 26 days.

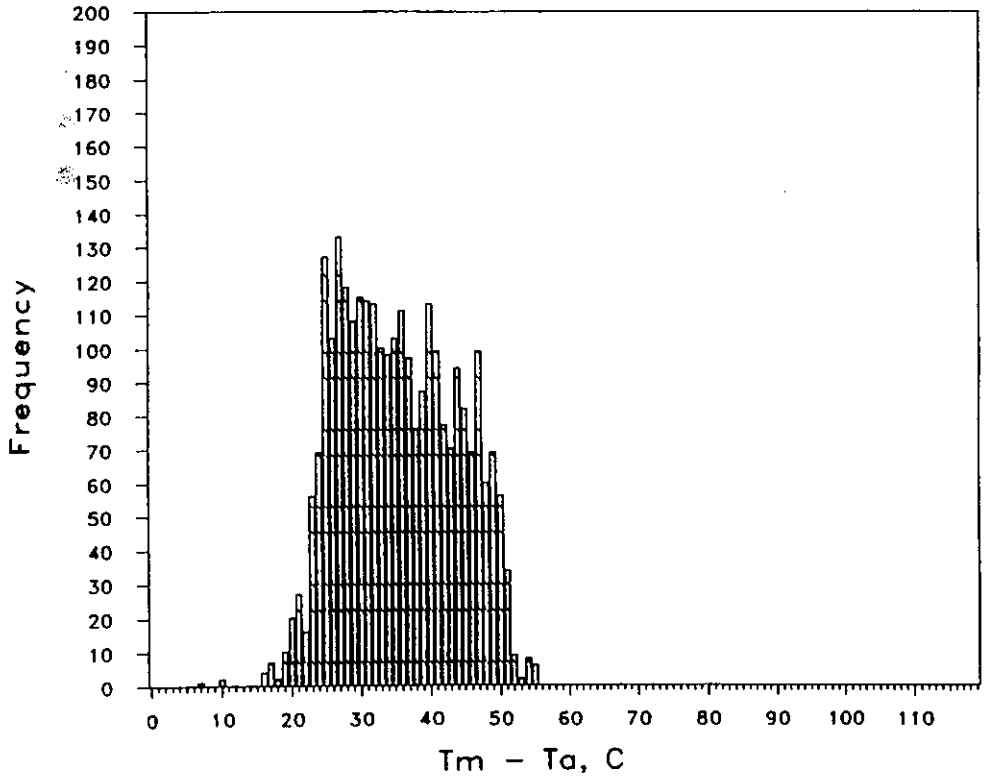

Figure 1: Temperature distribution of the measured points from the collector array at the Ry district heating plant.

From fig.1 it is obvious that such narrow temperature interval together with a definite scattering in the data makes it difficult to generate the efficiency curve by ordinary methods. It is evident that dynamic behaviour of the whole system would have a significant influence which should be also taken into the consideration. That is why the dynamic method [1] was implemented in this work in order to estimate the parameter values of the collector field.

4. EXPERIMENTAL RESULTS

Preliminary analysis of the experimental data was made by using a solar load ratio (SLR). Fig.2 represents a histogram based on 90 different daytime points obtained from the measurements as the average hour values. Number of the points were plotted versus the decimal logarithm of the SLR in order to investigate available range of weather and load conditions during the measurements.

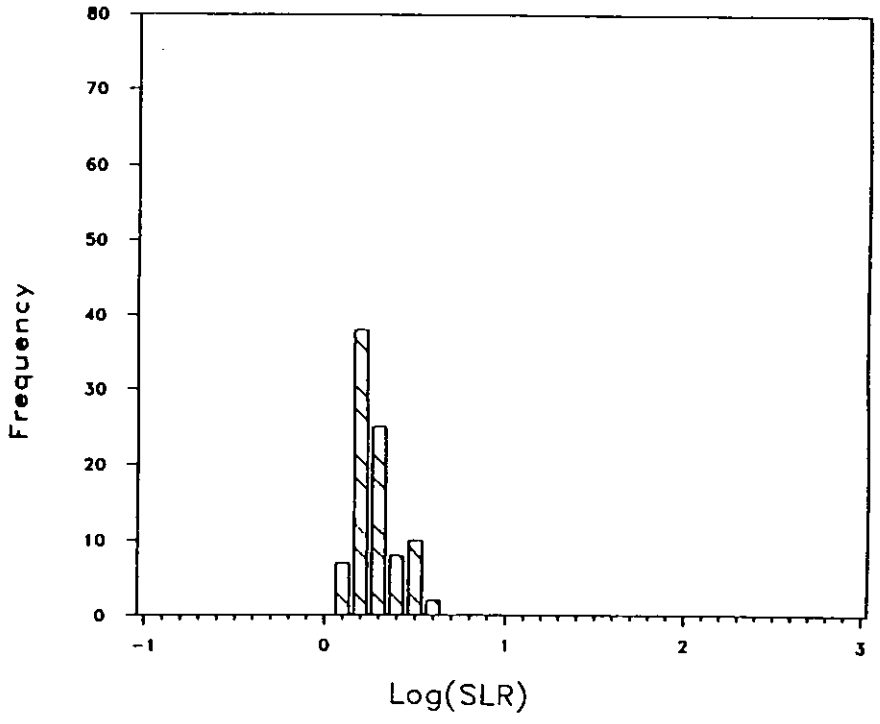

Figure 2: Frequency of average hour values versus the decimal logarithm of solar load ratio.

As inlet and outlet temperature sensors have been installed near the heat exchanger, heat losses from the pipes were included into the values of overall collector array losses. Calculated value of a heat loss coefficient for the pipes, connecting the collector field and the heat exchanger of the plant, was equal to 0.25 $W/m^2/K$. So this value have been subtracted from the total heat loss coefficient in order to evaluate separately heat losses of the solar collector field. Fitting of the collector field parameters was carried out on the basis of energy gain, measured during the tests. Estimated values of the collector field parameters are given in table 1.

Table 1: Results of parameter estimation for the Ry solar collector field.

Collector field parameters	Units	Values
Effective area	m^2	2310±110
Heat loss coefficient	$W/(m^2K)$	5.47±0.38
Thermal capacity for 1 m^2 of collector field aperture area	$kJ/(m^2K)$	12.23

Results, obtained from the indoor laboratory test for the single solar collector of the same type as at the Ry heating plant, are presented herein as a thermal efficiency curve:

$$\eta = 0.70 - 2.39(T_m - T_a)/G_t - 0.015(T_m - T_a)^2/G_t .$$

A comparison between stationary solar collector test and in-situ collector field tests was made and the efficiency curves for the both cases are plotted in fig.3. Data were represented within the temperature interval of $T_m - T_a$ = 20-50 °C, as it includes more than 98% of all the points, available from the measurements on

on the Ry collector field.

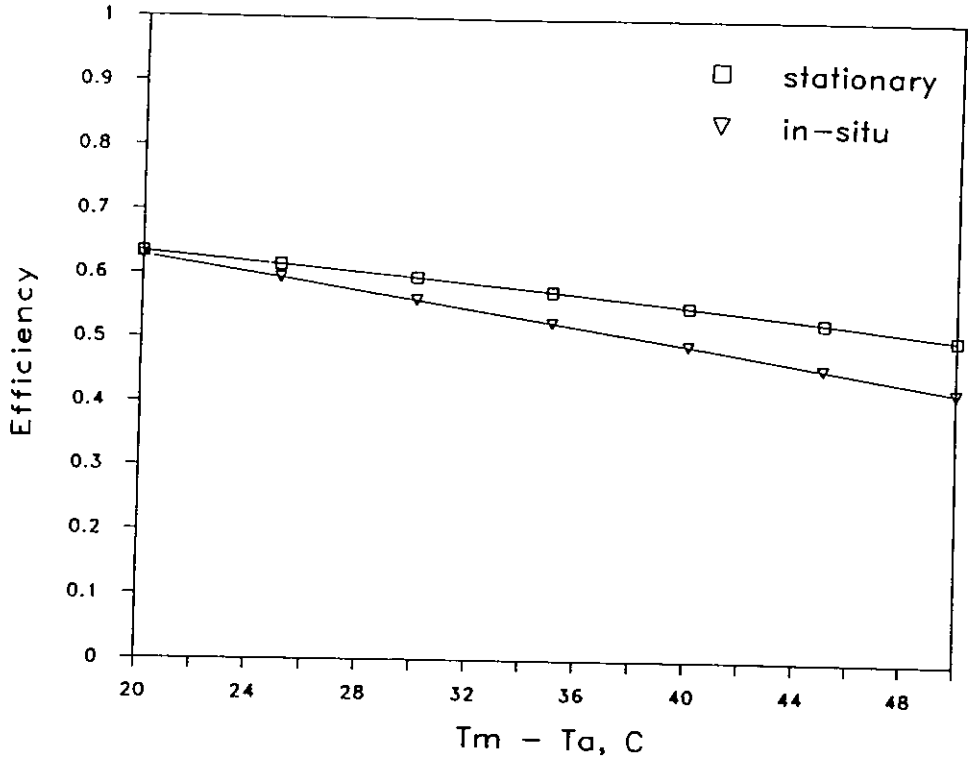

Figure 3: Thermal efficiency of the Ry collector field and a single solar collector of TEFNOTERM HT type.

Results of comparison show that single solar collector exibits a little higher thermal efficiency, than the collector field does. It can be assumed reasonable if take into account existance of heat losses of the piping between neibouring solar collectors and the fact, that such losses take place only in the collector field but not for the single solar collector, for which, as a rule, inlet and outlet temperatures are measured in direct nearness from the collector entrance and exit.

5. CONCLUSIONS

Application of the dynamic method for the parameter fitting of the large solar collector field can give rather reasonable results, despite a narrow temperature

distribution of experimental points during the measurements.
Our first experience of the work with the data from in-situ tests on the large field of the flat plate solar collectors allows to consider that its working performance is in general similar to that of a single solar collector and it may be described by ordinary thermal efficiency curve.

AKNOWLEDGEMENTS

This material is based in part upon work supported by the Danish Energy Agency. The authors express their hearty appreciations to Mr. Niels Andersson from the Folkecenter for renewable sources of energy (Hurup, Denmark) for providing us the experimental data from the Ry district heating plant for fitting procedure.

NOMENCLATURE

G_t	Solar irradiance in the collector plane, W/m^2
T_a	Ambient temperature, °C
T_m	Mean fluid temperature, °C
η	Thermal efficiency

REFERENCES

[1] Spirkl W., 'Dynamic Solar Domestic Hot Water Testing', Transactions of the ASME, 112, 1990, PP.98-101.

A DYNAMIC METHOD FOR COLLECTOR ARRAY TESTING AND EVALUATION USING MULTIPLE REGRESSION AND STANDARD SIMULATION PROGRAMS

Bengt Perers
Vattenfall Utveckling AB
c/o Miljökonsulterna
P.O. Box 154, 61124 Nyköping
Sweden

ABSTRACT

A measurement and evaluation method is described by which standard collector performance parameters can be derived directly from measured all day 1 hour outdoor data. Multiple regression is presently used to determine the model parameters. A one node capacitance correction for dynamic effects and separate incidence angle models for direct and diffuse radiation are essential for the accuracy of the method. The model is set up for useful energy Q_u (and not efficiency) which forces the parameters to values that are suitable for prediction of long term performance. The collector model and parameters correspond closely to those used in existing detailed simulation programs like TRNSYS, WATSUN, or MINSUN. The method can be used as an accurate bridge between short term testing and long term prediction by simulation. A great advantage of the method is also that data gaps can be allowed within a test period and that strange or erroneous data can be excluded without problem.

1. INTRODUCTION

The aim of this work is to find a practical and accurate enough connection between outdoor measured all day collector performance and collector efficiency parameters that can be used in standard simulation programs for long term performance prediction based

on 1 hour time steps. In the Swedish climate stationary outdoor test methods are very time consuming and expensive to use. For testing of large area collectors and in-situ testing of collector arrays, an improved outdoor test method is needed that can use all day values from normal operating conditions.

The basis for this work is the experience with dynamic on-line simulation directly in the measurement computer [1] which has been gained since 1979 in all our testing and monitoring projects.

A standard collector model, with correction terms for incidence angle effects and thermal capacitance effects, can describe the hourly and daily performance accurately enough to show whether the collectors and the system are performing as expected, and also to give some idea of what is wrong when the agreement is not so satisfactory. The inverse method of on-line simulation described here has been used at our laboratory for in-situ testing of collectors and collector arrays since 1985. Some of the first results are described in [2], [3] and [4].

The collector model used here is based on the almost 50 year old Hottel- Whillier-Bliss equation with improvements to take into account thermal capacitance effects, incidence angle effects and the temperature and wind dependence of the heat loss coefficient. The basic model and the correction terms used are described in [5]. A description and validation of improved collector models can also be found in [6] and [7] describing work within IEA SHAC Task VI and Task III.

The 1 hour time step is chosen mainly because of the standard resolution of available weather data for simulation programs. In practice it has been found that the 1 hour time step also implies that thermal capacitance effects in the collector can be treated with a one node model without going into detail in the collector design. This corresponds closely to theoretical work described in [8] investigating different thermal capacitance models by detailed simulation.

Improved outdoor test methods have been proposed and validated in [9] and by Emery (1984) to derive standard stationary collector parameters from outdoor testing. This method utilizes a more complete characterization of the collector including incidence angle and thermal capacitance effects. This leads to a wider range of acceptable climate conditions for the test, and a shorter test period.

The thermal capacitance correction term is only based on information about the mean fluid temperature variation within the hour (a new on-line data reduction in the measurement system is required). This means that the hourly values do not have to be in sequence. Databases with gaps or data from different test periods can be used without any problem.

This method has been tested now for one year at ITW in Stuttgart with very promising results [10] for a variety of different collectors. A comparison with parameters derived with conventional stationary testing shows an excellent agreement.

Within the IEA SHAC programme a special parameter identification program [11] has been developed for testing of SDHW systems. The program has also been tested for collector array evaluation with a similar one node dynamic collector model as in this method but without incidence angle correction [12]. The program in [11] contains all steps from checking of input data to extrapolation to long term performance.

One advantage of the method described in this paper is that the derived parameters are directly compatible with existing ISO collector test standards and standard system simulation programs like TRNSYS, WATSUN or MINSUN. Also the on-line data reduction is an advantage as each 1 hour data record will be a separate unit. They can be put together to save data from periods with measurement or operating problems. This is not so uncommon during in-situ or prototype testing to our experience.

2. PROPOSED COLLECTOR ARRAY MODEL FOR GLAZED COLLECTORS

The model described below is a mixture of already existing and validated correlation models for the complex instantaneous thermal and optical behaviour of a solar collector. The extension of the instantaneous models to hourly mean values is possible also for dynamic conditions as the integrated effect of thermal capacitance within the hour is taken care of in the model. The present model used for glazed collectors is:

$$q_u = F'(\tau\alpha)_e K_{\tau\alpha b}(\Theta) G_b + F'(\tau\alpha)_e K_{\tau\alpha d} G_d - F'U_0 DT - F'U_1 (DT)^2 + \\ - F'U_w DT \cdot w - (mC)_e dT_f/dt - U_p DT \qquad (1)$$

with:

q_u = collector array thermal output [W/m²]

$F'(\tau\alpha)_e$ = zero loss efficiency for direct radiation at normal incidence [-]

$K_{\tau\alpha b}(\Theta)$ = incidence angle modifier for direct radiation [-]

$K_{\tau\alpha d}$ = incidence angle modifier for diffuse radiation [-]

G_b = direct radiation in the collector plane [W/m²]

G_d = diffuse radiation in the collector plane [W/m²]

$F'U_0$ = heat loss coefficient for $T_f - T_a = 0$ [W/(m²K)]

$F'U_1$ = temperature dependence in the heat loss coefficient [W/(m²K²)]

$F'U_w$ = wind speed dependence in the heat loss coefficient [J/(m3K)]

U_p = piping heat loss coefficient per m2 collector area [W/m²K]

$(mC)_e$ = effective thermal capacitance including piping for the collector array [J/(m²K)]

DT = temperature difference, $T_f - T_a$ [K]

w = wind speed near the collector [m/s]

dT_f/dt = mean time derivative for the average fluid temperature T_f within the time step [K/s]

T_f = mean fluid temperature in the collector, $(T_{in} + T_{out})/2$ [°C]

T_a = ambient air temperature near the collector [°C]

Θ = incidence angle for the direct radiation in the collector plane [rad.]

Except for the wind dependence and thermal capacitance term most detailed simulation programs already use the same performance model. One problem is that some programs such as TRNSYS and WATSUN use models based on inlet temperature T_{in} whereas the model in this case is based on the mean fluid temperature T_f. The conversion between the two formats is described in [5].

The model is written as an *energy balance* as in the simulation programs and *not as collector efficiency* This is important for the parameter values as the multiple regression program should *minimize the error in useful energy* and not in efficiency, as this would lead to a too high influence of low radiation conditions on the parameter values.

3. TEST REQUIREMENTS

Standard test equipment can be used provided that all necessary variables in the model above are measured. The only change required is an on-line data reduction that calculates and stores the average mean fluid temperature change per second within the hour.

The only limitation for the use of the model is that the mean fluid temperature can only be determined as long as there is a continuous mass flow in the collector array during the hour. At the solar collector test field in Studsvik the collectors are operated with a continuous flow. This means that data for the whole day can be used. This can also be achieved during in-situ measurements by running the pump in the collector loop manually. This method uses the measured data much more intensively for the whole day.

Some extra care is required when using the sensors in practice. Placing, ventilation and radiation shielding of ambient temperature sensors is important in order to give a representative ambient temperature for the collector. A location in the shadow behind a freestanding collector has turned out to give a very good agreement with a fan ventilated reference sensor at the same height above ground. The alignment of the pyranometers also become more important in this case. An alignment error of 2° will give measurement errors in the range of 5% already at 50° off normal incidence.

From a practical point of view it is a great advantage that *data gaps can be accepted in this method.* This gives the possibility to delete strange or erroneous data or to mix data from different test sequences when evaluating the measurements.

4. RESULTS

At the Studsvik Solar Test Field 11 m2 modules of LGB (Long Ground Based) flat plate collectors have been tested. They can be site-built in sizes up to 70 m long [13]. In this case the collectors have a selective sunstrip absorber and a teflon inner glazing. Randomly chosen 65 hour periods of one hour mean values for each month from April

to September have been used to identify the model parameters. There was no selection of the periods except the avoidance of snow and frost on the collectors. Table 1 shows the results together with the expected parameter values from the collector design and materials used.

Table 1: Model parameters derived by multiple regression.

month	$F'(\tau\alpha)_b$ [-]	b_0 [-]	$F'(\tau\alpha)_b K_{\tau\alpha d}$ [-]	$F'U_L$ [W/(m²K)]	$(mC)_e$ [J/(m²K)]	st.dev. [W/m²]	R^2 [-]
expected	0.75	-0.15	0.68	-3.5	-10000	-	-
April	0.739	-0.185	0.652	-3.181	-8654	8.23	0.998
May	0.756	-0.165	0.712	-3.625	-12095	11.60	0.997
June	0.763	-0.257	0.738	-3.572	-9713	12.60	0.996
July	0.777	-0.188	0.742	-3.909	-9304	11.82	0.996
August	0.746	-0.165	0.660	-3.225	-9446	12.29	0.994
Sept.	0.743	-0.175	0.671	-3.168	-8986	8.95	0.998

All day values from sunrise to sunset have been used and in some cases also the hours of darkness. This means that the parameter values are valid not only for the operating time but will also give a good estimation of the transient behaviour outside the operating time.

5. DISCUSSION

The term $F'U_L$ in Table 1 is the *total heat loss factor*. For these randomly chosen data sets, the second order heat loss terms were just on the limit to be statistically significant (T-ratio just below 1) but were excluded in this presentation. The absolute values were near what could be expected.

Here the accuracy and mounting of the climate sensors has a significant influence and we are now refining this part of our measurement installation in Studsvik.

The seasonal variation is not completely understood but the model

$$K_{\tau\alpha b}(\Theta) = 1 - b_0(1/\cos(\Theta)-1) \quad (2)$$

used here to describe the incidence angle dependence is not good enough for angles exceeding 70° compared to flat glass transmission curves. The summer data here contain many hours with incidence angles greater than 70°. An incidence angle model that is more accurate for high incidence angles compared to flat glass curves is described in [6]:

$$K_{\tau\alpha b}(\Theta) = 1 - (\tan(\Theta/2))^n \, . \quad (3)$$

In practice, the absorber and shadowing from the frame of the collector glazing adds to the incidence angle effects. When taking the shadowing effect into account it turns out that Eq. (2) is better for most of the incidence angle range. Eq. 2 also gives a cut-off angle just as the shadowing effect. A structured collector glass was used in the collector test presented here which has a special incidence angle variation that also might give some influence.

Further investigations are required to find out the exact reason for the parameter variation. It should be pointed out that no selection or sorting of the data was done so there might be some influence just from extreme weather conditions also.

6. CONCLUSIONS

Multiple regression can be used to identify standard collector performance parameters from measured outdoor data.

Standard test equipment can be used but the mounting and placing of the climate sensors become more important as all day values are used and second order effects are taken into account.

By adding correction terms for incidence angle and thermal capacitance effects to the Hottel-Whillier-Bliss collector model, the all day performance on an hourly basis can be described accurately for most climate conditions in Sweden during the period April to

September.

By calculating and storing the temperature change of the collector mean fluid temperature each hour, the hourly thermal capacitance effects can be described very well with a one node model for the collector.

By running the pump in the collector loop continuously during the test period, all day data can be used which increases the variation range for the input variables. This will lead to better accuracy for the individual parameters and a shorter test period.

The derived collector parameters for 1 hour time step can be used directly in most detailed simulation programs.

REFERENCES

[1] Perers, B. and R. Roseen.
Solvärmecentralen i Studsvik - Resultat 1980 (Solar Heating Central - Results 1980).
STUDSVIK/E1-80/141, Studsvik AB, Sweden, 1980.

[2] Walletun, H. and B. Perers
Vindens inflytande på oglasade solfångare respektive solfångare med konvektionshinder (Wind influence for unglazed collectors and collectors with convection suppressing glazing).
STUDSVIK/ED-65/15, Studsvik Energy, Sweden, 1986.

[3] Perers, B. and P. Holst.
The Södertörn Solar District Heating Test Plant - Results 1982-1985.
STUDSVIK-87/1, Studsvik AB, Sweden, 1987.

[4] Perers, B.
Performance Testing of Unglazed Collectors, Wind and Long Wave Radiation Influence.
Report for IEA Task III. Studsvik Energy, Sweden, 1987.

[5] Duffie, J.A. and W.A. Beckman
Solar Engineering of Thermal Processes - Chapters 6 and 7.
John Wiley and Sons Inc., New York, 1980.

[6] Ambrosetti, P.
Das neue Bruttowärmeertragsmodell für Verglaste Sonnenkollektoren, Teil 1 Grundlagen (The new Gross Energy Contribution Model for Glazed Collectors, Part 1).
ISBN-3-85677-012-7, EIR Würenlingen, 1983.

[7] Gemmel, W.L., M. Chandrashekar and K.H. Vanoli.
Detailed Modelling of Evacuated Collector Systems.
IEA SHAC Task VI Report, 1986.

[8] Klein, S.A.
The Effects of Thermal Capacitance upon the Performance of Flat Plate Solar Collectors.
M.Sc. Thesis, University of Wisconsin, 1973.

[9] Proctor, D.
A Generalized Method for Testing all Classes of Solar Collectors - Part I, II, III.
Solar Energy, Vol. 32., No. 3, 1984.

[10] Guigas, M. R. Kübler and N. Fish.
Untersuchung von Hocheffizienten Flachkollektoren mit Hilfe einer Instationären Testmethode (Evaluation of High Performance Flat Plate Collectors with a Dynamic Test Method).
Proceedings Erstes Symposium Thermishe Solarenergie, 1991, Kloster Banz, pp. 290-295.

[11] Spirkl, W.
Dynamische Vermessung von Solaranlagen zur Warmwasserbereitung (Dynamic Testing of Solar Domestic Hot Water Systems).
Dipl.-Phys. Thesis. VDI Verlag, Reihe 6: Energieerzeugung, Nr. 241, München, 1990.

[12] Muschaweck, J.
Analyse einer solaren Brauchwasseranlage (Evaluation of a Solar Domestic Hot Water System).
Diplomarbeit, Universität München, 1989.

[13] Wilson, G.
Construction, Performance and Cost Analysis of the LGB-Collector.
North Sun Conference 1988, Swedish Council for Building Research D2:1989.
ISBN 91-540-4973-3.

[14] Perers, B. and H. Walletun
Dynamic Collector Models for 1 hr Timestep derived from Measured Outdoor Data.
ISES Solar World Conference 1991, pp. 1221-1226.